The Role of Rest and Stress Cardiac Energy Metabolism and Ectopic Lipid Deposition in Diabetic Cardiomyopathy

Eylem Levelt

St Peter's College

University of Oxford

Thesis Submitted for the Degree of Doctor of Philosophy

Trinity Term 2015

I dedicate this work to my daughter Emma.

Acknowledgements

It was an honour for me to be supervised by Prof. Kieran Clarke and Prof. Stefan Neubauer. I am very grateful for their support, steering and advice through the many learning stages of this thesis. Special thanks to Prof. Cameron Holloway, Dr Theodoros Karamitsos, Dr Oliver Rider, Dr Christopher Rodgers and Dr William Clarke, all of whom willingly gave me their time and expertise; for this I am forever grateful.

I am indebted to my colleagues for their willingness to help with the day-to-day running of this project. I would like to thank Dr Margaret Loudon, Dr Ntobeko Ntusi, Dr Rina Ariga, Dr Rohan Wijesurendra, Dr Jenny Rayner, Dr Victoria Stoll, Dr Alexander Liu and Dr Michael Pavlides for their true friendship on which I will count forever, and Dr Erica Dall'Armelina, and Dr Vanessa Ferreira for well-timed words of encouragement; I depended on them for advice. I am grateful to Mrs Jane Francis who has been heavily involved with the work in this thesis, for her help at every stage. I thank Dr Masliza Mahmod for her support over the years.

I especially want to thank my family. My gorgeous daughter, Emma. I am grateful for those lovely cuddles, which gave me strength beyond belief. I thank my wonderful husband, Sjoerd, who inspired me through his own achievements and has provided limitless support over the years. I have been blessed with magnificent support and love from my parents Hatice and Nurettin Aslan, and my wonderful sister Didem, and brother Fatih. Didem and

Fatih provided daily entertainment and kept me going. I thank my parents-in-law, Veronica Divendal and Peter Levelt, for their endless support and interest in my work.

Declarations

The work in this thesis is my own and original. Dr Christopher Rodgers and Dr William Clarke provided physics support leading to the results in chapter 4, and they were involved with scanning leading to the work described in chapter 6. Dr Rina Ariga and Mrs Jane Francis assisted in scanning and analysis of the studies of healthy volunteers. Dr Masliza Mahmod assisted in scanning in earlier studies. Dr Michael Pavlides, Dr Catherine Kelly and Mrs Sheena Thomas provided help with blinded analysis for chapter 5. Miss Joanna Sellwood assisted with recruitment and provided nursing care to the participants in these studies. Dr Alexander Liu carried out blinded analysis of the perfusion scans as a second operator leading to the work described in chapter 4.

Thesis Abstract

Type 2 diabetes mellitus (T2DM) is associated with an increased risk of heart failure and cardiovascular mortality even in the absence of coronary artery disease. Although the reasons for this are not clear, impaired cardiac high energy phosphate metabolism, coronary microvascular dysfunction and ectopic lipid deposition have emerged among the candidate mechanisms. Cardiac magnetic resonance imaging (CMR) and magnetic resonance spectroscopy (MRS) are powerful tools to characterise these conditions.

The findings here suggest that, in diabetes, coronary microvascular dysfunction may potentially exacerbate derangement of cardiac energetics under conditions of increased workload. The relationships amongst ectopic adiposity (myocardial, epicardial and hepatic), myocardial metabolic changes and left ventricular remodelling in T2DM were determined using proton magnetic resonance spectroscopy (^{1}H-MRS), cardiac computer tomography (CT) and multi-parametric liver MR. It was found that cardiac steatosis independently predicted left ventricular concentric remodelling and impairment of systolic strain in patients with T2DM. This work also demonstrated that ectopic adiposity is linked to insulin resistance, liver fibrosis and inflammation, and cardiac contractile dysfunction in diabetes, and that the coexistence of obesity and T2DM leads to higher epicardial fat volumes and significant non-alcoholic fatty liver disease compared to T2DM alone. These findings suggest that, since cardiac steatosis and ectopic adiposity are modifiable,

strategies aimed at reducing myocardial triglyceride levels may reverse concentric remodelling and improve contractile function in the diabetic heart. The work on field strength effects on cardiac ^{31}P-MRS has shown that 7T is feasible and reliable with reduced error and increased signal to noise compared to 3T.

In summary, the work in this thesis demonstrates the powerful role of CMR and MRS in elucidating the detrimental effects that originate from the metabolic abnormalities in the diabetic heart.

Abbreviations

2,3-DPG	2,3 diphosphoglycerate
^{31}P MRS	31-Phosphorus magnetic resonance spectroscopy
ACE-I	Angiotensin-converting enzyme inhibitors
AMARES	Advanced Method of Accurate, Robust and Efficient Spectroscopic fitting
ATP	Adenosine triphosphate
AW	Acquisition Weighting
BMI	Body Mass Index
BOLD	Blood oxygen level dependent imaging
CAD	Coronary artery disease
CMR	cardiac magnetic resonance
COV	Coefficient of variance
CRLB	Cramer-Ráo uncertainty
CSI	Chemical shift imaging
DM	Diabetes Mellitus

ECG	Electrocardiogram
EDV	End diastolic volume
EF	Ejection fraction
ESV	End systolic volume
FFA	Free Fatty Acid
FID	Free induction decay
HBA1c	Glycated Hemoglobin
HDL	High Density Lipoprotein
HLA	Horizontal Long Axis
HOMA-IR	Homeostatic Assessment of Insulin Resistance
LDL	Low Density Lipoprotein
LGE	Late gadolinium enhancement
LV	Left ventricle
MTG	Myocardial Triglyceride
MPRI	Myocardial perfusion reserve
MRI	Magnetic resonance imaging

NAFLD	Non-alcoholic fatty liver disease
NOE	Nuclear Overhauser Effect
NS	Not significant
PCr	Phosphocreatine
PPA	Phenyl phosphoric acid
PSF	Point spread function
RF	Radio frequency
RPP	Rate pressure product
SD	Standard Deviation
SERCA	Sarco/endoplasmic reticulum Ca^{2+}-ATPase
ShMOLLI	Shortened Modified Look- Locker inversion recovery
SI	Signal intensity
SNR	Signal to noise
SSFP	Steady state free precession
SV	Stroke volume
T	Tesla

TE	Echo time
TG	Triglyceride
TR	Repetition time
T1DM	Type 1 Diabetes Mellitus
T2DM	Type 2 Diabetes Mellitus

Table of Contents

List of Figures

Chapter 1

Chapter 2

Chapter 3

Chapter 4

Chapter 5

Chapter 6

List of Tables

Publications

Manuscripts currently undergoing rebuttal process

1) Levelt Eylem; Rodgers Christopher T; Clarke William T; Mahmod Masliza ; Ariga Rina; Francis Jane M; Liu Alexander ; Dass Saira ; Sabharwal Nikant; Robson Matthew D; Holloway Cameron J ; Rider Oliver J; Clarke Kieran; Karamitsos Theodoros D; Neubauer Stefan "**Cardiac energetics, oxygenation and perfusion during increased workload in patients with type 2 diabetes mellitus"**

2) Levelt E; Mahmod M ; Piechnik SK ; Ariga R ; Francis JM ; Rodgers CT; Clarke WT; Sabharwal N ; Schneider JE; Karamitsos TD ; Clarke K ; Rider OJ ; Neubauer S **"Relationship between Left Ventricular Structural and Metabolic Remodelling in Type 2 Diabetes Mellitus"**

3) Upton R; Levelt E; Ariga R; Mahmod M; Brophy C; Mangual J; Sellwood J; Pedrizzetti G; Clarke K; Neubauer S; Leeson P. **"Myocardial and Fluid Mechanics by Echocardiography detect subclinical Chnages in Type 2 Diabetes Mellitus."**

Manuscripts undergoing internal review process

1) Levelt E; Pavlides M; Mahmod M; Kelly C; Sellwood J; Thomas S; Francis JM; Schneider J; Rodgers CT; Clarke WT; Sabharwal N; Clarke K ; Antoniades C, Rider OJ; Neubauer S **"The Influence of Adiposity on Ectopic Lipid Deposition, Non-alcoholic Fatty Liver Disease and Cardiac Dysfunction in Type 2 Diabetes"**

2) Levelt, E; Piechnick SK; Mahmod M; Liu A; Ariga R; Francis JM; Robson MD; Clarke K; Neubauer S; Ferreira V; Karamitsos TD. **"Novel CMR technique for assessment of microvascular function in Type 2 Diabetes"**

3) Levelt Eylem; Clarke William T; Liu Alexander ; Stoll Victoria; Francis Jane M; Robson Matthew D; Clarke Kieran; Neubauer Stefan; Rodgers Christopher T. "**7T versus 3T ^{31}Phosphorus Magnetic Resonance Spectroscopy in Patients with Type 2 Diabetes Mellitus"**

Chapter 1
Introduction

1.1 Diabetes and Heart Disease

Recognized since the time of Aristotle, Diabetes Mellitus (DM) represents a serious disruption of fuel homeostasis with ravaging consequences throughout the body. The heart is a special target in patients with diabetes, with increased cardiovascular mortality among diabetes sufferers[1]. The synergy between coronary artery disease (CAD), hypertension and diabetes is clearly demonstrated by observations from the large studies of diabetic patients[2-4]. However, ventricular dysfunction has been identified also in patients with DM even in the absence CAD and hypertension, due to diabetic cardiomyopathy[5]. Large epidemiological studies support the existence of a diabetic cardiomyopathy in humans[1, 6]. The Framingham study demonstrated increased incidence of heart failure in both diabetic males (2.4:1) and females (5:1)[1]. The challenges in demonstrating a causal link between diabetes and heart failure, however, remain formidable. Inferred evidence for a diabetic cardiomyopathy in humans rests on a number of structural, functional, and metabolic observations.

The structural alterations in DM include, on the macroscopic level, as demonstrated by large screening databases, concentric left ventricular (LV) hypertrophy[1, 7, 8], concentric LV remodelling and increased heart mass, with mildly reduced left ventricular systolic performance[9]. On the microscopic level, histological studies demonstrate that diabetes is associated with myocyte hypertrophy, perivascular fibrosis, and increased quantities of matrix collagen, cellular triglyceride, and cell membrane lipid[10]. The diabetic heart becomes metabolically remodelled as a consequence of exposure to abnormal circulating substrates

and hormones. Early studies on substrate metabolism of the human heart have revealed that glucose uptake is decreased, whereas free fatty acid (FFA) uptake is increased by the heart of patients with diabetes[11, 12]. These structural and functional changes may be related to the nonenzymatic glycation of vascular and membrane proteins, increased cellular fatty acid uptake, and hyperglycemia-induced oxidative stress, which are characteristic of the diabetes state[11, 12]. The metabolic phenotype of diabetic heart disease is characterized by impaired myocardial energetics[13, 14] as indicated by reduced phosphocreatine to ATP (PCr/ATP) ratio and cardiac steatosis[13, 14] as a consequence of lipid accumulation assessed by ^{31}Phosphorus-Magnetic Resonance Spectroscopy and Proton (^{1}H)-Magnetic Resonance Spectroscopy, respectively[15, 16]. **Table 1.1** illustrates details of these early magnetic resonance spectroscopy studies.

Table 1.1: Magnetic Resonance Spectroscopy (MRS) Studies of Diabetes

Group	Year of Publication	Technique	Main Findings	Limitations
Scheuermann-Freestone et al. (21-T2DM patients and healthy controls)	2003	^{31}P-MRS Echocardiography characterisation of the cardiac function	1)Reduced resting myocardial PCr/ATP 2) Faster PCr/ATP reduction of the skeletal muscle with exercise 3) The negative correlation between myocardial PCr/ATP and plasma free fatty acids led to authors conclusion that impaired myocardial energy metabolism related to changes in circulating metabolic substrates.	1)No anatomical or functional assessment of ischemic heart disease 2)Cardiac volumes and function assessed by Echocardiography 3)Small sample size
Shivu et al. (25-T1DM patients and 26 healthy controls)	2010	^{31}P-MRS CMR First Pass Perfusion	1)Reduced myocardial PCr/ATP in young Type 1 DM patients 2) Impaired myocardial perfusion reserve index 3)impaired rest myocardial energetics irrespective of the duration of diabetes and MPRI	1)No anatomical assessment of ischemic heart disease 2)Small sample size for comparison of the newly diagnosed to longer-term diabetes patients data
McGavock et al. (Lean and obese controls, patients with impaired glucose tolerance and uncomplicated T2DM on mixture of antidiabetic treatment including Insulin, all stopped oral antidiabetics and eventually received 2 weeks of Insulin prior to the scans)	2007	^{1}H-MRS CMR	1) A stepwise increase in myocardial triglyceride levels from lean controls to patients with T2DM across the 4 study groups 2) IGT is accompanied by cardiac steatosis, thus showing cardiac steatosis to be an early manifestation of the disease pathogenesis 3)No association between the diastolic dysfunction(early diastolic peak filling rate assessed by CMR) and myocardial lipids	1)Subjects with IGT and those with T2DM were a decade older than the lean and obese controls, potentially confounding the results by age 2)T2DM patients received Insulin treatment, which is a lipogenic agent 3)No anatomical or functional assessment of ischemic heart disease
Rijzewijk et al (38 uncomplicated T2DM patients and 28 healthy volunteers)	2008	^{1}H-MRS CMR Dobutamine stress Echocardiography	1) Elevated myocardial triglyceride content in T2DM patients 2)Impaired diastolic function in T2DM patients 3)Myocardial lipids independently associated with E/A ratio	1)No anatomical assessment of ischemic heart disease 2)Small sample size

CMR indicates cardiac magnetic resonance; E/A, ratio of early peak filling rate to maximal left ventricular atrial peak filling rate; IGT, impaired glucose tolerance; MPRI, myocardial perfusion reserve index; ^{31}P-MRS, 31-Phosp horus Magnetic Resonance Spectroscopy; PCr/ATP, phosphocreatine to ATP ratio, T1DM, type 1 diabetes mellitus; T2DM type 2 diabetes mellitus.

Macroscopic structural changes such as left ventricular (LV) hypertrophy and interstitial fibrosis have been assessed by many studies. Increased LV mass was shown to occur independently of arterial blood pressure in type 2 diabetes mellitus (T2DM)[17]. As illustrated in **Table 1.2** several epidemiologic studies have suggested that there is a consistent association between diabetes and the presence of cardiac hypertrophy and myocardial stiffness independently of hypertension. The Framingham study investigators used echocardiography and reported a significant increase in LV wall thickness in women with diabetes[17] and in a further follow-up study, they showed that women with diabetes have a more pronounced increase in LV mass with advancing age compared to men[18]. Strong Heart Study showed that both men and women with diabetes had greater LV mass and wall thickness[19].

Table 1.2: Large Population Based Studies Assessing Structural and Functional Changes in Diabetic Heart Disease

Group	Year of Publication	Technique	Main Findings	DM Population Size
Galderisi et al. Framingham Heart Study	1991	Echocardiography	Increase in LV mass in women	111
Lee et al. Cardiovascular Health Study	1997	Echocardiography	Increase in LV mass in both genders	2697
Deveraux et al. Strong Heart Study	2000	Echocardiography	Increase in LV mass in both genders, reduction in Fractional shortening	1810
Palmieri et al. HyperGEN Study	2001	Echocardiography	Increase in LV mass in both genders and increase in relative wall thickness and reduction in Fractional shortening	386
Liu et al. Strong Heart Study	2001	Echocardiography	Progressive reduction of E/A ratio and prolongation of DT in DM and DM + HTN	616 DM 671 DM and Hypertension
Rutter et al. Framingham Heart Study	2003	Echocardiography	Progressive increase of LVM, RWT, and LA	186 DM
Turkbey et al. The Multi-Ethnic Study of Atherosclerosis (MESA)	2010	CMR	Obesity was associated with concentric LV remodeling without change in ejection fraction	272 DM>5000 participants with cardiovascular risk factors
Rosen et al. The Multi-Ethnic Study of Atherosclerosis (MESA)	2005	CMR	Concentric LV remodeling related to decreased peak systolic circumferential strain.	272 DM >5000 participants with cardiovascular risk factors

CMR indicates cardiac magnetic resonance; E/A, ratio of early peak filling rate to maximal left ventricular atrial peak filling rate; IGT, impaired glucose tolerance; DM , diabetes mellitus.

Functional changes in diabetic heart disease in humans are often characterized by diastolic dysfunction, with impairment of relaxation and passive filling of the LV, which may precede the development of systolic dysfunction[20-23]. In patients with well-controlled T2DM, the prevalence of diastolic dysfunction was shown to be up to 30% using echocardiography[21, 22]. The use of echocardiography tissue Doppler techniques suggests an even greater prevalence of diastolic dysfunction (up to 75%) among DM patients [24].

In diabetic cardiomyopathy with reduced LV ejection fraction, myocardial collagen deposition and advanced glycation end products **(**AGEs), which are proteins or lipids that become glycated after exposure to sugars, are thought to be among the primary pathological processes responsible for reduced elasticity of the myocardium in patients with diabetes[25]. Furthermore, in patients with T2DM, lipid vacuole infiltration has been shown to dissemble the myocardial contractile apparatus mechanically, leading to contractile dysfunction, and this may be an additional mechanism responsible[26]. Additionally, DM is associated with myocyte cell death; however, it is unclear whether diabetes can directly activate cell death or, rather, it activates pathways known to induce this process. Activation of the renin-angiotensin-aldosterone system was shown to be associated with increased oxidative stress and cardiomyocyte and endothelial cell death in diabetic hearts.

Follow-up study of 1021 middle-aged individuals with T2DM with normal renal function and free of clinical coronary artery disease or heart failure at baseline showed a total of 106

(10.1%) participants had experienced heart failure events during the 9-year follow-up[27]. The same study showed a 2.5-fold higher risk of developing heart failure in patients with retinopathy after controlling for confounding factors (age, sex, race, smoking, diabetes duration, insulin use, blood pressure, and lipid profile). This suggests the notion that, retinopathy reflecting small vessel disease seen in the retina may represent widespread systemic microcirculation disease, and lead to increased load to the heart and compromised cardiac performance (e.g., impair ventricular emptying and contractility) and may manifest as heart failure[27]; microvascular dysfunction in diabetes may play a role in diabetic cardiomyopathy.

Importantly, these structural, functional and metabolic changes were all shown to be predictors of mortality[7, 8, 28] and linked to contractile dysfunction[17, 18, 16].

1.2 Myocardial High Energy Phosphate Metabolism

The heart is an energy expensive organ. The myocardium consumes more adenosine triphosphate (ATP) than any other organ per gram of tissue. When the human heart only contains less than 1 gram of ATP, it uses up to 6 kilograms ATP a day on average to do its work[29]. Maintenance of adequate levels of cardiac high-energy phosphate metabolites, ATP, the energy source for contraction, and phosphocreatine (PCr), the major energy storage compound, are of vital importance for normal heart function. Thus it is tempting to

speculate that derangements in cardiac energetics can contribute significantly to disease aetiology and progression, even though it has not yet been established whether there is a causal relationship between energy starvation and contractile dysfunction. Supporting this, abnormal resting cardiac energetics has been shown to be a common feature of many cardiovascular pathologies including diabetic heart disease[13, 14], hypertrophic cardiomyopathy[30 31 32, 33], non-ischaemic heart failure[34 35 28], ischaemic heart disease[36,37], hypertension[38, 39] and valvular disease[40,36].

In the healthy heart, despite limited capacity to store ATP, cardiac pump work can be increased up to threefold[41]. The healthy myocardium has rapid response mechanisms to deal with acute changes in energy demand, providing a large metabolic reserve[41]. These mechanisms include increased contribution of carbohydrates for energy production through glycogenolysis,[42] increased glucose uptake and glycolysis,[43] and increased rates of phosphotransferase reactions.[44]

There are four major factors necessary for effective cardiac metabolism (Figure 1.1).

1. Adequate perfusion: A healthy myocardial blood supply with an appropriate hyperemic response during exercise is necessary to deliver both substrate and oxygen under resting and exercise condition.
2. Substrate utilisation: This involves uptake of mainly free fatty acids and glucose and their subsequent breakdown via beta oxidation and glycolysis. These processes result in the formation of acetyl coenzyme A (CoA), which is fed into the Krebs cycle and produces NADH and carbon dioxide (CO_2).

3. Energy production: High energy phosphate bonds are made in the form of ATP via a series of electron transfers in the mitochondria. Respiratory-chain complexes I through IV transfer electrons from NADH to oxygen, thereby creating a proton electrochemical gradient across the inner mitochondrial membrane as well as NAD and water. This gradient drives ATP synthase, which produces ATP by phosphorylating ADP (adenosine diphosphate). Uncoupling proteins cause mitochondria to produce heat rather than ATP.
4. Energy transfer and utilisation: The heart's energy transfer mechanism is the creatine kinase energy shuttle. Mitochondrial creatine kinase catalyzes the transfer of the high energy phosphate bond in ATP to creatine to form PCr. This molecule is smaller and less polar and hence diffuses out of the mitochondria into the cytoplasm. At the site of energy usage, mainly at the sarcomere and for ion pump function, ATP is reformed in the reverse reaction. Creatine, which is not produced in the heart, is taken up by the creatine transporter.

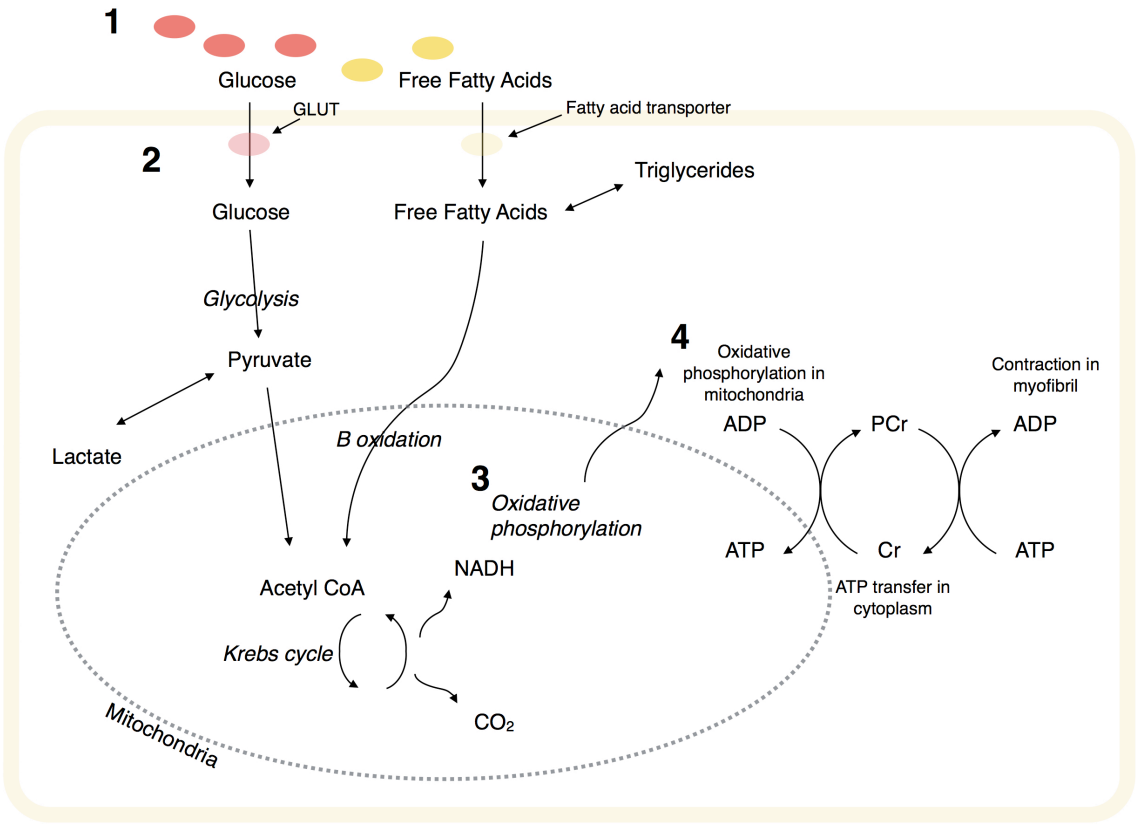

Figure 1.1: *Cardiac Energy Metabolism. Energy metabolism in the heart has four components: 1. Adequate blood supply; 2. Substrate utilisation; 3. Oxidative phosphorylation; 4. Energy transfer and utilisation. GLUT denotes glucose transporter, PCr phosphocreatine, Cr free creatine (E. Levelt DPhil Thesis).*

1.2.1 High Energy Phosphate Metabolism and Coronary Microvascular Function in Diabetes

Deranged cardiac energy metabolism has been implicated in both type 1[14] and type 2 DM[13]. Adding to the complexity of diabetic heart disease, myocardial energy depletion in patients with diabetes is a multifactorial phenomenon, related to limitations in uptake and utilisation of substrates,[10, 45] mitochondrial dysfunction[46] and impaired energy transfer from mitochondria to myofibrils.[47]

Diabetes mellitus is characterized by reduced glucose and lactate metabolism and increased FA metabolism.[48, 49] and metabolic inflexibility in substrate selection[10]. Increased FFA usage, and wasteful cycling of FFAs through intramyocardial lipolysis and esterification, result in energetic impairment[13, 50, 51].

A healthy myocardial blood supply with an appropriate hyperaemic response during exercise is necessary to deliver both substrate and oxygen under resting and exercise conditions. However, diabetic cardiomyopathy is characterized by microvascular disease resulting in a failure to increment the myocardial blood flow during acute increases in cardiac workload[14, 52-54]. Thus, abnormal energetics may be compounded by the microvascular dysfunction which occurs in DM with possible resultant tissue hypoxia. Microvascular dysfunction in DM has been extensively investigated using many modalities including MRI[14, 23, 52, 53] and positron emission tomography (PET)[55]. Ischaemia has been assumed as a result of perfusion deficits.

Myocardial hypoperfusion, in the absence of coronary disease, is a common feature of cardiomyopathies[56]. Microvascular dysfunction in diabetes is a multifactorial phenomenon, related to changes in perivascular and interstitial fibrosis[57], myocardial hypertrophy[58], reduced capillary density, and autonomic neuropathy[59]. The prognostic role of the myocardial perfusion reserve in diabetes has been described[60], but its role in the development of diabetic cardiomyopathy is not fully understood. Furthermore, myocardial hypoperfusion in diabetic heart might be severe enough to cause myocardial

deoxygenation. If proven this may be an important pathophysiologic trigger for diabetic cardiomyopathy.

1.3 Measuring cardiac energy metabolism

ATP is used for most energy consuming reactions in the heart, including contraction of cardiac myofilaments (70%) and for active pump function and calcium uptake via sarco/endoplasmic reticulum Ca^{2+}-ATPase (SERCA). Myocardial levels of ATP are kept relatively constant over a wide range of cardiac loads in the normal heart, buffered by the transfer of energy from PCr. The equilibrium constant of this creatine kinase reaction favors the synthesis of ATP over PCr by a factor of approximately 100. Hence, in disease states with inefficient energy production or energy utilisation, the ATP levels would initially remain constant at the expense of PCr; the ratio of PCr/ATP is therefore a sensitive indicator of the underlying energetic state of the heart.

Because the phosphoryl bond is so labile, obtaining reliable measures of the concentrations of ATP and PCr in tissue is a major challenge. Measurement of PCr and ATP content in myocardial biopsies is problematic as it is invasive and these molecules are unstable when analysed with wet chemical techniques.

Cardiac ^{31}P MRS is the only technique that allows non-invasive measurement of cardiac high-energy phosphate metabolism in vivo. The first publication in 1980 on *in vivo*

spectroscopy on rat hearts[61] paved the way for this non-invasive technique to be applied to the human heart[62]. The technique is now an established method used for investigating cardiac energetics and its response to treatment.

1.4 Ectopic adiposity and cardiovascular disease

The prevalence of T2DM continues to increase and is driven in part by the accompanying obesity epidemic. Adiposity is likely to be a strong contributor to non-ischemic cardiomyopathy in patients with diabetes[63]. Ectopic fat is defined by excess adipose tissue in locations not associated with adipose tissue storage by convention (e.g., the visceral cavity, intramuscular compartments, and the epicardial region). Accumulating evidence suggests that ectopic/visceral adiposity, confers a much higher cardiovascular risk than subcutaneous adiposity[64-66] and this may also play a role in the pathogenesis of non-ischemic cardiovascular diseases associated with diabetes and obesity[67]. Ectopic adiposity or 'acquired lipodystrophy' is linked to insulin resistance and diabetes. Insulin resistance may be responsible for the increased cardiovascular risk that is linked to ectopic adiposity. It has been clearly demonstrated that the degree of lipid infiltration into skeletal muscle and liver strongly correlates with insulin resistance[68-70].

Two hypotheses attempt to explain the link between ectopic adiposity, insulin resistance and cardiovascular risk. The first hypothesis, the 'ectopic fat storage syndrome', states that if fat mass cannot expand through the proliferation and differentiation of new adipocytes in

times of excess nutrient intake, then adipocyte hypertrophy results and excess dietary fat may be shunted to the liver, skeletal muscle and the beta cell. Importantly, if fat oxidation cannot be increased to compensate for the increased influx of lipid within these tissues, then intracellular accumulation of lipids will occur. A second paradigm, the 'endocrine hypothesis', is based on the growing number of factors that are released from adipocytes, with potent effects on metabolism and insulin sensitivity. This hypothesis no longer views the adipose tissue as a site of only energy storage, but considers adipose tissue as an endocrine gland secreting a variety of endocrine hormones such as leptin, interleukin-6, angiotensin II, adiponectin and resistin, and taking part in the regulation of diverse biological functions.

The growing recognition of the ectopic fat depots as an emerging cardiovascular risk factor, has led to interest in the development of methods allowing for the quantification of the different adipose tissue depots. Multidetector computed tomography (MDCT), MRI, ultrasonography, and ^{1}H-MRS have all been used to quantify adipose tissue amount or lipid content within an organ and they have been used to examine the association of various fat depots with both systemic and local manifestations of disease[15, 16, 64, 71-73].

Ectopic adiposity may influence the heart by several mechanisms, such as accumulation of adipose tissue surrounding the heart and coronary arteries, or via lipid accumulation within cardiomyocytes. Adipose tissue surrounding the heart, epicardial fat, wraps the coronary arteries, and is therefore a subtype of the perivascular adipose tissue that surrounds blood vessels. The anticontractile and vasoactive properties of the perivascular adipose tissue, via

the secreted substances, such as adiponectin and the adipocyte-derived relaxing factor, has previously been demonstrated[74, 75]. Importantly however, it has been demonstrated that the anticontractile property of perivascular adipose tissue is abolished in the presence of insulin resistance with the development of obesity[74].

1.5 Aims of this research

This is a multi-parametric magnetic resonance imaging (MRI) study.

This work aims to investigate the rest and stress energetic and oxygenation profile of diabetic heart, as well as the impact on left ventricular function and geometry created by differences in ectopic lipid deposition.

The following were then explored:

1. The impairment in cardiac metabolic reserve may decrease the ability of the diabetic heart to adapt to acute stress and potentially limit contractile reserve. As a proof-of-principle study, this thesis examined whether cardiac energetics are further impaired during exercise in diabetic cardiomyopathy.

2. Microvascular dysfunction is a well-known component of diabetic cardiomyopathy. This thesis explores, for the first time, tissue oxygenation in the diabetic heart. The relationship between exercise energetics, stress perfusion reserve and tissue oxygenation during stress was interrogated. It was hypothesised that the intrinsic

metabolic deficit and microvascular dysfunction in diabetes, either alone or in combination, will reduce the ability of the diabetic myocardium to adapt to acute increases in workload and exacerbate the energetic derangement.

3. Ectopic lipid deposition is a cardiovascular risk factor, with a novel appreciation. The impact of cardiac and hepatic steatosis, as well as epicardial fat accumulation on left ventricular function and geometry created by differences in lean and obese diabetes patients were explored.

4. Broader applications of ^{31}P-MRS have not yet seen widespread acceptance as a consequence of the method's low intrinsic signal-to-noise ratio (SNR). Higher field strength application of the technique may overcome this limitation. This work has compared clinical applications of cardiac 31P-MRS at 7 Tesla field strength to 3 Tesla in patients with diabetes.

Chapter 2
General Methods

2.1 General Methods

This study was approved by the South West Exeter Research Ethics Committee (ref: 13/ SW/0257) and Oxford Central Ethics Committee (REC Ref: 12/SC/0397). Each participant gave written informed consent to be involved. Subjects were recruited from the Thames Valley Primary Care Trust GP Surgeries. Healthy volunteers were recruited for a separate study with similar protocol, which was approved by the London Research Ethics Committee (Ethics Ref: 12/LO/1979). Healthy volunteers were recruited via word of mouth and study posters advertised on John Radcliffe Hospital information boards.

2.2 Eligibility Criteria

Subjects were eligible for inclusion in the study if:

- Aged between 18 and above.
- Willing to participate in a research study on a voluntary basis.

Type 2 DM group:

- Volunteers with type 2 DM and no hypertension, willing and able to give informed consent for participation in the study.
- Male or Female, aged 18 years or above.
- Participants on one or two oral antidiabetic agents.

- Blood pressure measurement at screening revealing results of systolic blood pressure ≤140 mmHg, and diastolic blood pressure of ≤85 mmHg.
- Able to perform exercise testing.
- Able (in the investigator's opinion) and willing to comply with all study requirements.

Healthy volunteers:

- Willing and able to give informed consent for participation in the study.
- Male or Female, aged 18-90 years.
- Age-matched healthy volunteers with no known history of cardiac disease, hypertension or diabetes.
- Able to perform exercise testing.
- Able (in the investigator's opinion) and willing to comply with all study requirements.

Subjects were **excluded** if any of the following were present:

- Pregnancy, or lactating mothers.
- Contra-indications to magnetic resonance imaging (pacemaker, cranial aneurysm clips, metallic ocular foreign bodies, severe claustrophobia).
- Significant coronary artery disease evident on CT coronary angiography.

- Diagnosis or history of Type 1 DM.
- Atrial fibrillation.
- Presence of severe asthma (contraindication to adenosine).
- Known hypersensitivity to adenosine or gadolinium.
- Terminally ill patients.
- Participants with a diagnosis of significant (> moderate, diagnosed by their GP or a Cardiologist) valve disease.
- Patients who are on Insulin therapy.
- Any other significant disease or disorder which, in the opinion of the investigator, may either put the participant at risk because of participation in the study, or may influence the result of the study, or the participant's ability to participate.
- Patients who were diagnosed with hypertension previously, or blood pressure measurement at screening revealing systolic levels > 140 mmHg and diastolic levels of > 85mmHg.
- All research participants with estimated glomerular filtration rate (eGFR) < 30ml/min (stage 3-5 renal disease) were excluded from the study. Participants had a blood test to assess kidney function at the first screening visit.
- Unable to perform exercise testing.

- Involvement in other studies thought to compromise resulting study data or the health of the participant.

- Current smoker *OR* a history of smoking in the past 3 years.

2.3 Clinical assessments

On **Visit 1** all subjects underwent a clinical assessment. This included history for:

- The presence of exclusion criteria as documented above.
- Drug history including allergies.
- Weekly alcohol level (units).
- Diabetes history, including duration since the diagnosis, symptoms, presence of diabetic complications.

Cardiovascular Examination was also performed to assess for the presence of ventricular hypertrophy and valvular heart disease. The following measurements were carried out:

- 3 blood pressure measurements at rest 5 minutes apart using a manual sphygmomanometer.
- Height (cm) and weight (kg) using calibrated scales.
- Creatine check to measure glomerular filtration rate.

Visit 2 included CT Coronary Angiogram. This was carried out at the Radiology Department. > 50% coronary artery luminal stenosis has been used as an exclusion criterion. Calcium

score and coronary stenosis have been assessed and reported by the John Radcliffe Hospital Radiologists and Cardiologist involved with CT Coronary Angiograms.

Visit 3 included CMR and MRS scans. On the day of arrival all participants had:

- Blood pressure measurements using a manual sphygmomanometer.
- 12 lead electrocardiogram, (ECG).
- Height (cm) and weight (kg) using calibrated scales.
- Blood tests after an 8 hour fast for serum cholesterol (total cholesterol, low density lipoprotein and high density lipoprotein) glucose, HBA1c, insulin, free fatty acids, triglyceride and aminotransferase (ALT), bilirubin and albumin.

2.4 Scan Protocols

Subjects underwent a comprehensive CMR protocol which measured the following

(i) Myocardial ^{31}P MRS at rest and during leg exercise.

(ii) ^{1}H MRS of the liver and the heart.

(iii) T1 Mapping of the liver, T2 star imaging of the liver.

(iv) Cardiac mass and function.

(v) T1 mapping of the 3 short axis slices of the heart(base, mid and apex).

(vi) T2 weighted imaging of the mid short axis slice of the heart.

(vii) Myocardial tagging.

(viii) Rest and adenosine stress Blood oxygen level dependent imaging (BOLD) to access tissue oxygenation.

(ix) Rest and stress adenosine perfusion.

(x) Late gadolinium enhancement, (LGE) to assess patchy fibrosis.

(xi) Post contrast T1 mapping (15 minutes from the injection of the gadolinium).

All scanning was conducted on a Siemens 3T Trio MR system (Erlangen, Germany). Average scan time is ~150 minutes; **figure 2.1** shows the scan timeline.

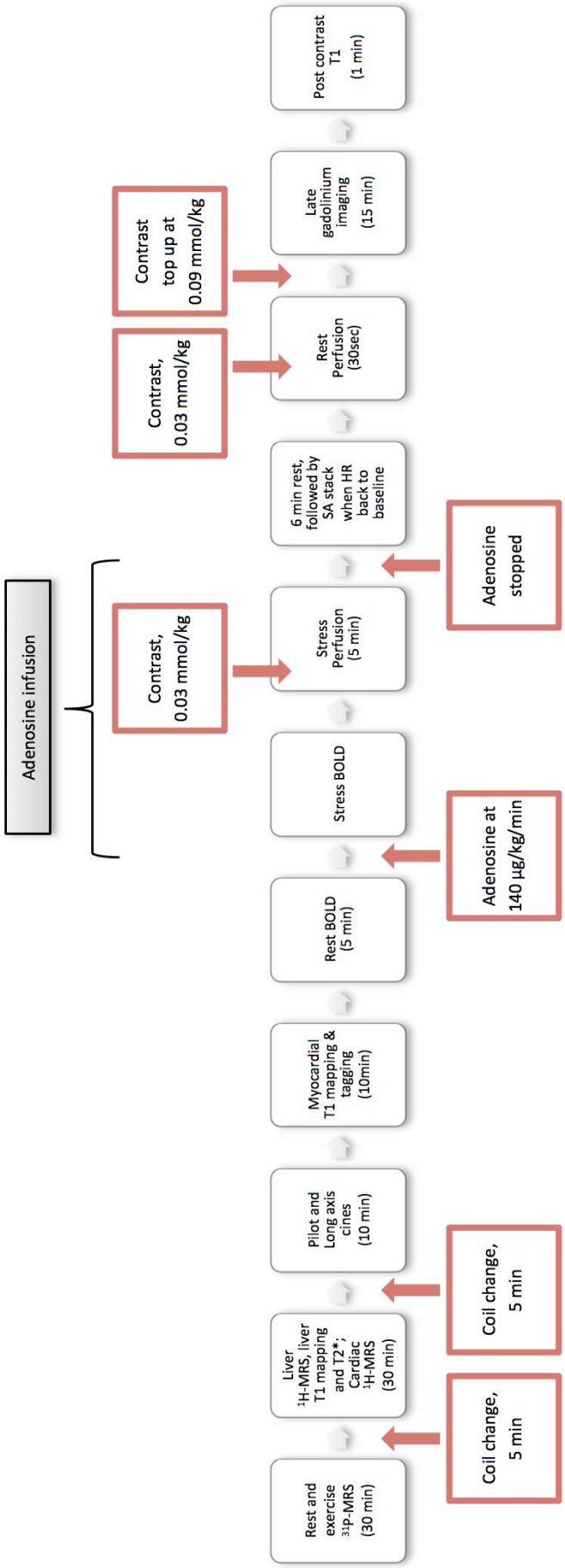

***Figure 2.1**: Timeline for the scan protocol*

2.4.1 Anthropometric Measurements

Height and weight were recorded and BMI calculated. Blood pressure was recorded as an average of 3 supine measures taken over 10 minutes (DINAMAP-1846-SX, Critikon Corp). Fasting venous blood was drawn for glucose, triglyceride, HBA1c, renal function and free fatty acids (FFA) tests as previously described[76]. Fasting insulin was also recorded in all diabetic patients. In agreement with the diabetes management guidelines[77] spot (random) urine sample albumin levels and the albumin: creatinine ratio was assessed in the majority of patients with T2DM (~69%, n = 32).

2.4.2 Coronary Computed Tomographic Angiography and Epicardial Fat Volume Assessment

An optional scan of coronary computed tomographic angiography (CCTA) was offered to diabetic patients to exclude obstructive coronary artery disease (> 50% of luminal stenosis) and for assessment of epicardial fat volumes. CT Coronary Angiography was performed with a GE VCT 64 slice scanner (GE Healthcare) and a Snapshot Pulse protocol with prospective ECG (electrocardiography) triggering. Participants received beta-blockade (intravenous Metoprolol) and sublingual GTN (if necessary and safe) prior to the scan to achieve a heart rate of < 65 beats per minute. During the CTCA acquisition, 70ml of iodinated contrast (Niopam 370, Bracco, UK) was injected at a rate of 6ml/sec followed by a 50ml saline flush. The scan was obtained 1-2 cm above the left main artery to 1-2 cm below the inferior myocardial apex in a single breath hold.

CT images were reconstructed using a medium-soft kernel (standard) with a slice thickness of 0.625mm and then transferred to a dedicated workstation for image processing, TeraRecon Aquarius iNtuition (version 4.4.11 TeraRecon Inc. San Mateo, CA). The adipose tissue volume was quantified using the contrast enhanced CT images. The layer of the epicardium was manually traced and using a semi-automated method a 3D image constructed. The volume was then calculated by a blinded operator (ST) and defined as the tissue with radiodensity -190 - -30 HU (Hounsfield Units).

2.4.3 ^{31}Phosphorus Magnetic Resonance Spectroscopy

3 Tesla and 7 Tesla spectroscopy protocol and analysis discussed in further detail in chapters 4 and 6.

2.4.4 Left ventricular function and mass

CMR was used for measuring left ventricular volumes and mass[78]. Cardiac volumes were acquired using Steady State Free Precession (SSFP) imaging. Pilot, horizontal long axis, vertical long axis and short axis stack images were acquired with the patient in the supine position. Each slice was 8 mm thick with a 3 mm gap and is prospectively gated with echo time, 1.5 ms; repetition time, 3 ms; flip angle, 50°. The slices were obtained during a breath-hold at the end of normal expiration to minimize the effects of respiratory motion.

LV short axis epicardial and endocardial borders were manually contoured at end diastole and end systole (figure 2.2), for determining end diastolic volume (EDV); end systolic volumes (ESV); stroke volume (SV) using cmr42© (Circle Cardiovascular Imaging Inc., Calgary, Canada). Ejection fraction (EF) and cardiac output (CO) were calculated (EF =

SV/EDV, CO = SV x heart rate. Myocardial mass was also calculated by subtracting the endocardial volume from the epicardial volume. Left ventricular mass was calculated based on prior knowledge of myocardial specific gravity (1.05 g/cm^3).

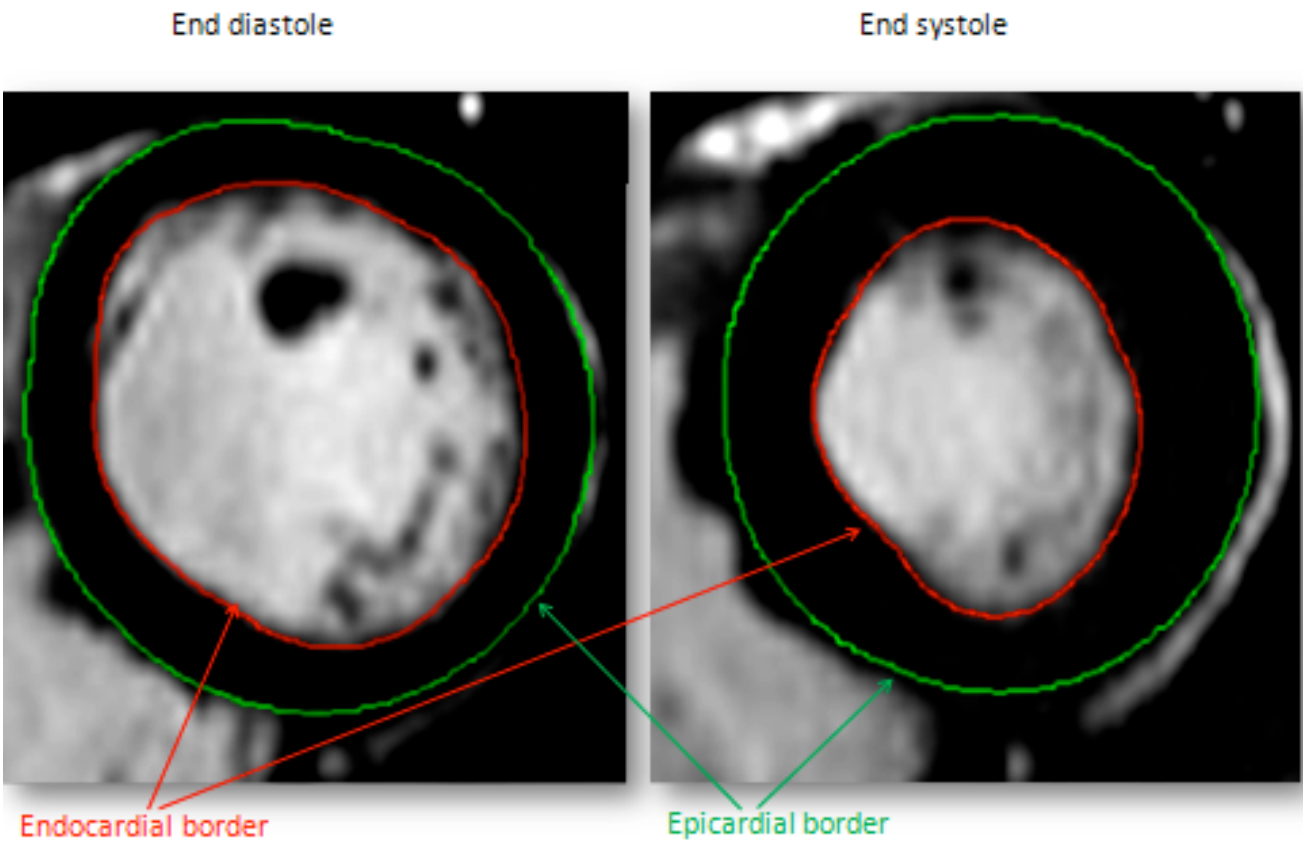

***Figure 2.2**: Epicardial and endocardial contours are drawn at end diastole and end systole.*

2.4.5 Strain Imaging

A gradient echo-based tagging pulse sequence was performed in the long-axis and in the short-axis slice, with a segmented k-space, multi-shot sequence (repetition time 4.47ms, echo time 7.4ms, and flip angle 25˚). Spatial modulation of magnetisation (SPAMM)[79]

produced images with a grid-based pattern of horizontally and vertically modulated 'stripes' 7mm apart, acquired during a single breath-hold, using a prospectively gated sequence. The temporal resolution (TR x no. of segments, 9) was 40.23 ms in all data sets, and 15-25 frames per cardiac cycle were recorded, depending on heart rate. Tagged images were analysed using Cim Tag2D version 7 (Auckland Medical Research, Auckland, New Zealand). Outcome parameters measured in this study were: global mid ventricular peak systolic circumferential strain, circumferential diastolic strain rate.

2.4.6 Blood Oxygenation Level Dependent (BOLD) CMR

BOLD-CMR was used for assessment of myocardial oxygenation response to Adenosine stress and it was performed at three levels: basal, mid ventricular and apical. Slices were acquired at mid-diastole using a T2-prepared ECG-gated SSFP sequence with the following parameters: repetition time/echo time, 2.86/1.43 ms; T2 preparation time, 40 ms; matrix, 168x192; field of view, 340x340 mm; slice thickness, 8 mm; and flip angle, 44°. Each BOLD image was obtained during a single breath-hold over 6 heart beats. Two images of the same slice were acquired at rest and during the infusion of adenosine (140 μg/kg/min, figure 2.3). The acquisition of stress BOLD images commenced at peak stress approximately 90 seconds after the initiation of adenosine infusion. If necessary, shimming and center frequency adjustments were performed before BOLD imaging to generate images free from off-resonance artefacts. Blood pressure was recorded at two minute intervals during the adenosine infusion.

For BOLD analysis, QMass software (version 6.2.3, Medis, Leiden, The Netherlands) was used. Myocardial signal intensity, (SI) was measured after manually tracing the endocardial and epicardial contours. Basal and midventricular short-axis BOLD images were divided into 6 segments (inferior septum, anterior septum, anterior, anterolateral, inferolateral, and inferior), and the apical BOLD slice was divided to 4 segments (septum, anterior, lateral and inferior) according to American Heart Association 17-segment model (excluding segment 17 – true apex). All three short axis slices were analyzed and the mean of the three were reported as the mean BOLD signal intensity change (SIΔ).

In this cardiac gated sequence, variations of heart-rate also affect the signal intensity due to its effect on T1 relaxation, and the following equation was used for correction:

$$S = S_0 \Big/ \left(1 - \beta e^{\frac{-T_R}{T_1}}\right)$$

with T1 = 1220 ms [80] and β = 0.59 (determined empirically for this sequence) where S_0 is the measured signal intensity, S is the corrected signal intensity and TR is the image dependent time between acquisitions of sections of k-space, governed by the heart rate. TR is replaced by the RR interval.

The relative corrected signal intensity change was calculated as follows:

$$SI\Delta\ (\%) = \frac{\text{Mean SI (stress)} - \text{mean SI (rest)}}{\text{Mean SI (rest)}} \times 100$$

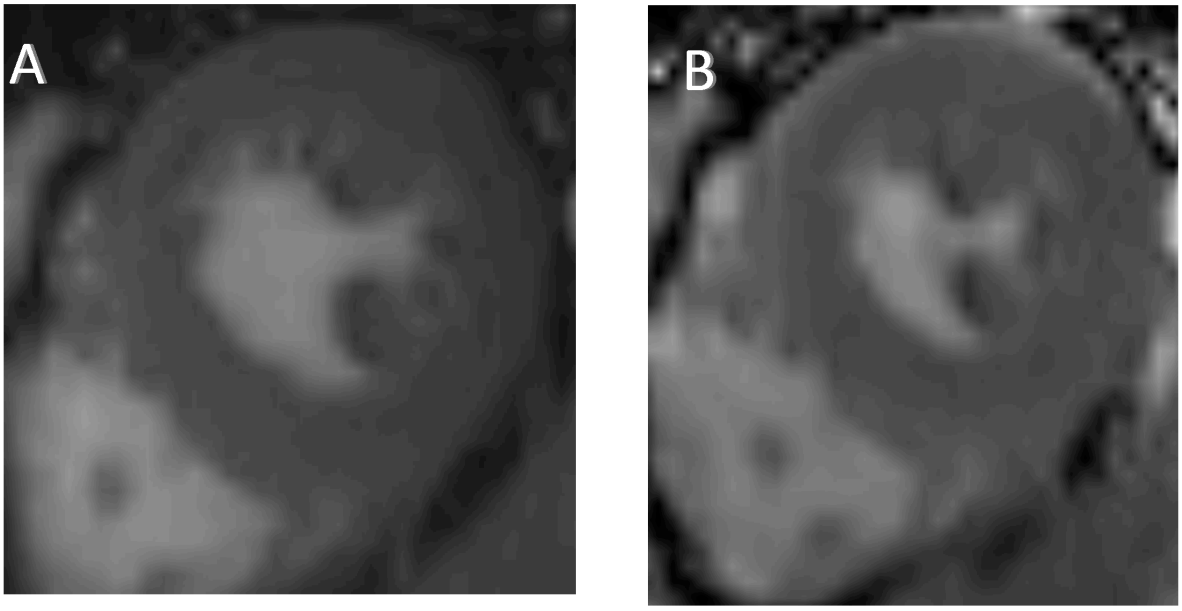

Figure 2.3: *BOLD image a) rest and b) Adenosine stress.*

2.4.7 Perfusion

Three short axis cine images (base, mid-ventricular and apical) were chosen from the short axis stack, identical to those of BOLD images, taking care to avoid the LV outflow in systole. Adenosine (140µg/kg/min) was infused through a large bore cannula in the ante-cubital fossa. Images were acquired at peak stress after commencement of adenosine. Heart rate and blood pressure are measured before, at two minute intervals during, and after adenosine stress. To assess regional perfusion, a bolus of intravenous magnetic resonance contrast agent (0.03mmol/kg body weight of Gadodiamide, Omniscan; GE Healthcare, Amersham, United Kingdom, injection rate, 6 mL/s) was administered, followed by a saline flush of 15 mL at the same rate at the end of the adenosine infusion. Stress perfusion was measured every heartbeat during the first pass using a T1 -weighted fast (spoiled) gradient echo sequence in the 3 short-axis imaging planes. Perfusion pulse sequence parameters

were as follows: repetition time (per image), 180 ms; echo time, 0.99 ms; matrix, 128x80; and slice thickness, 8 mm. All perfusion images were acquired in the 3 short-axis orientations only. Rest perfusion imaging was performed after 20 minutes and another dose of contrast (0.03mmol/kg body weight) was given (figure 2.4).

For perfusion analysis, cmr42 software (version 6.2.3, Medis, Leiden, and The Netherlands) was used. The epicardial and endocardial contours were traced. The basal and mid ventricular slices were divided into 6 equiangular segments and the apical slice into 4 segments (according to American Heart Association 17-segment model, excluding segment 17 – true apex). The signal intensity of the pixels before and during contrast injection was measured to generate signal intensity curves for each segment. The upslope or rate of change of signal intensity in the myocardium was then derived (i.e., the first derivative of the signal intensity curve)[81]. This rate of contrast enhancement in myocardial tissue was normalised to the rate of contrast enhancement in the LV cavity and the myocardial perfusion reserve index (MPRI) was then calculated by dividing the results at maximal vasodilation through the results at rest[82, 83]. MPRI is a semi-quantitative method and has been widely adapted for perfusion analysis[83]. Figure 2.5 illustrates signal intensity curves at rest and during adenosine stress of a patient with T2DM.

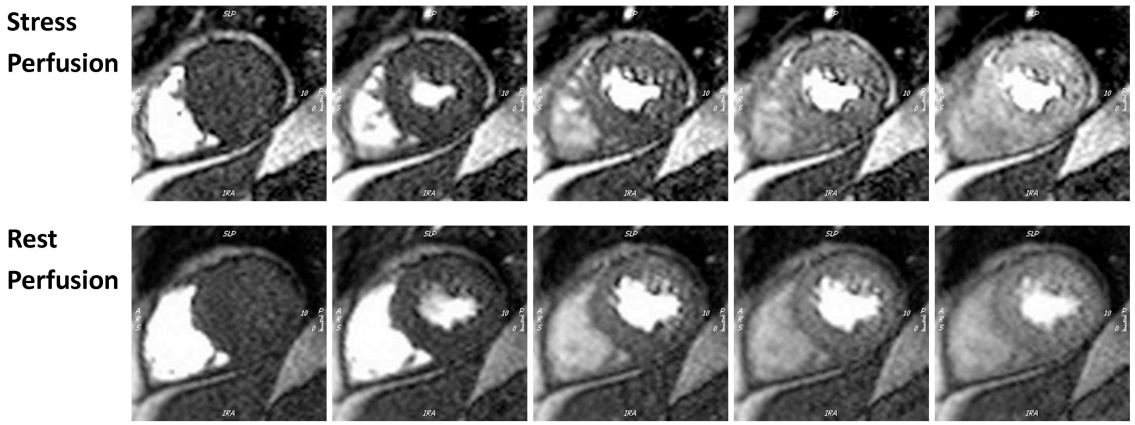

***Figure 2.4**: First pass myocardial CMR perfusion imaging. Series on top row show sequential perfusion images during adenosine stress and bottom row during rest perfusion imaging in a patient with T2DM. Initially contrast enters the right ventricle, then left ventricle and flushes through the myocardium.*

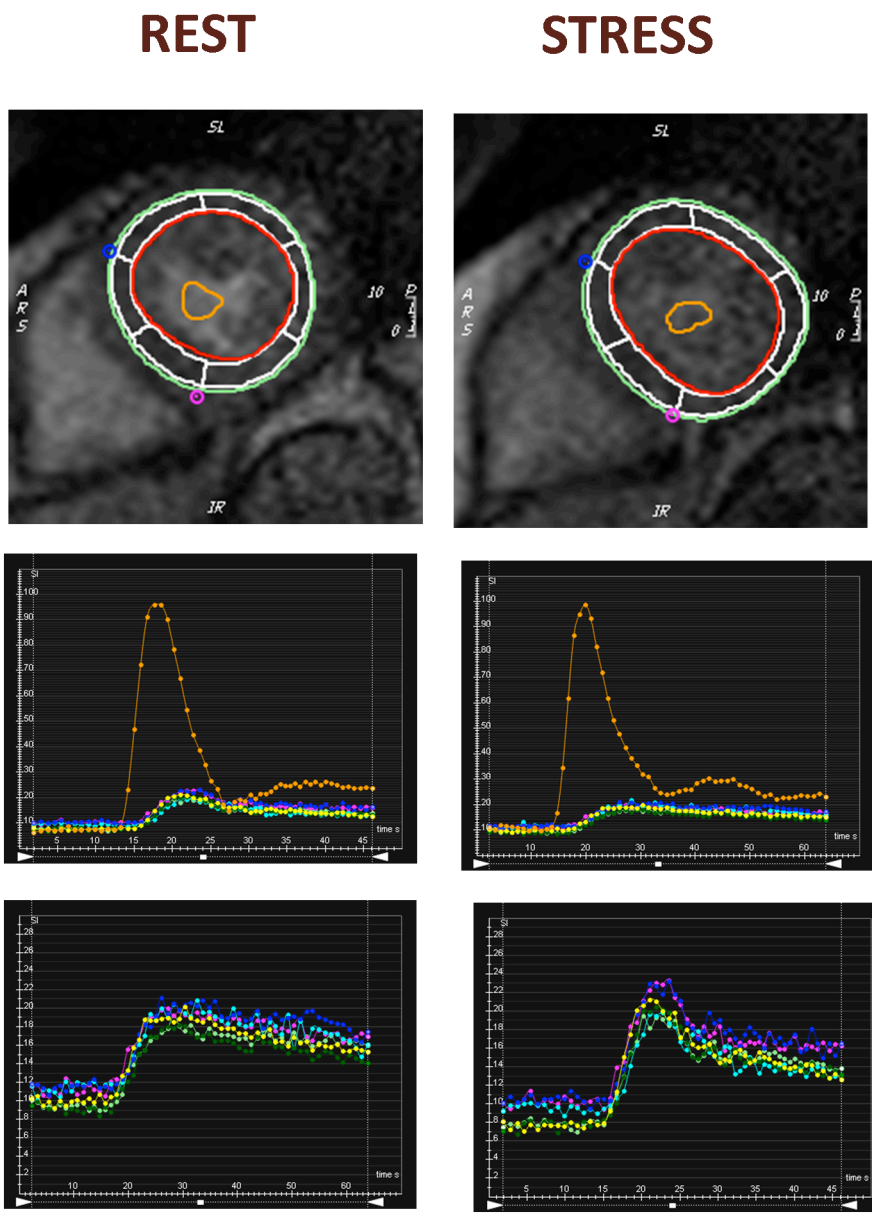

***Figure 2.5**: Myocardial intensity slope curves of a patient with T2DM at rest and during stress, middle row represents these slope curves with the blood pool included (yellow curve). Colours each represent a different LV segment.*

2.4.8 Late Gadolinium Enhancement

For late gadolinium enhancement (LGE) CMR, a top-up bolus of 0.06 mmol/kg of body weight of a gadolinium-based contrast agent (Gadodiamide, Omniscan; GE Healthcare, Amersham, United Kingdom) followed by a 10-mL saline flush were administered through an intravenous cannula inserted into the antecubital fossa. Electrocardiographically gated images were acquired after a 3 minute delay in long- and short-axis planes using a breath-hold T1 -weighted segmented inversion-recovery turbo fast low-angle shot sequence previously described[84]. The scan parameters used were: slice thickness 8 mm, flip angle 20°, Repetition time/ Echo time = 3 ms/7.5 ms.

Areas of LGE were visually scored as absent or present by consensus of 2 experienced operators.

Rest and stress BOLD, perfusion and LGE images were acquired on matching basal, midventricular and apical slices.

2.4.9 Shortened Modified Look-Locker Inversion (ShMOLLI) T1 Mapping

Shortened Modified Look-Locker Inversion recovery T1 maps were generated from the mid short-axis images with variable inversion preparation time.[85] Typical acquisition parameters were: echo time (TE)/repetition time (TR) = 1.07/2.14 ms, flip angle = 35°, field of view = 340×255 mm, matrix size = 192×144, 107 phase-encoding steps, interpolated pixel size = 0.9×0.9, GRAPPA = 2, 24 reference lines, cardiac delay time TD = 500 ms, 206 ms acquisition time for single image, phase partial Fourier 6/8. Shimming and center frequency

adjustments were performed to generate images free from off-resonance artefacts. For the analysis of ShMOLLI T1-maps, the LV myocardium of the short axis slice acquired at baseline was contoured using dedicated software, as previously described,[85] providing a single average myocardial T1 value per each individual.

Consistent with established methods of estimating myocardial extra cellular volume fraction (ECV) using a delayed postcontrast bolus protocol,[86] precontrast and postcontrast myocardial and blood T1 values were measured. Estimation of ECV and lambda (λ- partition coefficient) as indices of diffuse myocardial fibrosis, were based on multipoint regression,[87] incorporating all available precontrast and postcontrast points, in order to increase the robustness of the estimates by increasing the number of underlying data points. ECV was calculated as (1 – haematocrit). For calculation of postcontrast T1 values, a single mid-ventricular short axis slice was acquired for postcontrast T1 maps at 15 after the administration of contrast (Gd-DOTA).

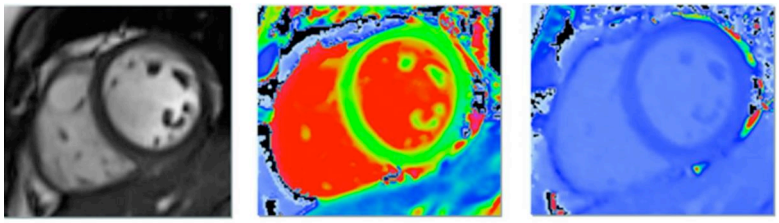

Figure 2.6: *Examples of a T1 map, post-contrast T1 map with a corresponding short axis cine image from a patient with T2DM.*

2.4.8 ^{1}H-Magnetic Resonance Spectroscopy

A rapid, proton magnetic resonance spectroscopy method was used to evaluate myocardial lipid levels in a single breath-hold at 3 T using a commercial whole-body system for the measurement of lipid (based on the specific resonance of methylene – CH_2) as a percentage of water signal in the same region of the myocardium. Technical challenges in the development of ^{1}H-MRS include low signal to noise ratio (SNR) due to low absolute metabolite concentrations, achieving adequate water suppression and long distances from the radio-frequency (RF) coils. Previous work has reported the intraobserver and interobserver variabilities in our center showing our reproducibility of ^{1}H MRS for measuring myocardial lipid levels in a short breath-hold was acceptable in five repeated measurements within the same subject and this was published previously[88]. Within-subject reproducibility of myocardial lipid levels over repeated ^{1}H-MRS measurements in a single breath-hold showed a coefficient of variation of 19%.

^{1}H-MRS was performed on a 3 T Siemens Tim Trio using the whole body coil and the 6-channel anterior and 24-channel posterior phased-array coils for signal receiving. Mid-ventricular long and SA cine were acquired to determine the trigger delay for mid-diastole. A calibration pulse sequence was implemented to evaluate the optimal water suppression pulse scaling factor. Cardiac gated spectra were acquired using different water correction scaling factors and the one yielding the most effective water-suppression was chosen. A 22x18x32mm stimulated echo acquisition mode (STEAM) voxel was planned on the corresponding cine frame. A water spectrum (3 averages; repetition time (TR) of at least 4

s) was acquired in a single breath-hold to use as internal reference. Next, five to six water-suppressed scans (5 averages each; TR of at least 2 s) were acquired at mid-diastole in a series of single breath-holds.

Individual coil signals were combined within Matlab using specifically written modules. The water-suppressed scans were constructively averaged, including frequency correction. Spectra were quantified using the Advanced Method of Accurate, Robust and Efficient Spectroscopic (AMARES) fitting algorithm. Metabolite peaks (including lipid/triglycerides) were analyzed and prior knowledge was used for all peak locations by using soft constraints. All peaks were fitted using Lorentzian lineshapes.[88] As ^{1}H-MRS analysis has no subjective element to it and is not operator dependent, inter-observer and intra-observer variability tests were not performed.

To obtain hepatic ^{1}H-MRS, an 8-ml voxel (2x2x2) was positioned in the liver, avoiding gross vascular, biliary structures and adipose tissue depots. Both spectra with and without water suppression were obtained to calculate hepatic triglyceride content as a percentage relative to water (triglyceride/water x100).

2.4.9 Statistical Analysis

All statistical analysis was performed with commercially available software packages (IBM SPSS Statistics, version 20). All data were checked for normality using Kolmogorov–Smirnov test and presented as mean ± standard deviations, and median (interquartile range) as appropriate. Normally distributed data sets were analysed with the independent Student *t* test. The chi-square test was used to compare discrete data as appropriate.

Bivariate correlations were performed using Pearson's or Spearman's method as appropriate. To assess the associations concentric remodelling and metabolic parameters, linear regression across all subjects was performed. Linearity was assessed visually. Variables with $P < 0.05$, and the strongest relationship with concentric remodelling were then included in multiple linear regression models by a stepwise selection method to assess the "best" subset in predicting cardiovascular remodelling. Non significance was assumed at $P > 0.05$.

Chapter 3

Relationship between Left Ventricular Structural and Metabolic Remodelling in Type 2 Diabetes Mellitus

3.1 Abstract

Aims

Concentric left ventricular (LV) remodelling is associated with adverse cardiovascular events and is frequently observed in patients with type 2 diabetes mellitus (T2DM). The cause of concentric remodelling, in diabetes per se, is unclear, but may well be related to cardiac steatosis and impaired energetics. As a result, the relationship between myocardial metabolic changes in T2DM and LV geometric remodelling was investigated.

Research Design and Methods

46 patients with T2DM (mean age 55 ± 9 years, body mass index (BMI) 29.6 ± 5.7 kg/m^2), mean HBA1c 7.5 ± 1.2%, and 20 matched controls (mean age 54 ± 10 years, BMI 28.6 ± 2.8 kg/m^2) underwent cardiovascular magnetic resonance to assess concentric LV remodelling (LV mass: end-diastolic volume ratio, LVMVR), function, tissue characterisation, ^{1}H- ,^{31}P MRS for myocardial triglyceride (MTG) and PCr/ATP respectively.

Results

When compared to BMI and BP matched controls, diabetes, even in the absence of hypertension (average BP 129/76 mmHg) was associated with: concentric remodelling (LVMVR 0.98 ± 0.16 vs 0.74 ± 0.14, P < 0.001), two-fold higher MTG (1.13 ± 0.78 vs 0.64 ± 0.52, P = 0.017), impaired myocardial energetics (PCr/ATP, 1.69 ± 0.29 vs 2.05 ± 0.34; P < 0.001), impaired systolic strain (14.5 ± 3.5% vs 18.3 ± 2.6%, P < 0.001) and no evidence of fibrosis. LVMVR showed a positive correlation with MTG (R = 0.41, P = 0.003) and negative

correlation with PCr/ATP (R = -0.30, P = 0.02). Importantly, cardiac steatosis independently predicted concentric remodelling (β = 0.473, P = 0.001) and systolic strain (β = -0.400, P = 0.003).

Conclusions

Concentric LV remodelling in diabetes may be explained by increased MTG. As cardiac steatosis is modifiable, strategies aimed at reducing MTG may be beneficial in reducing concentric remodelling.

3.2 Introduction

Diabetes mellitus (DM) is associated with an increased risk of both heart failure[6] and cardiovascular mortality[1]. The reasons for this, in the absence of coronary artery disease (CAD), are not clear, but one candidate mechanism that has emerged is concentric LV hypertrophy, which is frequently observed in patients with type 2 diabetes mellitus (T2DM)[9, 89] and is a strong predictor of adverse cardiovascular events[8] preceding the development of clinical heart failure[90].

The precise underlying mechanism of concentric LV remodelling in patients with DM, in the absence of significant arterial hypertension, remains unclear. One potential driver of LV concentric remodelling in patients with T2DM is cardiac steatosis, where excess myocyte accumulation of triglyceride leads to hypertrophic signaling[91, 92]. The link between lipotoxicity and concentric LV remodelling has been demonstrated in animal models of excess lipid accumulation[7, 93] and within humans with generalised lipodystrophy[94] who exhibit severe concentric LVH and significant cardiac steatosis. Proton (^{1}H) magnetic resonance spectroscopy (MRS) allows the non-invasive measurement of cardiac TG content, and in patients with T2DM, cardiac steatosis has been shown to be a prominent and early feature of obesity[95] and diabetic cardiomyopathy[15].

In addition, impaired myocardial high energy phosphate metabolism is another prominent feature of the diabetic cardiomyopathy[13]. ^{31}Phosphorus magnetic resonance spectroscopy (^{31}P-MRS) allows cardiac energetics to be measured non-invasively. Whether a relationship between concentric LV remodelling and reduced myocardial energetics exists in T2DM is

unknown, but given the link between PCr/ATP ratio and mortality[28], this is worthy of investigation.

Interstitial fibrosis has also been implicated in the pathogenesis of LV hypertrophy [96] and has been identified in the more advanced stages of diabetic cardiomyopathy[5]. The role of interstitial fibrosis in the pathogenesis of LVH in stable/early diabetic cardiomyopathy is much less clear as abnormal myocyte hypertrophy rather than fibrosis appears to predominate in the early stages[97]. Cardiac magnetic resonance (CMR) T1 mapping for extracellular volume (ECV) quantification allows non-invasive quantification of interstitial fibrosis[86], which was shown to correlate well with collagen proportion on histology[98].

A combination of CMR imaging with ^{1}H-MRS and ^{31}P-MRS has therefore been used to assess the relationship between LV concentric remodelling, cardiac fibrosis, steatosis and myocardial energetics in T2DM, and the results were compared to non-diabetic age, body mass index (BMI) and blood pressure matched controls, with similar LV ejection fraction.

3.3 Methods

Study Protocol

Forty-six patients with T2DM and twenty controls were recruited. All recruits fulfilled the inclusion and exclusion criteria described in chapter 2.

All study subjects underwent CMR scanning at 3 T as follows:

1. ^{31}P-MRS to assess PCr/ATP as a measure of myocardial energetic status at rest.

2. ^{1}H-MRS to quantify myocardial steatosis.

3. Cine imaging to measure LV function, mass and volume.

4. Tagging CMR to assess LV strain.

5. ShMOLLI T1 mapping to assess tissue characterization.

6. Late gadolinium enhancement to exclude scarring and evaluate interstitial fibrosis.

3.3 Statistics

All statistical analysis was performed with commercially available software packages (IBM SPSS Statistics, version 20). All data were checked for normality using Kolmogorov–Smirnov test and presented as mean ± standard deviations, and median (interquartile range) as appropriate. Normally distributed data sets were analysed with the independent Student *t* test. The chi-square test was used to compare discrete data between patients with T2DM and controls, as appropriate. Bivariate correlations were performed using Pearson's or Spearman's method as appropriate. To assess the associations concentric remodelling and metabolic parameters, linear regression across all subjects was performed. Variables with $P < 0.05$, and the strongest relationship with concentric remodelling were then included in multiple linear regression models by a stepwise selection method to assess the "best" subset in predicting cardiovascular remodelling. Non significance was assumed at $P > 0.05$.

3.4 Results

Subject Characteristics

Study population

Forty-six patients (24 male, mean age 55 ± 9 years, body mass index (BMI) 29.6 ± 5.7 kg/m^2) with T2DM, median diabetes duration 7 years [IQR: 1-8] and mean HBA1c of 7.5 ± 1.2%, and twenty controls (9 male, mean age 54 ± 10 years, BMI 28.6 ± 2.8 kg/m^2) were studied.Patients were of similar age, gender, weight and blood pressure with controls. As expected, diabetes was associated with higher fasting blood glucose, HBA1c, free fatty acids (FFA), triglyceride levels and lower high-density lipoprotein cholesterol. About 74% of the diabetic patients were on statin therapy hence the lower total cholesterol and low-density lipoprotein cholesterol levels were detected in patients compared to controls. Urine albumin: creatinine ratio and urine albumin results were within normal limits, but only assessed in 32 patients due to urine sample unavailability in the remaining patients.

Demographic, clinical, and biochemical data are shown in **Table 3.1**.

Table 3.1: Clinical, Biochemical Characteristics

Variable	Controls N = 20	Type 2 DM patients N = 46	P value
Age, y	54 ± 10	55 ± 9	0.583
BMI, kg/m^2	28.6 ± 2.8	29.6 ± 5.7	0.463
Male,%	45	50	0.714
Diabetes duration, y	…	7[IQR:1-8]	
Systolic blood pressure, mmHg	128 ± 12	129 ± 8	0.583
Diastolic blood pressure, mmHg	74 ± 8	76 ± 7	0.311
Plasma fasting glucose, mmol/L	4.9 ± 0.5	8.9 ± 3.1	< 0.001
Glycated hemoglobin, %	5.4 ± 0.3	7.5 ± 0.2	< 0.001
Glycated haemoglobin, mmol/mol	37 ± 3	57 ± 15	< 0.001
Plasma triglycerides, mmol/L	1.59 ± 0.68	1.60 ± 0.78	0.931
Plasma free fatty acids, mmol/L	0.38 ± 0.23	0.61 ± 0.36	0.017
Total cholesterol, mmol/L	5.6 ± 0.9	3.9 ± 0.9	< 0.001
HDL, mmol/L	1.53 ± 0.61	1.18 ± 0.29	0.005
LDL, mmol/L	3.41 ± 0.53	2.04 ± 0.74	< 0.001
Creatinine, mmol/L	72 ± 19	65 ± 17	0.228
Urine albumin, mg/L, (N = 32)	…	16 ± 30	
Urine albumin: creatinine ratio, mg/mmol, (N = 32)	…	1.7 ± 3	
Medications, n (%)			
Metformin, n (%)	-	41 (89)	
Sulphonylurea	-	14 (30)	
Aspirin	-	5 (11)	
Statin	-	34 (74)	
ACE-I	-	12 (26)	

Continuous data are mean ± SD unless otherwise indicated. Categorical data are frequency (percent) unless otherwise indicated. T2DM indicates type 2 diabetes mellitus; BMI, body mass index; y, years; HDL, high density lipoprotein; LDL, low density lipoprotein; ACE-I angiotensin-converting enzyme inhibitors.

The Effects of Diabetes on LV Geometry and Function

T2DM was associated with concentric LV remodelling. Although LV mass was not different between T2DM and controls (p = 0.183), LV end-diastolic volume was 16% smaller in T2DM (p = 0.004). As a result, T2DM was associated with increased LVMVR by 31% compared to controls, (0.97 ± 0.17, vs 0.74 ± 0.14g/ml, P < 0.001; **Figure 3.1, A**; **Table 3.2**), suggesting significant concentric remodelling. Importantly, this concentric remodelling was not correlated with blood pressure (R = -0.002, P = 0.989).

Despite normal LV ejection fraction (LVEF), mid-ventricular systolic circumferential strain was impaired in patients with T2DM (T2DM 14.5 ± 3.5%, vs controls 18.3 ± 2.6%, P < 0.001; **Figure 3.1B**), indicating subtle contractile dysfunction. The differences in diastolic strain rate between the T2DM patients and controls did not reach statistical significance (T2DM 60 ± 24s^{-1}, vs controls 65 ± 13s^{-1}, P = 0.057). Interestingly, there was a negative correlation between LVMVR and systolic circumferential strain (R = -0.430, P < 0.001).

Table 3.2: LV Geometry and Function

	Controls N = 20	**Type 2 DM N = 46**	**P value**
LV end-diastolic volume, ml	148 ± 8	124 ± 4	0.004
LV end-systolic volume (ESV), ml	43 ± 4	37 ± 2	0.351
LV stroke volume (SV), ml	104 ± 5	86 ± 3	0.055
LV ejection fraction, %	71 ± 1	70 ± 1	0.586
LV wall thickness, mm	9.6 ± 0.29	10.4 ± 0.26	0.047
LV mass, g	109 ± 7	120 ± 4	0.183
LV mass index, g/m^2	53.1 ± 3.6	60.2 ± 1.7	0.05
LV mass to LV end-diastolic volume, g/ml	0.74 ± 0.14	0.97 ± 0.17	< 0.001
Native myocardial T1 value, ms	1184 ± 28	1194 ± 32	0.23
Extra Cellular Volume fraction, %	0.29 ± 0.03	0.29 ± 0.02	0.773

Continuous data are mean ± SD unless otherwise indicated. Categorical data are frequency (percent) unless otherwise indicated. T2DM indicates type 2 diabetes mellitus; CMR, cardiac magnetic resonance; LV, left ventricular.

Cardiac Steatosis, Myocardial Energetics, Concentric Remodelling and Strain

Myocardial triglyceride levels were not normally distributed, therefore non=parametric tests were used for comparison of the data between the patients and the controls. Diabetes was associated with an almost two-fold elevation of myocardial triglyceride (T2DM 1.13 ± 0.78, vs controls 0.64 ± 0.52, P = 0.017; **Figure 3.1, C**) and was also associated

with ~30% reduction in the myocardial PCr/ATP ratio (T2DM 1.68 ± 0.28, vs controls 2.05 ± 0.34, P < 0.001 ; **Figure 3.1, D**). When investigating the whole group, there was a positive correlation between the MTG and concentric LV remodelling (R = 0.410, P = 0.003) and a negative correlation between the myocardial energetics and the LVMVR (R = -0.30, P < 0.020). Stepwise multivariable regression of these variables revealed myocardial steatosis (β = 0.473, P = 0.001) to be the only independent predictor of the concentric remodelling (overall R^2 of the model = 0.304, P = 0.001).

Furthermore, steatosis also negatively correlated with systolic strain (R = -0.400, P = 0.003) and it was also the only independent predictor of the systolic strain (β = -0.400, P = 0.003) on stepwise multivariable regression analysis. However, there was no correlation between diastolic strain rate and steatosis (R = 0.158, P = 0.263).

When investigating the data pertaining to the patients only, this positive association between the MTG and the concentric LV remodelling remained significant (R = 0.433, P = 0.007). Furthermore, MTG remained an independent predictor of LV concentric remodelling (β = 0.430, P = 0.014) when BP, BMI, age and HBA1c were not independently associated with concentric remodelling in this study. This correlation between the LV concentricity and MTG was, however, not significant for the controls (R = -0.282, P = 0.309).

Similarly, steatosis also negatively correlated with systolic strain when investigating the data pertaining to the patients only, (R = -0.309, P = 0.039). Stepwise multivariable regression of these variables, however, revealed the independent association between myocardial steatosis and the peak circumferential systolic strain to be non-significant when

investigating only patients' data, despite a strong trend (β = -0.327, P = 0.054). This correlation between the MTG and peak circumferential systolic strain, however, was not significant for the controls (R = -0.250, P = 0.368).

That the correlation between the MTG, LV concentricity and systolic strain was significant only in the patient data and not in the control data is not surprising and suggests MTG to be detrimental only at higher levels.

T1 mapping , extracellular volume (ECV) quantification and late Gadolinium Enhancement

There was no significant difference in native myocardial T1 values between the T2DM patients and the controls (T2DM 1194 ± 32, vs controls 1184 ± 28; P = 0.23). Similarly, ECV did not differ between the groups (T2DM 0.29 ± 0.02, vs controls 0.29 ± 0.03, P = 0.773). On visual assessment of the LGE images, no areas of enhancement indicative of scarring in either ischaemic or non-ischaemic patterns were identified in any of the participants.

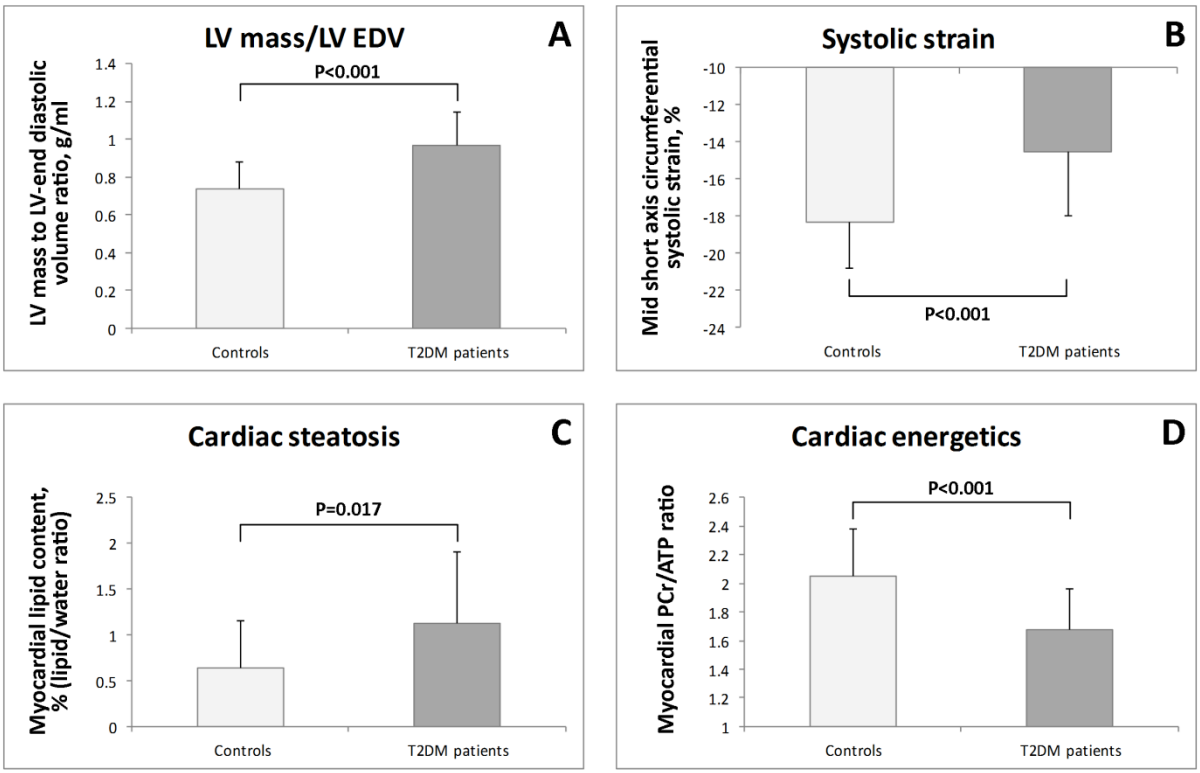

Figure 3.1 *Differences in cardiac geometry and function between patients with T2DM and controls:* ***(A)*** *LV Mass: LV-EDV ratio (g/ml);* ***(B)*** *Systolic strain %;* ***(C)*** *Myocardial triglyceride content (%);* ***(D)*** *Myocardial energetics (PCr/ATP ratio).*

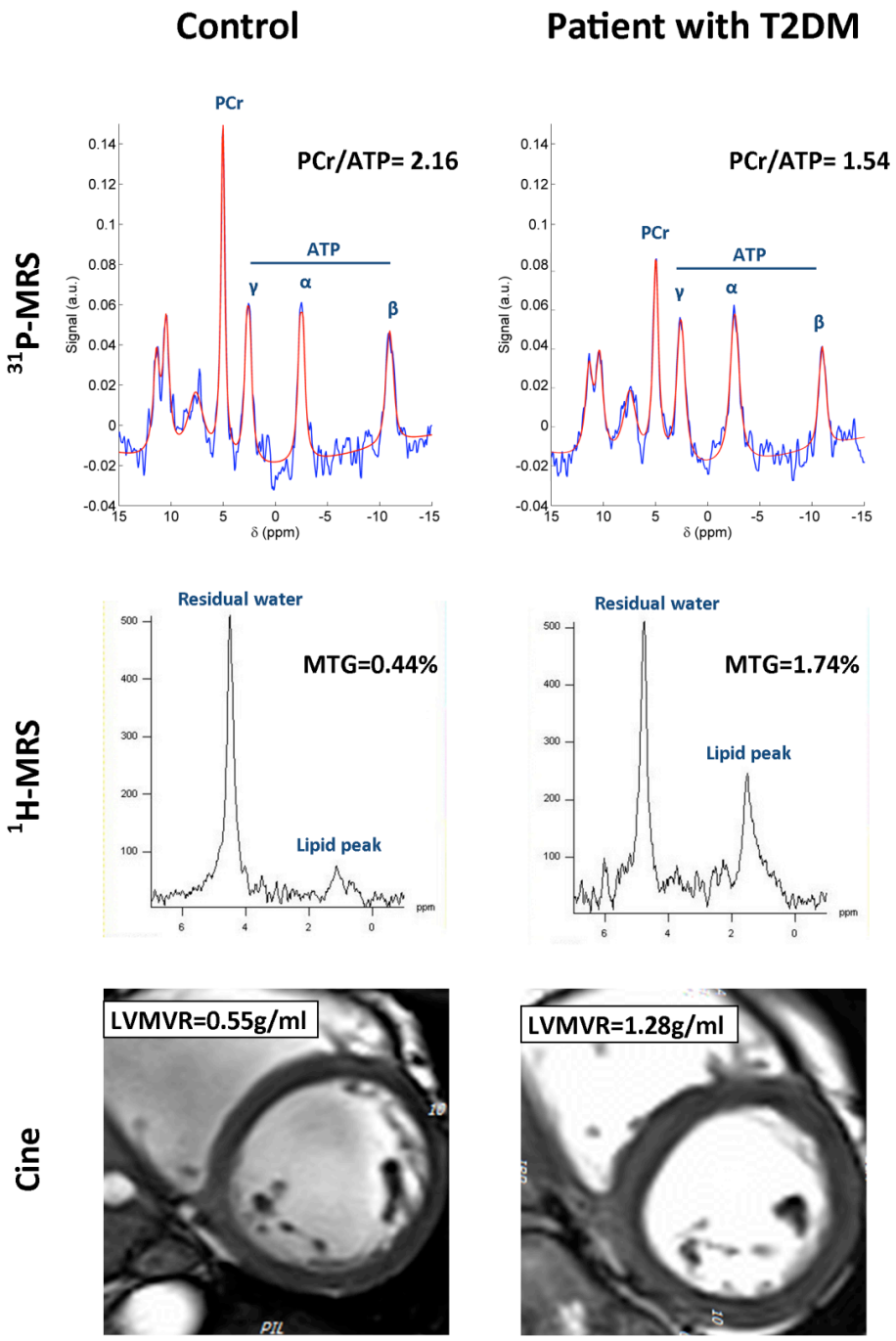

Figure 3.2: *Representative examples of cardiac ^{31}P-MRS, ^{1}H-MRS and cine imaging in a control and a patient with T2DM. Top panel: normal control ^{31}P-MRS with PCr/ATP = 2.16, vs patient with T2DM PCr/ATP = 1.66; second panel: normal control 1H-MRS with myocardial lipid to water ratio = 0.44%, vs patient with T2DM = 1.74%; third panel: normal control cine image with LV mass : LV end-diastolic volume ratio = 0.55 g/ml, vs patient with T2DM = 1.28 g/ml.*

3.3 Discussion

Concentric LV remodelling is an adverse prognostic marker of cardiovascular events[99], and is linked to contractile dysfunction[100]. Using CMR and MRS, I show here that diabetes, in the absence of significant hypertension, is associated with concentric LV remodelling, and I confirm the findings of previous studies, showing pronounced cardiac steatosis[15] and decreased energetics in patients with T2DM. I have also shown that despite normal LVEF, systolic strain was significantly impaired in diabetics, indicating a subtle contractile dysfunction, and was negatively correlated with both reduced myocardial energetics and concentric LV remodelling. Importantly, I have shown here that the degree of myocardial triglyceride accumulation is predictive of concentric LV remodelling and cardiac contractile function. As myocardial steatosis has been shown to be modifiable[101, 102] this provides the potential for novel therapies aimed at reducing concentric LV remodelling and improving cardiac function in diabetes. Finally, as no significant difference in ECV and native (pre-contrast) T1 mapping was found between the patients with T2DM and controls, it is unlikely that interstitial fibrosis plays a significant role in the pathogenesis of concentric LV remodelling in this well controlled stable T2DM population.

LV Geometric Remodelling and the Functional Changes in the Diabetic Heart

It is now widely known that a strong relationship exists between LVH and subsequent cardiovascular morbidity (relative risk 2.3) as well as all-cause mortality (relative risk 2.5). In addition, concentric LV remodelling and hypertrophy carries an even greater risk[39]. It has

now been established that T2DM itself, independent of hypertension and coronary heart disease[1, 6, 9], results in concentric LV remodelling[103]. Here, the presence of concentric LV remodelling has been confirmed, importantly in a stable and well controlled T2DM population. This suggests that the process of concentric remodelling is not limited to poorly controlled diabetics, or those with renal dysfunction[5], and occurs in the absence of significant systemic hypertension.

Relationship between LV Geometric Remodelling and Cardiac Steatosis in the Diabetic Heart

Ectopic lipid deposition in the diabetic heart is a well-documented process, and non-invasive studies using ^{1}H-MRS have reported elevated levels of cardiac triglyceride in human diabetes[15]. However, the link between cardiac steatosis and diabetes, above and beyond that observed in obesity, and its potential role in concentric LV remodelling within diabetes, has not been explored in humans. This study now demonstrates that diabetes *per se* is linked to significant cardiac steatosis, and that the degree of steatosis is linked to the degree of concentric LV remodelling.

The importance of cardiac steatosis in the pathophysiology of concentric LV remodelling has been assessed in experimental models. In diabetes, where fatty acid supply exceeds the oxidative capacity of the heart, this leads to diversion of lipids away from oxidative processes and towards non oxidative processes with the production of lipotoxic intermediates such as ceramide and diacyl-glycerol[104]. These lipotoxic intermediates have

been shown to activate signalling pathways affecting ATP production, insulin sensitivity, myo-cellular contractility, and apoptosis[104]. Recently, it has also been demonstrated that cardiac steatosis potentiates the effects of Angiotensin 2 on the heart[105]. Given the fact that Angiotensin 2 is a potent hypertrophic stimulus and that both Angiotensin 2 receptor density and mRNA expression are elevated in the diabetic heart[45], this is likely to be an important driver for hypertrophy. In addition, animal models of overexpression of fatty acid transporters and increases in triglyceride synthesis both result in severe cardiac steatosis and concentric LV hypertrophy[92,36]. This provides a mechanistic link between cardiac steatosis, lipotoxicity and concentric LV remodelling in diseases of upregulated fatty acid metabolism such as diabetes. Importantly, successful reduction of myocardial steatosis with glucagon-like peptide-1 receptor (GLP-1) agonists[101] and mineralocorticoid receptor blockers[102] have both been shown to reverse concentric LV remodelling.

Here, it has been demonstrated that myocardial steatosis is a predictor of concentric LV remodelling and subclinical contractile dysfunction in patients with T2DM. This supports the notion that the development of concentric LV remodelling in T2DM is mechanistically linked to cardiac steatosis, and that cardiac lipotoxicity represents a significant component of this process. This suggests that therapies and interventions aimed at reducing myocardial triglyceride may well promote beneficial reverse remodelling in humans.

LV Concentric Remodelling and Myocardial Energetics

A healthy heart is able to metabolise a range of substrates, including fatty acids, glucose, amino acids, ketone bodies and lactate, to fulfil the demand for ATP production. Depending

on the availability of substrates and the physiological conditions, the heart will switch its metabolic preference amongst substrates. This metabolic flexibility allows the heart to maximise ATP production to the prevailing conditions, and is regulated by substrate concentrations, hormones, oxygen availability and workload[106]. This flexibility is lost in diabetes and myocardial substrate selection is shifted almost exclusively to fatty acid metabolism[45]. Increased delivery of fatty acids, insulin resistance, activation of the peroxisome proliferator–activated receptor-α (PPAR-α) signalling, and inhibition of pyruvate dehydrogenase all act in diabetes to increase mitochondrial fatty acid uptake and use, and to inhibit glucose uptake and oxidation[45]. The crucial importance of this increase in fatty acid metabolism lies in the fact that mitochondrial redox state, and as a result the free energy of hydrolysis of ATP, is affected by the substrate oxidised. This over utilisation of fatty acids results in a reduced ATP yield and a loss of mitochondrial efficiency[45]. The interplay between myocardial energetic status and geometrical changes in diabetes has previously not been explored. This study reports that in the context of well controlled diabetes, myocardial energetics, in the form of PCr/ATP ratios, are impaired, and are linked to concentric remodelling.

Functional Consequences of Steatosis and Concentric Remodelling.

Starting as an adaptation to reduce LV wall stress, LV concentric remodelling eventually contributes to increased rates of cardiovascular events via deleterious effects on ventricular function[100]. It is shown here that T2DM is linked to concentric remodelling, and that this concentric remodelling is correlated with reduced energetics, myocardial steatosis

and, importantly, contractile dysfunction in the form of impaired systolic strain, and, as a trend, diastolic dysfunction with lower diastolic strain rate. Thus, although these data do not prove a direct causal link, they are suggestive of a pathophysiological role of concentric LV remodelling in the development of contractile dysfunction in T2DM acting via cardiac steatosis and impaired energetics. Importantly, all these findings occurred above and beyond the effects of increased adiposity, which has previously been shown to be linked to impaired energetics,[63] subclinical systolic dysfunction, diastolic dysfunction, cardiac steatosis and concentric LV remodelling[95]. This suggests that these findings are much more likely due to diabetes *per se* than to coexisting obesity.

Microalbuminuria is strongly associated with risk of cardiovascular disease, but the nature of this link remains controversial and poorly understood[107]. In this study, in patients with stable T2DM, free of coronary artery disease, no association between the urine albumin excretion and the LV remodelling, contractile dysfunction, cardiac energetics or steatosis was observed.

3.4 Limitations

Of the 46 patients with T2DM, 11 patients (24%) did not consent to have CCTA performed and as such it is possible that occult coronary artery disease could be present in this minority of patients.

Insulin measurements were not taken in the control group. Although diabetes was excluded on fasting glucose measurements, this does preclude the investigation of the role of insulin resistance in the pathogenesis of cardiac steatosis.

Urine albumin levels were recorded only in ~69% (n = 32) of the patients with T2DM.

3.5 Conclusion

When compared to BMI matched controls, patients with well controlled T2DM exhibit LV concentric remodelling in the absence of arterial hypertension. This concentric remodelling is associated with cardiac steatosis, myocardial energetic impairment and subclinical systolic dysfunction. As myocardial steatosis is independently predictive of concentric remodelling and cardiac systolic strain, it may play an important role in adverse geometric remodelling in T2DM. Importantly, as myocardial TG content is modifiable, strategies aimed at reversing myocardial steatosis may be beneficial in reversing LV remodelling, and potentially improve contractile function and prognosis in patients with diabetes.

Chapter 4

Cardiac energetics, oxygenation and perfusion during increased workload in patients with type 2 diabetes mellitus

4.1 Abstract

Aims

Patients with type 2 diabetes mellitus (T2DM) are known to have impaired resting myocardial energetics and impaired myocardial perfusion reserve, even in the absence of obstructive epicardial coronary artery disease (CAD). Whether or not the pre-existing energetic deficit is exacerbated by exercise, and whether the impaired myocardial perfusion causes deoxygenation and further energetic derangement during exercise stress, is uncertain.

Methods and Results

Thirty-one T2DM patients, on oral antidiabetic therapies with a mean HBA1c of 7.4 ± 1.3%, and seventeen matched controls underwent adenosine stress cardiovascular magnetic resonance (CMR) for assessment of perfusion (myocardial perfusion reserve index-MPRI) and oxygenation (blood-oxygen level dependent-BOLD signal intensity change-SIΔ). Cardiac Phosphorus-MR spectroscopy was performed at rest and during leg exercise. Significant CAD (> 50% coronary stenosis) was excluded in all patients by coronary computed tomographic angiography.

Resting PCr/ATP was reduced by 17% in patients (1.74 ± 0.26, P = 0.001) compared to controls (2.07 ± 0.35); during exercise there was a further 12% reduction in PCr/ATP (P = 0.005) in T2DM patients, but no change in controls. MPRI and oxygenation response Adenosine stress were decreased in T2DM (MPRI 1.61 ± 0.43 vs 2.11 ± 0.68 in controls, P =

0.002; BOLD SIΔ 7.3 ± 7.8% vs 17.1 ± 7.2% in controls, P < 0.001). Exercise PCr/ATP correlated with MPRI (r = 0.50, P = 0.001) and with BOLD SIΔ (r = 0.32, P < 0.05), but there were no correlations between rest PCr/ATP and MPRI or BOLD SIΔ.

Conclusions

The pre-existing energetic deficit in diabetic cardiomyopathy is exacerbated by exercise; stress PCr/ATP correlates with impaired perfusion and oxygenation. These findings suggest that, in diabetes, coronary microvascular dysfunction exacerbates derangement of cardiac energetics under conditions of increased workload.

4.2 Introduction

Diabetes Mellitus (DM) is associated with increased risk of congestive heart failure (CHF)[6] and cardiovascular mortality.[1] Myocardial energy depletion[14, 13] and coronary microvascular dysfunction[54] are features of diabetic heart disease. Myocardial energy depletion in patients with diabetes is a multifactorial phenomenon, related to limitations in uptake and utilisation of substrates,[45, 49] mitochondrial dysfunction[46] and impaired energy transfer from mitochondria to myofibrils.[47] These metabolic changes, in combination with coronary microvascular dysfunction, may decrease the ability of the diabetic heart to adapt to acute increases in workload. Further derangement of the energetic deficit on increased workload could potentially limit myocardial contractile reserve and exacerbate diastolic dysfunction.[108, 109]

Phosphorus-magnetic resonance spectroscopy (^{31}P-MRS) allows non-invasive assessment of the myocardial phosphocreatine to ATP concentration ratio (PCr/ATP), which is a sensitive indicator of the myocardial energy status.[28] Using ^{31}P-MRS our group, and others, have shown that the diabetic heart is energetically compromised, with a decreased PCr/ATP, at rest.[14,13] However, changes in cardiac metabolic reserve and energy metabolism in diabetic patients under conditions of increased workload have not been studied. Furthermore, blood-oxygen level-dependent (BOLD) cardiovascular magnetic resonance (CMR) or oxygenation-sensitive CMR has the ability to noninvasively assess myocardial tissue oxygenation during vasodilator stress. Oxygenation-sensitive CMR capitalizes on the paramagnetic properties of deoxygenated hemoglobin, which acts as an intrinsic contrast

mechanism in oxygenation-sensitive MR sequences.[110-112] Thus, CMR allows a comprehensive investigation of the interplay between metabolic and ischaemic changes in the diabetic heart.

The primary objective of this study was to assess whether the pre-existing cardiac energetic deficit is exacerbated by exercise in patients with type 2 diabetes mellitus (T2DM) as a measure of metabolic reserve. The second objective was to assess myocardial perfusion reserve and oxygenation during vasodilator stress, and to examine their relationship with myocardial energy status in T2DM patients, who were free of significant epicardial coronary artery stenosis. It was hypothesised that the intrinsic metabolic deficit and microvascular dysfunction in diabetes, either alone or in combination, will reduce the ability of the diabetic myocardium to adapt to acute increases in workload and exacerbate the energetic derangement.

4.3 Methods

Study Population

Thirty-nine subjects with T2DM on oral antidiabetic therapies and seventeen volunteers of similar age and body mass index (BMI) to the patients were recruited. T2DM was diagnosed according to the World Health Organization criteria.[113] All patients were recruited from the general practice surgeries in Oxfordshire, United Kingdom. The study complied with the

Declaration of Helsinki, and it was approved by the National Research Ethics Committee (REC Ref 13/SW/0257) and informed written consent was obtained from each participant.

Inclusion and Exclusion Criteria

Subjects were excluded if they had a history of cardiovascular disease, chest pain, tobacco smoking, uncontrolled hypertension (resting systolic blood pressure (BP) > 140 mmHg and diastolic BP > 90 mmHg), contraindications to MR imaging, ischaemic changes on 12-lead ECG, or renal impairment (estimated glomerular filtration rate below 30 mL/min). T2DM participants were excluded if they were taking insulin. Additionally, patients were screened for obstructive epicardial CAD (> 50% of luminal stenosis) by coronary computed tomographic angiography (CCTA) scan. Subjects with no evidence of significant epicardial CAD on CCTA underwent CMR, ^{31}P-MRS, transthoracic echocardiography and fasting blood tests.

Study Protocol

All study subjects underwent CMR scanning at 3 T as follows:

1. CT coronary angiography to exclude significant CAD (> 50% coronary stenosis).
2. ^{31}P-MR Spectroscopy to obtain the rest and exercise PCr/ATP.
3. Cine imaging to measure LV function, mass and volume.
4. Tagging CMR to assess LV strain.

5. Rest and Adenosine stress BOLD imaging to assess oxygenation.

6. Rest and Adenosine stress perfusion to measure myocardial perfusion reserve index.

7. Late gadolinium enhancement to assess fibrosis.

^{31}P-MR Spectroscopy Exercise Protocol

MR spectroscopy was performed to obtain the rest and exercise PCr/ATP from a voxel placed in the mid-ventricular septum, with the subjects lying prone with their heart over the centre of the ^{31}P heart/liver coil in the iso-centre of the magnet as previously described.[118, 120] Acquisition time was 9 minutes during rest and 9 minutes during leg exercise lying prone, with 2.5 kg weights attached to both ankles.

The rate pressure product (RPP) was calculated using the product of the heart rate and systolic blood pressure, providing a measure of cardiac work. The starting RPP was calculated during the baseline resting spectral acquisition. On completion of the resting scan, volunteers were asked to initiate exercise with repeated and alternate knee flexion, aiming to double the baseline RPP, with feedback given throughout. When maintained at a steady level of exercise, reached after 1 min, the exercise scans were acquired. Haemodynamic measurements were taken and recorded every minute and the mean exercise RPP calculated. Subjects were also encouraged to maintain a steady exercise level during the 9-minute acquisition of spectra. The volunteers stopped exercising on completion of the exercise spectrum.

^{31}P-MRS spectra were processed with a custom Matlab (The Mathworks Inc., Nattick, MA) implementation of the Advanced Method of Accurate, Robust, and Efficient Spectroscopic (AMARES) fitting algorithm[114,115], using prior knowledge[116] specifying 11 Lorentzian peaks (α,β,γ-ATP multiplet components, PCr, PDE, and 2×2,3-diphosphoglycerate [2,3-DPG]), fixed amplitude ratios and scalar couplings for the multiplets, and a fixed begin time.[117]

Peak areas were corrected for Nuclear Overhauser Effects (NOE) using the following empirical correction factors[118]: PCr 0.80, β-ATP 0.88, α-ATP 0.88, γ-ATP 0.79, 2,3-DPG 0.70. Partial saturation was corrected for the excitation flip angle at the centre of the chosen voxel [119]: PCr 3.8 s, γ-ATP 2.4 s, α-ATP 2.5 s, β-ATP 2.7 s, 2,3-DPG 1.39 s, and PDE 1.1 s. The resulting ATP amplitudes were averaged and corrected for blood contamination by subtracting 11% of the total 2,3-DPG amplitude.[34]

4.4 Statistical Analysis

All data are expressed as mean ± standard deviations, apart from diabetes duration which is expressed as median with interquartile range, and were checked for normality using the Kolmogorov–Smirnov test. Comparisons between the 2 groups were performed by Student t-test. The chi-square test or Fisher's exact test was used to compare discrete data as appropriate. Bivariate correlations were performed using Pearson's or Spearman's method, as appropriate. Comparisons between rest and exercise energetics in patients and controls were performed with two-tailed paired t-test. A P-value < 0.05 was considered significant.

All statistical analyses were performed with IBM SPSS Statistics version 20 (IBM, Armonk, New York, USA).

A priori sample size calculation was performed to detect a 13% drop in PCr/ATP ratio in the T2DM cohort during stress. Based on pilot data (PCr/ATP rest 1.91 ± 0.25, stress 1.65 ± 0.28) assuming two-tailed paired *t*-test analysis ($\alpha = 0.05$ and $\beta = 0.8$), calculations suggested that 11 T2DM participants would be needed. A second a priori sample size calculation was also performed to detect a 10% difference in PCr/ATP ratio in T2DM when compared with normal. Assuming two-tailed independent *t*-test analysis ($\alpha = 0.05$ and $\beta = 0.8$) pilot data (PCr/ATP T2DM 1.81 ± 0.30, normal populations 2.11 ± 0.25) suggested that 14 T2DM and 14 normal subjects would be needed to detect a 14% difference in PCr/ATP ratio at rest. Due to excellent recruitment, these targets were achieved in this study.

4.5 Results

Participant Characteristics

Of the thirty-nine diabetic patients screened in the study, eight were excluded: 4 had significant obstructive coronary artery disease on CCTA, 1 had high systolic blood pressure on screening (> 140mmHg) and deep lateral T wave inversions on ECG, 1 had claustrophobia, 1 could not fit in the scanner due to body habitus and 1 patient withdrew consent after the first study visit. Consequently, thirty-one patients (17 male, mean age 55 ± 9 years; BMI 28.7 ± 5.6 kg/m^2) with T2DM, median diabetes duration 7 years [IQR: 1-8]

and mean glycated haemoglobin level 7.4 ± 1.3%, and seventeen controls (9 male, mean age 50 ± 14 years; BMI 27.1 ± 5.0 kg/m^2) were studied.

Demographic, clinical, biochemical and echocardiographic data are shown in **Table 4.1**. There were no significant differences in age, gender, systolic BP and BMI between diabetic patients and controls. Diastolic BP and resting heart rate were statistically higher in the diabetic cohort, although remained within the normal range. Diabetes was associated with higher fasting blood glucose and plasma free fatty acid (FFA) content. A significant proportion of my diabetic cohort (77%) was on statin therapy, hence total cholesterol and low-density lipoprotein cholesterol levels were lower in T2DM patients compared to controls.

Table 4.1: Baseline characteristics of the study cohort

Variable	Controls N = 17	Type 2 DM patients N = 31	P value
Age, y	50 ± 14	55 ± 9	0.102
BMI, kg/m2	27.1 ± 5.0	28.7 ± 5.6	0.302
Male,%	53	58	0.739
Diabetes duration, y	…	7 [IQR:1-8]	
Systolic blood pressure, mmHg	121 ± 12	127 ± 14	0.135
Diastolic blood pressure, mmHg	69 ± 9	77 ± 8	0.007
Plasma fasting glucose,mmol/L	4.9 ± 0.3	9.1 ± 3.2	< 0.001
Glycated hemoglobin, %	…	7.4 ± 1.3	
Insulin, pmol/L	…	135 ± 131	
Plasma triglycerides, mmol/L	1.46 ± 0.7	1.47 ± 0.8	0.986
Plasma free fatty acids, mmol/L	0.36 ± 0.20	0.60 ± 0.31	0.007
Total cholesterol, mmol/L	5.2 ± 0.9	3.9 ± 0.8	< 0.001
HDL, mmol/L	1.36 ± 0.4	1.22 ± 0.4	0.273
LDL, mmol/L	3.16 ± 0.6	1.9 ± 0.6	< 0.001
Medications, n (%)			
Metformin, n (%)	-	31(97)	
Sulphonylurea	-	21(68)	
Aspirin	-	11(35)	
Statin	-	24(77)	
ACE-I	-	21(68)	

Continuous data are mean ± SD unless otherwise indicated. Categorical data are frequency (percent) unless otherwise indicated. T2DM indicates type 2 diabetes mellitus; BMI, body mass index; y, years; HDL, high density lipoprotein; LDL, low density lipoprotein; ACE-I angiotensin-converting enzyme inhibitors.

Myocardial structure and systolic function

CMR results for LV volumes and function are summarized in **Table 4.2**. There was no significant difference in LV ejection fraction between patients with T2DM and controls. Diabetes was associated with concentric LV remodelling (LV Mass: Volume ratio T2DM, 0.98 ± 0.21 vs controls, 0.70 ± 0.12; $P < 0.001$), with reduced LV diastolic volumes ($P < 0.001$) and increased maximal wall thickness ($P < 0.05$). Despite these differences in LV structure, LV mass did not differ between the two groups. Mid-ventricular systolic circumferential strain was impaired in patients with T2DM compared to controls, indicating subtle contractile dysfunction.

Table 4.2 CMR results in patients vs. controls

Variable	Controls N = 17	Type 2 DM patients N = 31	P value
LV End diastolic volumes, ml	161 ± 39	125 ± 30	0.001
LV End systolic volumes, ml	48 ± 16	40 ± 18	0.137
LV stroke volume, ml	105 ± 25	88 ± 25	0.022
LV Ejection fraction, %	70 ± 5	69 ± 9	0.535
LV mass index, g/m^2	52 ± 14	60 ± 13	0.056
LV mass, g	109 ± 30	121 ± 31	0.235
LV diastolic wall thickness, mm	9.3 ± 1.2	10.6 ± 1.8	0.016
LV mid-ventricular circumferential systolic strain, % (negative)	19 ± 3	14 ± 2	< 0.001
LV mass/End diastolic volume g/ml	0.70 ± 0.12	0.98 ± 0.21	< 0.001
LV mid-ventricular diastolic strain rate, s^{-1}	65 ± 13	62 ± 26	0.749

Continuous data are mean ± SD unless otherwise indicated. Categorical data are frequency (percent) unless otherwise indicated. T2DM indicates type 2 diabetes mellitus; CMR, cardiac magnetic resonance; LV, left ventricular.

Hemodynamic Measurements

Rest, physiological stress and pharmacological stress blood pressure and heart rate responses are summarized in **Table 4.3**. Adenosine stress and exercise led to similar percentage increases in rate pressure product.

Table 4.3 Haemodynamic Measurements

Variable	Controls	T2DM	P Value
	^{31}P-MRS Exercise Stress		
Rest heart rate, bpm	55 ± 10	69 ± 8	< 0.001
Stress heart rate, bpm	78 ± 10	84 ± 10	0.076
Rest blood pressure, mmHg	121 ± 12	127 ± 14	0.135
Stress blood pressure, mmHg	126 ± 15	147 ± 20	0.002
Rest RPP, bpm*mmHg	6832 ± 1441	8766 ± 1318	< 0.001
Stress RPP, bpm*mmHg	9926 ± 1761	12264 ± 2204	0.002
Increase in RPP, %	**48 ± 30**	**41 ± 22**	**0.381**
	Adenosine Stress CMR		
Rest heart rate, bpm	60 ± 13	69 ± 9	0.036
Stress heart rate, bpm	77 ± 16	85 ± 9	0.054
Stress blood pressure, mmHg	121 ± 9	130 ± 15	0.075
Rest RPP, bpm*mmHg	6982 ± 1494	9382 ± 2106	0.001
Stress RPP, bpm*mmHg	10048 ± 2856	12479 ± 2819	0.014
Increase in RPP, %	**44 ± 26**	**35 ± 29**	**0.369**

Continuous data are mean ± SD unless otherwise indicated. Categorical data are frequency (percent) unless otherwise indicated. T2DM indicates type 2 diabetes mellitus; CMR, cardiac magnetic resonance; bpm, beats per minute; BP, blood pressure; RPP, rate pressure product.

Changes in rest and exercise myocardial energetics

Diabetes was associated with a 17% decrease in PCr/ATP at rest compared with controls (P = 0.001) and there was a further 12% decrease in PCr/ATP with exercise (mean rest PCr/ATP 1.74 ± 0.26 to mean exercise PCr/ATP 1.54 ± 0.26; P = 0.005; **Figure 4.1**). In contrast, there was no significant change in PCr/ATP in healthy controls with exercise. **Figure 4.2** shows representative rest and exercise ^{31}P-MR spectra.

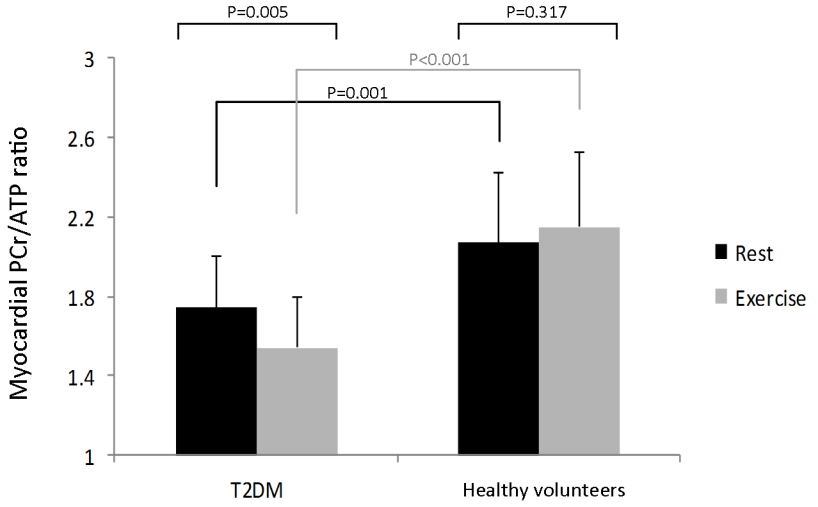

Figure 4.1: *Column graphs with means and standard deviations showing differences in rest and exercise myocardial PCr/ATP ratios between controls and patients with T2DM. Bars show mean PCr/ATP ratios and error bars indicate standard deviations. NS = Non-significant.*

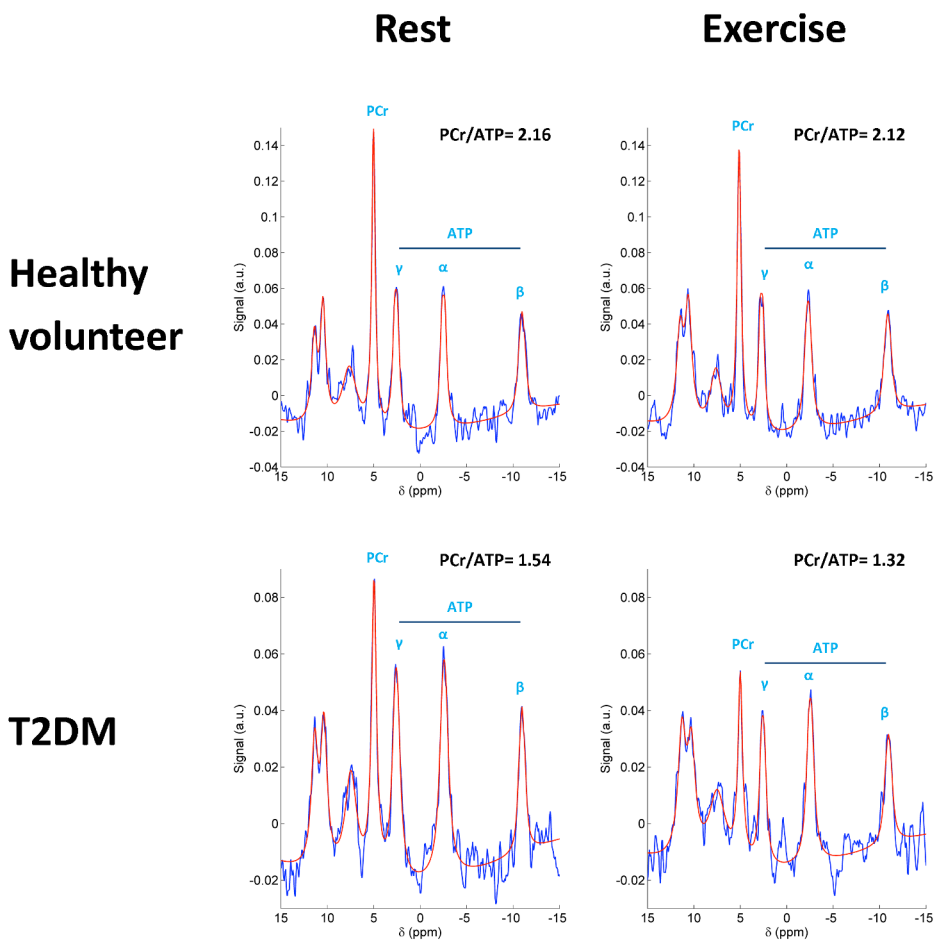

Figure 4.2: *Representative rest and exercise ^{31}P-MR spectra examples. Rest and exercise myocardial phosphorus spectra in a healthy volunteer (top row) and a patient with T2DM. Note a further decrease of already lower rest PCr/ATP in the patient with T2DM during exercise.*

Changes in rest and exercise myocardial energetics

Mean MPRI in the T2DM group was 24% lower than in controls (P = 0.002; **Figure 4.3**). During vasodilator stress, patients with T2DM showed evidence of blunted oxygenation response, (SIΔ: T2DM 7.3 ± 7.8%) compared with controls (SIΔ: 17.1 ± 7.2%, P < 0.001; **Figure 4.3**). **Figure 4.4** shows representative CMR images of oxygenation and perfusion.

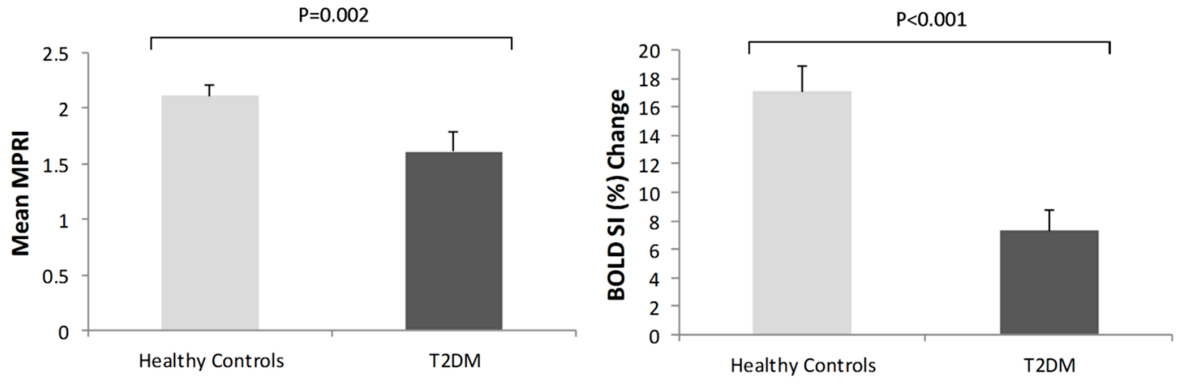

Figure 4.3: *Column graphs with means and standard deviations showing differences in MPRI and BOLD SI (%) change between controls and patients with T2DM. Bars show mean PCr/ATP ratios and error bars indicate standard deviations.*

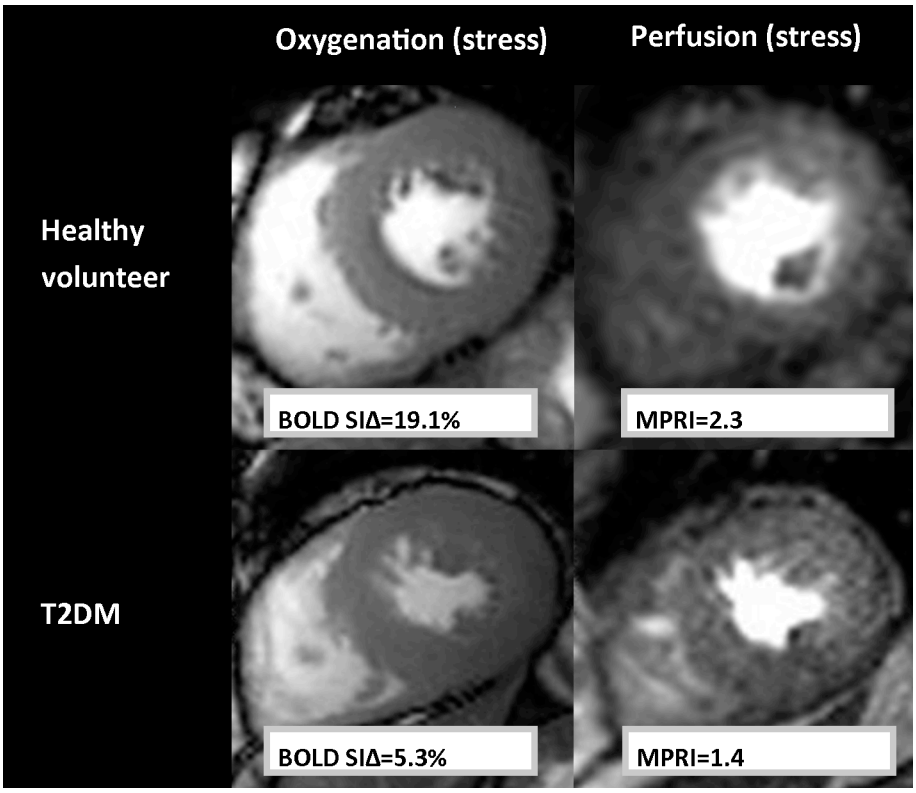

Figure 4.4: *Representative cardiovascular magnetic resonance perfusion and oxygenation examples. Oxygenation, and corresponding perfusion images in a healthy volunteer (top row) and a patient with T2DM. Perfusion reserve (mean myocardial perfusion reserve index-MPRI) and oxygenation signal intensity change (BOLD SIΔ) were impaired in the patient.*

Assessment of Myocardial Scarring Using Late Gadolinium Enhancement Imaging

On visual assessment of LGE images, no areas of myocardial enhancement indicative of replacement or interstitial fibrosis were identified in either diabetic patients or normal controls.

Correlations amongst myocardial oxygenation, perfusion, energetics and strain

When investigating the data for the whole study participants, MPRI had no significant correlation with PCr/ATP at rest. However, a positive correlation with PCr/ATP was obtained during exercise ($r = 0.50$, $P = 0.001$). Impaired MPRI was associated with blunting of myocardial oxygenation during vasodilator stress ($r = 0.40$, $P < 0.05$). There was also a positive correlation between exercise PCr/ATP and oxygenation SIΔ ($r = 0.32$, $P < 0.05$), whilst there was no correlation between the rest PCr/ATP and oxygenation SIΔ. Systolic circumferential strain, correlated with rest PCr/ATP ($r = 0.40$, $P < 0.05$) and exercise PCr/ATP ($r = 0.50$, $P = 0.003$).

When investigating the patients only data, the positive association between the exercise PCr/ATP and MPRI did not reach statistical significance ($r = 0.247$, $P = 0.205$). Similarly, when investigating the controls only data, the positive association between the exercise PCr/ATP and MPRI did not reach statistical significance ($r=0.225$, $P= 0.258$). Nevertheless, as reported above, for the overall group, exercise PCr/ATP was modestly associated with the

MPRI. This is likely reflective of the small sample group size and future studies should aim to assess this with a larger group of patients and controls.

Finally, plasma FFA levels correlated inversely with oxygenation SIΔ ($r = -0.35$, $P < 0.05$), but there was no significant correlation between the plasma fasting glucose and the oxygenation SIΔ. There was no significant correlation of MPRI with fasting plasma FFA or glucose levels. When fasting plasma glucose levels correlated inversely with exercise PCr/ATP ($r = -0.40$, $P < 0.05$) and rest PCr/ATP ($r = -0.50$, $P = 0.002$), fasting plasma FFA levels only correlated inversely with exercise PCr/ATP ($r = -0.50$, $P = 0.004$), but not with rest PCr/ATP.

4.6 Discussion

In this study, CMR and ^{31}P-MRS were used to study patients with T2DM free of significant obstructive epicardial CAD on CCTA. The effects of diabetes on cardiac metabolic reserve, and how metabolic reserve relates to both myocardial oxygenation and perfusion reserve, were assessed. It was demonstrated that during exercise, the pre-existing energetic deficit in patients with diabetes, as determined by PCr/ATP, is exacerbated. Reduced MPRI in T2DM is not a universal finding[23], however, similarly to some other studies, impaired myocardial perfusion reserve in diabetes is once again confirmed[14, 53, 122]. I now also show here that patients with diabetes not only have impaired perfusion, but also evidence of

blunted myocardial oxygenation at stress. Finally, it has been demonstrated here that although myocardial energy metabolism at rest does not correlate with coronary microvascular dysfunction, and is primarily a result of an intrinsic metabolic deficit, during exercise microvascular dysfunction exacerbates the energetic deficit.

Diabetes and Cardiac Metabolic Reserve

Myocardial energetic compromise, indicated by decreased PCr/ATP, is a predictor of mortality,[28] linked to contractile dysfunction,[28, 108] and is a well-recognized complication of diabetes.[13, 14] Here, for the first time, I demonstrate exacerbation of this energetic deficit during exercise in stable patients with diabetes, indicating impaired cardiac metabolic reserve.

The healthy myocardium has rapid response mechanisms to deal with acute changes in energy demand, providing a large metabolic reserve.[41] These mechanisms include increased contribution of carbohydrates to energy production by glycogenolysis,[42] increased glucose uptake and glycolysis,[43] and increased rates of phosphotransferase reactions.[44] The primary energy reserve compound in the heart is PCr and the enzyme creatine kinase is thought to allow the transfer of the high-energy phosphate bond between ATP and PCr, through the phosphotransferase reactions, in order to diffuse energy from the mitochondria to the myofibrils as PCr.[108] These changes require the metabolic machinery to be flexible, when in contrast diabetes is associated with metabolic inflexibility. The further drop of PCr/ATP during exercise in these patients with diabetes can

potentially be explained by metabolic inflexibility,[49] insufficient oxygen delivery, in addition to an impaired oxidative metabolism in diabetes resulting in reduced ATP production.[46, 123]

The causal role of altered energetics in contractile dysfunction in diabetic hearts is controversial, and this controversy remains unsettled. In my study, I also provide evidence in support of a relationship between energy starvation and contractile dysfunction in diabetic hearts, by showing correlations between myocardial systolic strain and the rest and stress PCr/ATP.

Myocardial Tissue Perfusion and Oxygenation in Diabetic Cardiomyopathy

Diabetic cardiomyopathy is characterized by microvascular disease, resulting in a failure to increment myocardial blood flow during acute increases in cardiac workload.[14, 53, 54, 122] Coronary microvascular dysfunction in diabetes is a multifactorial phenomenon, related to changes in perivascular and interstitial fibrosis,[57] reduced capillary density, and autonomic neuropathy.[59] Myocardial hypoperfusion does not always reflect tissue ischemia, as oxygen demand may vary in different pathophysiologic states. Indeed, some degree of dissociation exists between flow and oxygenation in the setting of CAD and dilated cardiomyopathy.[110, 120] It is therefore likely that perfusion is not the only determinant of oxygenation, and the metabolic state also plays a significant role.

Unlike myocardial perfusion, little is known about myocardial tissue oxygenation in patients with diabetes. BOLD CMR detects changes in tissue deoxyhemoglobin during manoeuvres that affect oxygen consumption and it is therefore used as a surrogate measure of tissue

oxygenation and metabolic activity. The assessed BOLD SI change with vasodilator stress reflects changes in the capillary bed which contains nearly 90% of the myocardial blood flow, and therefore the balance of oxygen supply and demand[124, 125]. The ability of oxygenation-sensitive CMR to detect microcirculatory changes has also been shown in patients with hypertension[126] and in patients with hypertrophic cardiomyopathy including mutation carriers without left ventricular hypertrophy[127].

The interplay between myocardial perfusion and oxygenation in diabetes has not been explored before. The oxygenation response during vasodilatory stress in diabetes is likely to be affected by the combination of decreased supply and increased demand for oxygen. This study shows that, in the context of reasonably well controlled diabetes, there is a modest relationship between myocardial perfusion and oxygenation during stress, and both are impaired. These findings support that the hypoperfusion as a result of microvascular dysfunction plays a role in the impaired ability to increase and/or maintain intravascular myocardial oxygenation during vasodilatory stress in diabetes. Furthermore, as outlined earlier, diabetic cardiomyopathy is associated with metabolic inefficiency, due to an increased reliance on fatty acids. To yield a consistently sufficient ATP supply, the diabetic heart matches the energy production to the requirement by increasing myocardial oxygen consumption[128,129]. Here it is shown that increased FFA availability is related to impaired myocardial oxygenation in diabetes, with a modest correlation between blunted oxygenation response and the plasma FFA levels.

With the results of the myocardial oxygenation assessments the prior literature on diabetic heart disease is extended by the indication that diabetes is associated with a reduced capacity to augment intramyocardial oxygenation, and a number of potential mechanisms for this association are proposed.

The relationship between myocardial energetics, perfusion and oxygenation

Here, this study has confirmed a reduced myocardial perfusion reserve in patients with T2DM and for the first time it has been demonstrated that this reduction is associated with a further decrease in the PCr/ATP ratio during increased workloads, when in contrast there is no association between the myocardial PCr/ATP ratio at rest and MPRI. This study therefore shows that microvascular dysfunction and the exacerbated energetic deficit during stress are related in diabetes.

A borderline correlation between the PCr/ATP ratio obtained during exercise and BOLD SI change was also shown. It is possible that the exaggerated increase in ATP demand during exercise explains the augmented increase in oxygen extraction and hence the blunted oxygenation response to stress.

The endothelium has been recognised to be a major regulator of vascular tone and growth. Both experimental and clinical studies have demonstrated the association between diabetes and endothelium-dependent relaxation impairment[130, 131]. Whilst in this study myocardial perfusion reserve was assessed during Adenosine stress, this parameter is both endothelium- and non–endothelium-dependent and does not allow to distinguish between

the two, as such it is possible that the lower MPRIs observed in the diabetic patients in this study might be the result of decreased vasodilation via both endothelium dependent and independent pathways, although an observational study such as ours cannot clearly identify the mechanisms responsible for the reduced coronary vasodilation response to adenosine**.**

4.7 Study Limitations

This study is limited by a relatively small sample size, in line with its proof-of-principle nature, and further studies are needed to understand the complex interaction between metabolic reserve and other factors. The principal limitation of this study is the lack of repeated assessment of myocardial function during stress. However, previous studies have shown exaggerated diastolic and systolic dysfunction in response to stress in patients with diabetes.[132, 133] Subjecting the participants to a third stress protocol (in addition to leg exercise during the acquisition of ^{31}P-MRS and adenosine stress for the assessment of MPRI and oxygenation signal intensity change) was deemed too high a burden on study subjects as this would lead to significantly longer adenosine infusion times, higher risk of adverse event rates and high drop-out rates. For the same reasons invasive coronary angiography for assessment of endothelium-dependent coronary vasodilatation and coronary vascular smooth muscle responsiveness was also not carried out.

The leg flexion stress was submaximal during the 9 minutes of acute physical exercise, with an average RPP increase of 40-50% in patients and controls, likely representing the physical constraints of exercising in an MRI scanner. However, this moderate exercise reflects typical levels of exercise that patients with diabetes would perform in daily life. While mean rest and exercise RPP were higher in diabetics, increases in RPP were similar in the two groups.

Adenosine stress tests for CMR perfusion, BOLD-SI imaging are distinct from the physiological stress during the spectroscopy. This is due to the limitations of the techniques; it is not technically achievable to carry out these tests together, CMR and MR spectroscopy require different coils for image acquisition and data on PCr/ATP and CMR perfusion, BOLD-SI cannot be simultaneously obtained. It has however been ensured that all data sets were acquired within the same scanning session and in closest proximity with each other as the techniques allow for.

CCTA was not performed in the normal volunteers to prevent unnecessary ionizing radiation exposure. Significant coronary artery disease was deemed to be unlikely in this normal cohort and this is further supported by the fact that perfusion and oxygenation values were within the normal range.

4.8 Conclusions

The pre-existing energetic deficit in diabetic cardiomyopathy is further exacerbated during exercise. While the myocardial PCr/ATP ratio at rest is not related to coronary microvascular dysfunction and is primarily a result of intrinsic metabolic dysfunction, during exercise, microvascular dysfunction appears to exacerbate the energetic deficit. Diabetes is associated with a reduction in perfusion reserve severe enough to lead to blunted myocardial oxygenation response during adenosine stress and further exacerbation of the energetic abnormalities during increased workload. These mechanisms may contribute to the pathophysiology of the cardiomyopathy process in diabetes.

4.9 Clinical Implications

The current study provides important insights into the interplay of perfusion, oxygenation and metabolic changes during stress in the diabetic heart. Presence of markers of poor prognosis such as myocardial energetic compromise and impaired perfusion reserve[28, 108], which have both been linked to contractile dysfunction and are predictors of mortality[28, 108, 134] has been identified here. Moreover, these findings were detected in a subclinical setting of well-controlled and stable patients, and more profound alterations may be expected in overt diabetic cardiomyopathy.

The findings here suggest that strategies aimed at improving metabolic reserve and myocardial oxygenation together, such as pharmacological activation of the hypoxia-

inducible factor (HIF) pathway, which increases angiogenesis, oxygen carrying capacity and metabolically upregulates oxygen-independent ATP synthesis[135], may in the future become therapeutic targets for patients with diabetic cardiomyopathy.

Future proof-of-principle clinical studies may use stress myocardial PCr/ATP and the BOLD SI change to monitor the early energetic and vascular response of the heart to novel therapies, and it is possible that these methods may provide surrogate markers of long-term prognostic effects.

Chapter 5

The Influence of Adiposity on Ectopic Lipid Deposition, Non-alcoholic Fatty Liver Disease and Cardiac Dysfunction in Type 2 Diabetes

5.1 Abstract

Background

Ectopic adiposity is frequently observed in obesity and type 2 diabetes mellitus (T2DM), is linked to insulin resistance, and may contribute to non-ischemic cardiomyopathy in these conditions.

Aims

The aim of this research was to investigate the relationship between ectopic adiposity, and both myocardial and hepatic structural, metabolic and functional changes in T2DM.

Methods

Twenty-seven obese T2DM patients (O-T2DM) (BMI 33 ± 3 kg/m^2), and fifteen lean T2DM patients (L-T2DM) (BMI 23 ± 2 kg/m^2), matched for age, gender, diabetes duration, treatment and HBA1c underwent cardiac CT (epicardial fat quantification), a multi-parametric liver MRI scan, including ^{1}H-MRS for hepatic triglyceride (HTG), T1 and T2* mapping yielding an 'iron-corrected T1' (cT1) and liver inflammation and fibrosis score (LIF-score: a parameter which allows non-invasive quantification of fibroinflammatory liver disease), cardiac MRI (cine and tagging), ^{1}H-, ^{31}P-MRS for myocardial triglyceride (MTG) and PCr/ATP respectively. Healthy volunteers underwent identical MRI protocols.

Results

Epicardial fat volumes (99 ± 41 cm^3 vs 72 ± 22 cm^3, P = 0.04), liver triglyceride (14.28 ± 8.41%, vs 8.43 ± 5.54%, P = 0.03), liver inflammation and fibrosis score (2.6 ± 0.8 vs 1.3 ± 0.7, P < 0.001) were higher in O-T2DM compared to L-T2DM, when MTG (1.22 ± 0.93% vs 1.14 ± 0.63%, P = 0.80) and myocardial PCr/ATP (1.67 ± 0.33 vs 1.68 ± 0.31, P = 0.92) were not significantly different. Left ventricular ejection fraction (68 ± 8%, vs 74 ± 5%, P = 0.01), peak systolic circumferential strain (13.4 ± 3.6% vs 15.8 ± 2.8%, P = 0.04) were lower in O-T2DM compared to L-T2DM. The estimate of insulin resistance obtained by homeostasis model assessment correlated with epicardial fat volumes (R = 0.446, P = 0.03), and liver fibrosis and inflammation score (R = 0.684, P = 0.001). L-T2DM was also however associated with elevated cT1, indicating liver fibrosis compared to healthy volunteers (P = 0.004).

Conclusions

Ectopic adiposity is more pronounced in O-T2DM patients and is linked to insulin resistance, liver fibrosis and inflammation, and cardiac contractile dysfunction.

5.2 Introduction

The prevalence of type diabetes mellitus (T2DM) continues to increase and is driven in part by the accompanying obesity epidemic. T2DM is associated with an increased risk of heart failure[6] and cardiovascular mortality[1]. Adiposity is likely to be a strong contributor to non-ischemic cardiomyopathy in patients with diabetes[63]. However, it is also well known that there are many lean diabetes patients and many overweight individuals without diabetes and relatively little is known about the cardiac disease phenotype of diabetic patients with low-normal body mass index (≤25 kg/m^2).

Accumulating evidence suggests that ectopic/visceral adiposity, confers a much higher cardiovascular risk than subcutaneous adiposity[64-66] and this may also play a role in the pathogenesis of non-ischemic cardiovascular diseases associated with obesity[67]. This is further supported by the association between non-alcoholic fatty liver disease (NAFLD) and epicardial fat thickness, which are markers of ectopic adiposity, and the cardiac structural and functional changes[136, 137]. The precise underlying mechanism linking ectopic adiposity in obesity and T2DM to CVD remains unclear, but one candidate mechanism that has emerged is insulin resistance.

Computed tomography (CT), and Proton (^{1}H-) magnetic resonance spectroscopy (MRS) are excellent tools in the study of ectopic adiposity, as they allow for quantification of variations in body fat distribution, and provide a more complete understanding of associated metabolic risk. Furthermore, multi-parametric magnetic resonance imaging (MRI) allows non-invasive measurement of liver fibrosis, inflammation and haemosiderosis

in addition to steatosis with a high diagnostic accuracy[138], and all these may have independent effects on metabolic risk. Non-alcoholic fatty liver disease (NAFLD) represent a spectrum of liver pathology ranging from simple steatosis (accumulation of fat without associated inflammation) to non-alcoholic steatohepatitis (NASH; accumulation of fat associated with inflammation) and fibrosis which can progress to cirrhosis. In NAFLD assessment, multi-parametric MRI has shown good diagnostic accuracy for staging fibrosis and identification of steatohepatitis[138]. The objective of this study was to use these state of the art MR methods to assess and compare abnormalities of (1) LV morphology, (2) LV systolic and diastolic function (3) resting LV energy metabolism (4) Epicardial fat content, and (5) liver fibrosis, steatosis and haemosiderosis, that may be detected in obese (BMI ≥ 30 kg/m^2) type 2 DM patients and lean (BMI ≤ 25 kg/m^2) T2DM patients, with similar diabetes duration, treatment and comorbidities except for difference in BMI. It was hypothesised that the diabetes associated cardiac changes will be amplified by the co-existence of obesity, increasing the overall likelihood of developing heart failure in this population, and that the visceral adiposity/ectopic lipid deposition may play a pathophysiological role in diabetes/obesity related cardiomyopathy, which may be linked to insulin resistance.

5.3 Method

Study Population and Protocol

Twenty-seven obese type 2 DM patients and fifteen lean type 2 DM patients underwent CMR scanning protocol at 3 T as follows:

1. ^{31}P-MRS for assessment of myocardial PCr/ATP ratio as a measure of myocardial energetic status.

2. Cardiac and Liver ^{1}H-MRS for assessment of myocardial and hepatic steatosis.

3. Cine imaging to measure LV volumes, mass and function.

4. Multiparametric liver protocol for calculation of iron corrected T1 and the Liver Inflammation and Fibrosis score.

Inclusion and Exclusion Criteria

Subjects were excluded if they had a history of cardiovascular or liver disease, chest pain, tobacco smoking, hypertension (resting systolic blood pressure (BP) > 140 mmHg and diastolic BP > 90 mmHg), contraindications to MR imaging, ischemic changes on 12-lead ECG, or renal impairment (estimated glomerular filtration rate below 30 mL/min), alcohol intake above 21 units weekly for men or 14 units for women, and if they were taking insulin.

Anthropometric Measurements

Height and weight were recorded and BMI calculated. Blood pressure was recorded as an average of 3 supine measures taken over 10 minutes (DINAMAP-1846-SX, Critikon Corp). Fasting venous blood was drawn for glucose, triglyceride, HBA1c, renal and liver function and free fatty acids (FFA), full blood count tests as previously described[76]. Plasma glucose levels and fasting insulin were also recorded and homeostasis model assessment of insulin resistance (HOMA-IR) was used to evaluate insulin resistance (fasting serum insulin (μU/L) × fasting plasma glucose (mmol l^{-1})/22.5)[139].

Liver Magnetic Resonance Protocol

The liver multi-parametric MR protocol was previously described[138]. MR scans were performed using a 3-Tesla scanner (Tim Trio, Siemens Healthcare, Germany). Transverse abdominal T1 and T2* MR maps were acquired for the estimation of tissue water content and liver iron respectively. Patients attended for their MRI scans after an overnight fast.

Iron corrected T1 and the Liver Inflammation and Fibrosis score

T1 relaxation time increases with increases in tissue water content such as in fibrosis and inflammation. However, the presence of iron, which can be accurately measured from T2* maps, has an opposing effect on the T1. An algorithm has been created that allows for the bias introduced by elevated iron to be removed from the T1 measurements, yielding the iron corrected T1 (cT1).

Optimal cT1 cut-off points for the differentiation of: none, mild, moderate and severe liver disease have been derived from the association of cT1 with histological fibrosis in a previous study from our centre[138]. These cut-offs were used to develop the Liver Inflammation and Fibrosis (LIF) score, a standardised score (0-4).

LiverMultiScanTM (LMS, Perspectum Diagnostics, Oxford, UK) is a software product, developed specifically to measure cT1 and LIF scores from T1 and T2* maps. For this study, LMS was used to analyse anonymised images off-site, by investigators blinded to the clinical data. LIF scores were measured in a single, operator-defined, region of interest away from vascular and biliary structures.

5.3 Statistical analysis

All statistical analysis was performed with commercially available software packages (IBM SPSS Statistics, version 20). All data were checked for normality using Kolmogorov–Smirnov test and presented as mean ± standard deviations. Normally distributed data sets were analysed with the independent Student *t* test. The chi-square test was used to compare discrete data as appropriate. Bivariate correlations were performed using Pearson's or Spearman's method as appropriate. Correlations were assessed with all study subjects included. Significance was assumed at $P < 0.05$.

Statistical assessments of a gender differences in cardiac and hepatic features between subjects who were separated into world health organisation BMI categories and gender

groups were performed with analysis of variance (ANOVA) with post hoc Bonferroni corrections for between-group comparisons (4 groups).

5.4 Results

Study Population

Demographic, clinical, and biochemical data are shown in **Table 5.1**.

Twenty-seven obese T2DM patients (14 male, mean age 56 ± 8 years, BMI 33 ± 3 kg/m^2), with mean diabetes duration of 6.1 ± 4.7 years, mean HBA1c of 7.7 ± 1.4% and fifteen lean T2DM patients (9 male, mean age 56 ± 9 years, BMI 23 ± 2 kg/m^2), with mean diabetes duration of 6.6 ± 6.5 years, mean HBA1c of 7.4 ± 0.9%, were studied. Patients in both groups were of similar age, gender, and there were no significant differences in systolic and diastolic blood pressures, diabetes duration, diabetes treatment or metabolic profile.

Table 5.1: Clinical, Biochemical Characteristics

Variable	Lean T2DM patients N = 15	Obese T2DM patients N = 27	P value
Age, y	56 ± 9	56 ± 8	0.94
BMI, kg/m^2	23 ± 2	33 ± 3	< 0.001
BSA, m^2	1.84 ± 0.21	2.02 ± 0.21	0.011
Male,%	60	41	0.24
Diabetes duration, y	6.1 ± 4.7	6.6 ± 6.5	0.78
Systolic blood pressure, mmHg	131 ± 8	130 ± 9	0.76
Diastolic blood pressure, mmHg	76 ± 7	76 ± 7	0.74
Plasma fasting glucose, mmol/L	8.5 ± 3.0	9.2 ± 3.2	0.46
Glycated hemoglobin, %	7.4 ± 0.9	7.7 ± 1.4	0.40
Hematocrit, %	42 ± 3	43 ± 3	0.58
Insulin, pmol/L	107 ± 142	218 ± 255	0.21
HOMA-IR, %	1.43 ± 0.72	3.23 ± 2.26	0.02
Plasma triglycerides, mmol/L	1.92 ± 1.76	1.71 ± 0.81	0.62
Plasma free fatty acids, mmol/L	0.60 ± 0.43	0.68 ± 0.43	0.53
Total cholesterol, mmol/L	3.8 ± 0.8	4.1 ± 1.0	0.35
HDL, mmol/L	1.23 ± 0.29	1.20 ± 0.31	0.71
LDL, mmol/L	1.79 ± 0.81	2.16 ± 0.80	0.15
Medications, n (%)			
Metformin, n (%)	14 (93)	23 (85)	0.45
Sulphonylurea	4 (27)	12 (44)	0.27
Aspirin	2 (13)	7 (26)	0.35
Statin	8 (60)	19 (70)	0.51
ACE-I	7 (47)	10 (37)	0.56

Continuous data are mean ± SD unless otherwise indicated. Categorical data are frequency (percent) unless otherwise indicated. T2DM indicates type 2 diabetes mellitus; BMI, body mass index; BSA, body surface area; y, years; HDL, high density lipoprotein; LDL, low density lipoprotein; HOMA-IR, homeostasis model assessment of insulin resistance; ACE-I angiotensin-converting enzyme inhibitors.

Cardiac Geometry and Function

CMR results for LV volumes and function are summarized in **Table 5.2**. There were no significant differences in LV end-diastolic volumes between the obese T2DM and the lean T2DM patients (129 ± 29 ml, vs 118 ± 25 ml respectively, P = 0.20), LV mass (120 ± 29 g, vs 121 ± 32 g respectively, P = 0.90) or in maximal LV wall thickness (10.4 ± 0.9 vs 11.0 ± 2.3 respectively, P = 0.42). Similarly, the mean LV mass to volume ratios, were not significantly different between the groups (0.88 ± 0.19 vs lean T2DM patients 0.98 ± 0.27, P = 0.15), indicating no significant difference in LV structural remodelling.

LV ejection fraction was significantly lower in obese T2DM patients compared to lean T2DM DM patients (68 ± 8%, vs 74 ± 5% respectively, P = 0.01), although this remained within normal limits. Similarly peak systolic circumferential strain was impaired in obese T2DM patients compared to lean T2DM patients (13.4 ± 3.6% vs 15.8 ± 2.8% respectively, P = 0.04). As expected there was a positive correlation between the peak systolic circumferential strain and LV ejection fraction (R = 0.46, P = 0.004). The differences in diastolic strain rate between the obese T2DM patients and the lean T2DM patients did not reach statistical significance (56 ± 27 s^{-1}, vs 67 ± 19 s^{-1} respectively, P = 0.07).

Left atrial volumes were significantly increased in the obese T2DM patients compared to lean T2DM patients (75 ± 17 ml, vs 58 ± 12 ml respectively, P = 0.001).

Table 5.2 CMR and Cardiac MRS Findings

	Lean T2DM patients N = 15	**Obese T2DM patients N = 27**	**P value**
LV end-diastolic volume, ml	118 ± 25	129 ± 29	0.20
LV end-diastolic volume, indexed to BSA ml/m^2	61 ± 9	66 ± 11	0.12
LV ejection fraction, %	74 ± 8	68 ± 8	0.01
LV mass, g	121 ± 32	120 ± 29	0.90
LV mass index, g/m^2	65 ± 14	58 ± 10	0.07
LV mass to LV end-diastolic volume, g/ml	0.98 ± 0.27	0.88 ± 0.19	0.15
Left atrial volume,mm^3	58 ± 11	75 ± 17	0.001
Left atrial volume, indexed to BSA mm^3/ m^2	30 ± 11	36 ± 8	0.05
Peak systolic circumferential strain, negative (-) , %	15.8 ± 2.8	13.4 ± 3.6	0.04
Peak circumferential diastolic strain rate, s-1	67 ± 19	56 ± 27	0.07
Myocardial PCr/ATP ratio	1.68 ± 0.31	1.67 ± 0.33	0.92
Myocardial triglyceride, %(Lipid/water ratio)	1.14 ± 0.63	1.22 ± 0.94	0.80

Continuous data are mean ± SD unless otherwise indicated. Categorical data are frequency (percent) unless otherwise indicated. BSA indicates body surface area; T2DM, type 2 diabetes mellitus; CMR, cardiac magnetic resonance; LV, left ventricular, PCr, Phosphocreatine.

Cardiac & Hepatic Steatosis, Epicardial Fat Volume

There was no significant difference in myocardial triglyceride content between the obese T2DM patients and the lean T2DM patients (1.22 ± 0.93, vs 1.14 ± 0.63 respectively, P =

0.80). Hepatic triglyceride content was ~69% higher in obese T2DM patients (14.28 ± 8.41, vs 8.43 ± 5.54, P = 0.03, **Figure 5.1, A**). Hepatic triglyceride content correlated negatively with the peak systolic circumferential strain (R = -0.40, P = 0.02) and diastolic strain rate (R = -0.51, P = 0.003), but not with LV ejection fraction (R = -0.24, P = 0.15). Myocardial triglyceride content did not correlate with epicardial fat volumes (R = 0.31, P = 0.14), nor hepatic triglyceride content (R = -0.05, P = 0.81).

Obese patients with T2DM had higher epicardial fat volumes compared to lean T2DM patients (96 ± 40 cm^3 vs 71 ± 21 cm^3, P = 0.04, **Figure 5.1, B**). Epicardial fat volumes correlated negatively with peak systolic circumferential strain (R = -0.48, P = 0.008) and diastolic strain rate (R = -0.44, P = 0.02), but not with LV ejection fraction (R = -0.22, P = 0.22). Epicardial fat volumes also correlated with coronary calcium score (R = 0.63, P = 0.04). **Figure 5.2** shows representative images of epicardial fat volume in a lean and obese T2DM patient.

11 patients (n = 5 obese T2DM, n = 6 lean T2DM) had evidence of coronary calcification, with no significant difference in coronary calcium score (35 ± 55, vs 71 ± 99, P = 0.50).

Hepatic fibrosis and T1 mapping

Liver enzymes and multiparametric liver MRI results for hepatic fibrosis, steatosis and haemosiderosis are summarized in **Table 5.3**.

The mean cT1 was higher in the obese T2DM patients compared to lean T2DM patients (942 ± 116 ms vs 810 ± 61 ms respectively, P = 0.004, **Figure 5.1, C**) indicating liver

fibrosis/inflammation. The mean hepatic iron content was not different between the groups (1.3 ± 0.2 vs lean T2DM 1.4 ± 0.1, P = 0.93). Hepatic fat levels correlated positively with cT1 (R = 0.66, P = 0.001).

LIF score was higher in the obese T2DM patients compared to lean T2DM patients (2.6 ± 0.8 vs 1.3 ± 0.7, respectively, P < 0.001, **Figure 5.1, D**), indicating inflammation and fibrosis within the liver. There was also a positive correlation between LIF score and epicardial fat volume (R = 0.57, P = 0.01). **Figure 5.3** shows representative liver ^{1}H-MR spectra, shMOLLI liver T1 map and cardiac tagging in a lean and obese T2DM patient.

Only 5 obese T2DM patients and 2 lean T2DM patients had elevated liver enzymes (ALT > 45 IU/L), despite the significant changes detected by the multiparametric liver MRI.

Table 5.3 Liver Assessments

	Lean T2DM patients N = 15	**Obese T2DM patients N = 27**	**P value**
Liver Enzymes			
Bilirubin, umol/L	12 ± 6	11 ± 4	0.20
ALT, IU/L	31 ± 22	35 ± 17	0.55
Alk Phosphatase, IU/L	156 ± 49	160 ± 47	0.80
Albumin, g/L	45 ± 2	46 ± 3	0.63
Multiparametric Liver MRI			
cT1,ms	810 ± 61	942 ± 116	0.004
T2*,ms	20 ± 4	18 ± 5	0.35
Hepatic triglyceride content, % (Lipid/water ratio)	8.4 ± 5.6	14.3 ± 8.4	0.03
Liver iron, mg/g	1.34 ± 0.13	1.33 ± 0.19	0.93
LIF Score	1.26 ± 0.65	2.61 ± 0.82	< 0.001

Continuous data are mean ± SD unless otherwise indicated. Categorical data are frequency (percent) unless otherwise indicated. T2DM indicates type 2 diabetes mellitus; CMR, cardiac magnetic resonance; cT1, corrected T1; ms, milliseconds; mg/g, milligram/gram; LIF, liver inflammation and fibrosis score.

Myocardial Energetics

^{31}P-MRS results for myocardial energetics are summarized in **Table 5.4**. There was no significant difference in myocardial PCr/ATP ratio between the obese T2DM patients and the lean T2DM patients (1.67 ± 0.33, vs 1.68 ± 0.31 respectively, P = 0.92). There were no

significant correlations between the myocardial PCr/ATP ratio and hepatic triglyceride content (R = -0.168, P = 0.36), or with epicardial fat volume (R = -0.227, P = 0.27).

Table 5.4 Cardiac MRS Findings

	Lean T2DM patients N = 15	**Obese T2DM patients N = 27**	**P value**
Myocardial PCr/ATP ratio	1.68 ± 0.31	1.67 ± 0.33	0.92
Myocardial triglyceride, %(Lipid/water ratio)	1.14 ± 0.63	1.22 ± 0.94	0.80

Continuous data are mean ± SD unless otherwise indicated. Categorical data are frequency (percent) unless otherwise indicated. T2DM indicates type 2 diabetes mellitus; CMR, cardiac magnetic resonance; LV, left ventricular, PCr, Phosphocreatine.

Insulin resistance

Insulin resistance indicated by HOMA-IR was significantly higher in the obese T2DM patients compared to the lean T2DM patients (3.23 ± 2.26, vs 1.43 ± 0.72, P = 0.02). There was a significant positive correlation between HOMA-IR and liver cT1 (R = 0.684, P = 0.001), LIF score and between HOMA-IR and LIF score (R = 0.684, P = 0.001) indicating the level of liver damage may have a pathophysiological link to insulin resistance. Moreover, epicardial fat correlates with HOMA-IR (R = 0.446, P = 0.03). There was also a negative correlation between HOMA-IR and circumferential systolic strain (R = -0.508, P = 0.004).

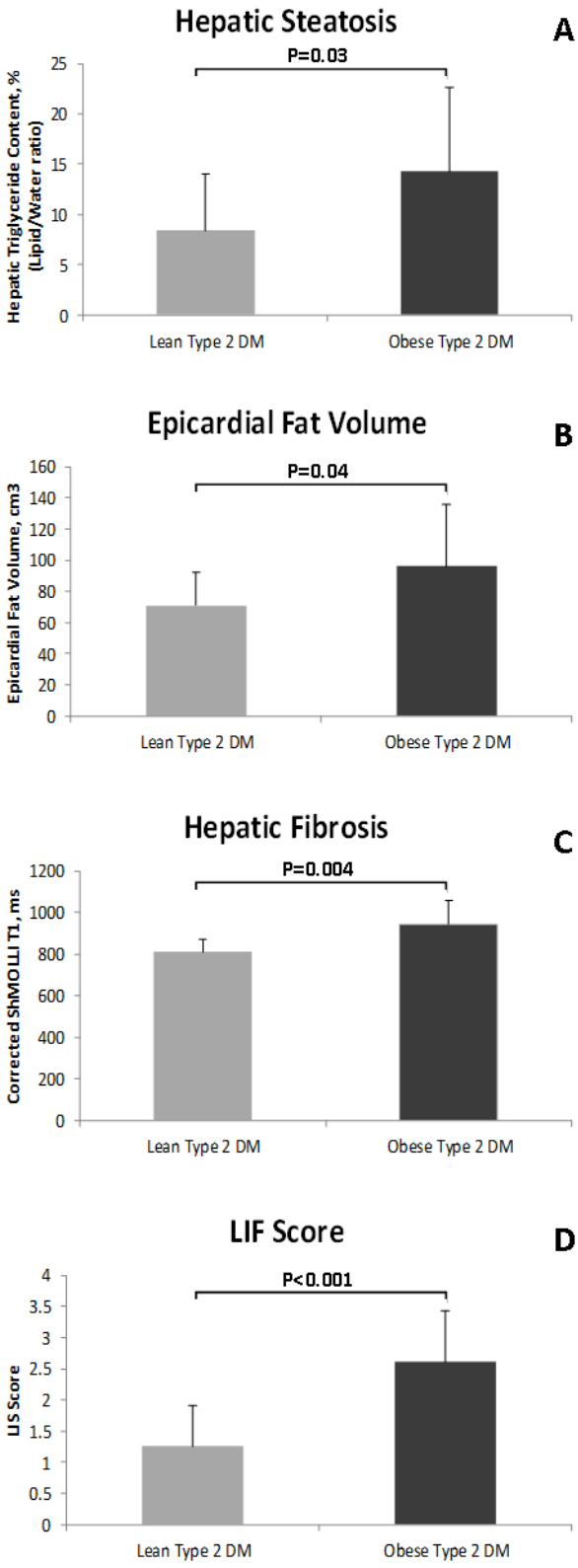

***Figure 5.1**: Differences in epicardial fat volumes, hepatic steatosis, hepatic fibrosis, and liver inflammation and fibrosis score between lean and obese patients with T2DM; **(A)** Epicardial Fat Volume (cm^3); **(B)** Hepatic triglyceride content (%); **(C)** hepatic corrected T1 map (ms); **(D)** LIF score.*

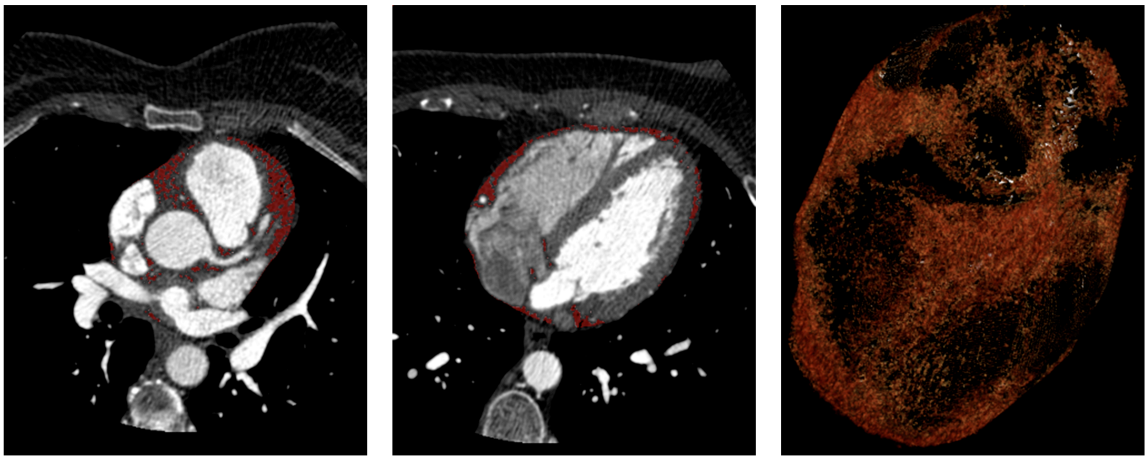

Lean Type 2 DM patient, epicardial fat volume = 37.75cm^3

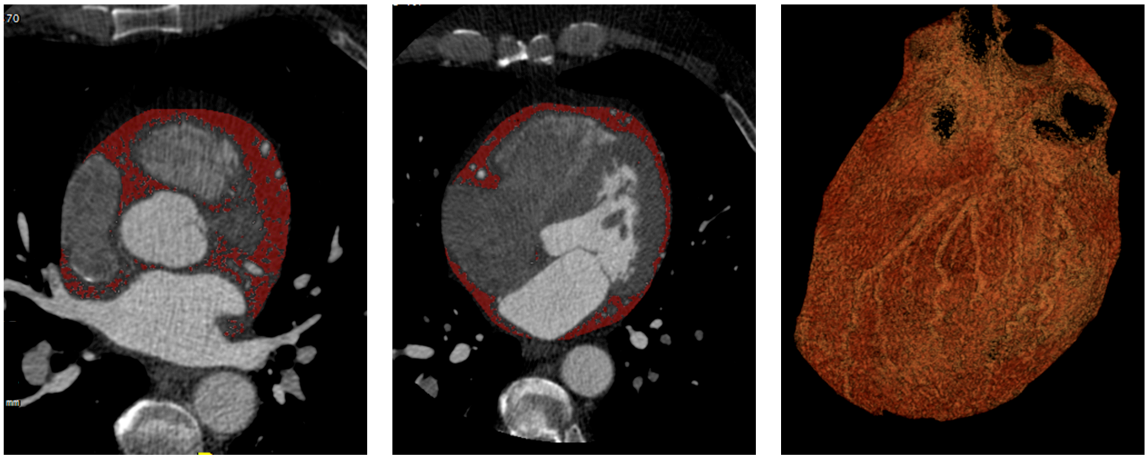

Obese Type 2 DM patient, epicardial fat volume = 192.59cm^3

Figure 5.2: *Representative examples of CT epicardial fat volumes in a lean and an obese patient with T2DM. Top panel: lean patient with T2DM with epicardial fat volume = 37.75 cm^3; second panel: obese patient with T2DM with epicardial fat volume = 192.59 cm^3.*

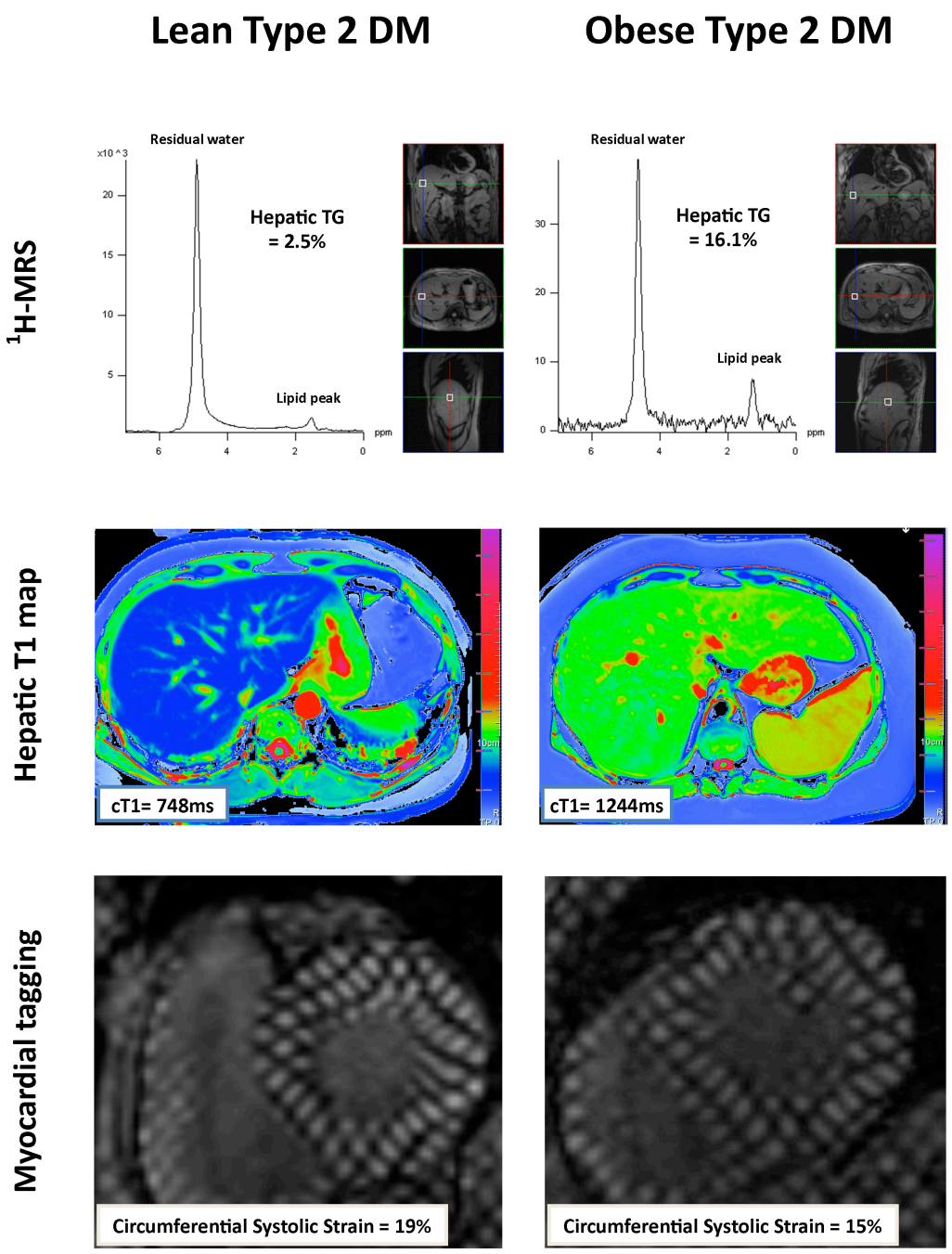

Figure 5.3: *Representative examples of ^{1}H-MRS , trans axial liver ShMOLLI T1 map and mid ventricular tagging in a lean and an obese patient with T2DM. Top panel: lean patient with T2DM ^{1}H-MRS with hepatic TG = 2.6, vs obese patient with T2DM hepatic TG = 16.1; second panel: lean patient with T2DM liver ShMOLLI T1 map with corrected T1 = 748 ms, vs obese patient with T2DM = 1244 ms; third panel: lean patient with T2DM mid ventricular myocardial tagging with circumferential systolic strain = 19%, vs obese patient with T2DM = 15%.*

Gender-specific differences in cardiac and hepatic characteristics for the study group

The gender differences in cardiac and hepatic features of diabetes have been further explored. Subjects were separated into world health organisation (WHO) BMI categories and gender groups (7 lean female, 10 lean male, 15 obese female and 10 obese male).

Age, BMI, systolic blood pressure, diabetes duration and metabolic profile were similar between men and women, stratified by lean, or obese diabetic groups, diastolic blood pressures were higher in both the lean and the obese diabetic men compared to lean and obese diabetic women **(Table 5.5).**

Table 5.5:
Clinical, Biochemical Characteristics

Variable	Lean T2DM female N=7	Lean T2DM male N=10	Obese T2DM female N=15	Obese T2DM male N=10	p Value
			Clinical		
Age, y	58 ± 10	56 ± 9	55 ± 8	56 ± 8	0.88
BMI, kg/m2	24.0 ± 2	24 ± 2	34 ± 5	33 ± 4	<0.001
Diabetes duration, y	8 ± 6	5 ± 6	7 ± 5	5 ± 4	0.52
Systolic blood pressure, mm Hg	130 ± 9	133 ± 6	128 ± 10	133 ± 5	0.15
Diastolic blood pressure, mm Hg	71 ± 7*, **	80 ± 4	73 ± 9*, **	80 ± 3	0.005
Plasma fasting glucose, mmol/L	10 ± 3	7 ± 3	9 ± 3	9 ± 2	0.21
Glycated hemoglobin, %	7.6 ± 0.9	6.9 ± 0.7	7.6 ± 1.2	8.1 ± 1.6	0.23
Insulin pmol/L	71 ± 32	115 ± 173	298 ± 325	175 ± 69	0.19
HOMA-IR, %	1.6 ± 0.7	1.2 ± 0.7	3.4 ± 2.7	3.6 ± 1.5	0.04
Plasma triglycerides, mmol/L	2.3 ± 2.5	1.5 ± 0.7	1.8 ± 0.9	1.7 ± 0.7	0.62
Plasma free fatty acids, mmol/L	0.68 ±0.1	0.57 ± 0.1	0.68 ± 0.6	0.67 ± 0.1	0.89
Total cholesterol, mmol/L	4.0 ± 0.3	3.8 ± 0.8	4.2 ± 1.2	3.9 ± 0.7	0.83
HDL, mmol/L	1.4 ± 0.5	1.2 ± 0.3	1.2 ± 0.3*	1.1 ± 0.2	0.11
LDL, mmol/L	1.7 ± 0.5	1.9 ± 0.7	2.2 ± 1	2.1 ± 0.6	0.51

Values are mean ±standard deviation. T2DM indicates type 2 diabetes mellitus; BMI, body mass index, y, years; L, litre; HDL, high density lipoprotein; LDL, low density lipoprotein

P values are for ANOVA for groups specified.

*P < 0.05, normal weight males vs. normal weight females.

#P < 0.05, obese males vs. normal weight males.

†P < 0.05, obese females vs. normal weight females.

≠P < 0.05, obese females vs. obese males.

** P < 0.05, lean females vs. obese males

Comparison of the CMR and the MRS data **(Table 5.6)** showed that the LVEDV, LV mass was smaller in the lean female diabetes patients, compared to lean male diabetics and obese male diabetics, but not compared to obese female diabetics. Interestingly, in males, LV-EDV, LV mass, LV wall thickness, left atrial volumes were all similar between the lean and obese males. Apart from the difference in left atrial volumes (higher in obese female diabetics) there were no significant differences in LV mass, volumes and ejection fraction and wall thickness between obese and lean female diabetics. There were no differences in myocardial lipids and energetics across the groups.

As a result, the differences between the obese and lean T2DM patients when looking at the data of both genders together in left atrial volumes were driven by the increase in the left atrial volume of the female obese T2DM patients, and the peak circumferential systolic strain was lowest in the obese male T2DM patients and closer to normal in the lean female T2DM patients.

Comparison of the hepatic lipid and cT1 data **(Table 5.6)** showed that the obese diabetic men and obese women had significantly elevated cT1 compared to lean diabetic men, when both genders of the obese group cT1 levels did not reach statistical significance when compared to lean female diabetes patients. The numeric differences in hepatic lipids did not reach statistical significance between the gender and BMI classified groups.

Table 5.6: Multiparametric MRI and MR Spectroscopy characteristics for the study group separated into WHO BMI categories and gender groups

Variable	Lean T2DM female N=7	Lean T2DM male N=10	Obese T2DM female N=15	Obese T2DM male N=10	p Value (ANOVA)
MRI					
LV end-diastolic volume, ml	100 ± 11*, **	138 ± 32	122 ± 20	136 ± 31	0.02
LV end-systolic volume, ml	26 ± 6	40 ± 20	35 ± 6	50 ± 16	0.005
LV stroke volume, ml	74 ± 7	98 ± 17	87± 15	86 ± 26	0.07
LV ejection fraction, %	74 ± 4**	72 ± 7	71 ± 3≠	63 ± 11#	0.006
LV wall thickness, mm	10.1 ± 3.2	11.2 ± 1.2	9.8 ± 1.5	11.7 ± 2.1	0.09
LV mass, g	96± 27*, **	140 ± 22	110 ± 28	134 ± 23	0.002
LV mass index, g/m2	56 ± 15**	70 ± 11	55 ± 11	61 ± 30	0.01
LV concentricity, g/ml	0.89 ± 0.36	1.01 ± 0.17	0.81 ± 0.14	0.98 ± 0.21	0.11
Left atrial volume, mm^3	52 ± 11	67 ± 19	76 ± 14†	69 ± 17	0.02
Native myocardial T1 value, ms	1195 ±8	1183 ±6	1193 ±5	1194 ±9	0.06
Extra cellular volume fraction	0.31 ± 0.02	0.28 ±0.02	0.31 ± 0.02	0.28 ± 0.02	0.005
Mid short axis peak systolic circumferential strain, negative (-) , %	17.0 ± 3.2**	15.1 ± 3.7	15.1 ± 1.6≠	10.9 ± 1.6	0.001
Peak circumferential diastolic strain rate, s^{-1}	71 ± 28	62 ± 14	56 ± 18	58 ± 39	0.69
Hepatic cT1, ms	831± 57	782 ± 55	948 ± 123 **ω**	956 ± 98#	0.009
MRS					
PCr/ATP ratio	1.53 ± 0.28	1.83 ± 0.29	1.66 ± 0.37	1.64 ± 0.27	0.29
Hepatic	6 ± 4	10 ± 5	14 ± 8	17 ± 9	0.03

triglyceride content, %(Lipid/water ratio) Myocardial lipid content, %(Lipid/water ratio)	0.88 ±0.40	1.16 ± 0.60	1.09 ± 0.64	1.65 ± 1.4	0.47

Continuous data are mean ± SD unless otherwise indicated. Categorical data are frequency (percent) unless otherwise indicated. MRI, indicated Magnetic Resonance Imaging,; LV, left ventricular; RV, right ventricular; SR, strain rate, MRS indicates Magnetic Resonance Spectroscopy PCr, phosphocreatine; ATP, adenosine triphosphate.

*P < 0.05, lean females vs. lean males.
#P < 0.05, obese males vs. lean males.
†P < 0.05, obese females vs. lean females.
≠P < 0.05, obese females vs. obese males.
** P < 0.05, lean females vs. obese males
ω P < 0.05, obese females vs. lean males.

5.5 Discussion

Epicardial fat and liver fat are markers of ectopic adiposity, linked to insulin resistance in overweight/obese patients with T2DM, and are modifiable cardiovascular risk factors[140, 141]. Using CMR, MRS, cardiac CT, and multiparametric liver scan, it is shown here, that obesity, in the presence of diabetes, is associated with higher epicardial fat volumes, significant NAFLD and liver fibrosis and inflammation, higher insulin resistance, but not with exacerbated deficit in myocardial energetic status or more pronounced cardiac steatosis. It is also demonstrated that despite no significant difference in diabetes duration, treatment, medical history or the metabolic profile, obesity in patients with T2DM was associated with worse cardiac contractile function indicated by significantly lower systolic strain, and lower, but within normal limits LVEF; but no difference in LV morphology compared to diabetes in

the lean patients. Importantly, it has been demonstrated here for the first time, not only the hepatic triglyceride content, but also liver fibrosis and inflammation score, correlate significantly with epicardial fat volumes. Moreover, in line with previous studies, these markers of ectopic fat deposition correlate with insulin resistance[73, 142], and with systolic strain and diastolic strain rates, suggesting body fat distribution may contribute to insulin resistance and cardiovascular disease in patients with diabetes. As ectopic adiposity is modifiable[143], this strategy provides the potential for novel therapies aimed at reversing insulin resistance, improving cardiac and liver function in obesity and diabetes.

Ectopic Adiposity, Insulin Resistance and Cardiac Dysfunction

It is now widely accepted that adipose tissue is a dominant regulator of lipid and glucose metabolism. Growing observations support the concept that insulin resistance is prompted, and sustained by, dysregulated fat tissue[94, 144-148]. In addition, insulin resistance and ectopic adiposity carries even a greater cardiovascular risk[149, 150]. It has now been established that obese subjects with T2DM are at high risk of developing ectopic adiposity[151].

Epicardial adipose tissue is an ectopic fat depot with dichotomous functional characteristics, adverse and protective, interacting locally with the coronary arteries and the myocardium through paracrine or vasocrine pathways. Under physiological conditions, epicardial fat supplies energy and heat to the myocardium and exerts a protective modulation of the coronary arteries[74, 75, 152]. Its pathological increase, and the co-existence of other metabolic and hemodynamic abnormalities, turn it into an adverse lipotoxic, prothrombotic and proinflammatory organ[150].

Here, higher epicardial fat volumes in obese patients with T2DM compared to lean diabetics was shown. It has also been confirmed that epicardial fat is associated with liver steatosis[153], when myocardial triglyceride content may present a separate entity that is influenced by factors beyond visceral adiposity, suggested by the dissociation of myocardial steatosis from epicardial and liver fat in this study[154]. Moreover, this study provides evidence for the relationship between ectopic adiposity, insulin resistance and cardiovascular disease. These findings suggest that the strategies aimed at improving

adipocyte function may lead to reversal of insulin resistance and this may promote improvement of cardiac function in the diabetic heart.

Non-alcoholic Fatty Liver Disease, Hepatic Fibrosis, Obesity and Type 2 DM

NAFLD is one of the most common manifestations of excessive fat accumulation in the liver. It is among the leading causes of death in T2DM[155] and linked to hepatic insulin resistance[156]. Despite this strong association and the emergence of NAFLD as a novel cardiovascular risk factor, only a few studies have addressed the presence of myocardial structural and functional changes in patients with NAFLD. Specifically, NAFLD, diagnosed either by ultrasonography or by liver biopsy, was shown to be associated with a higher prevalence of low coronary flow reserve[157], coronary calcification[158], significant impairment in echocardiographic diastolic function[137], concentric remodelling and reduced longitudinal shortening[159].

This study is the first to date to non-invasively assess the severity of liver damage using a multi-parametric MRI protocol and delineate the influence of obesity in patients with T2DM on the presence of NAFLD and its impact on cardiac structure. This study has demonstrated that significant NAFLD is present in asymptomatic obese T2DM patients compared to lean diabetics, importantly with no significant difference in ALT levels. Using multiparametric MRI of liver, it has been shown here, fibrosis was linked not only with the parameters of cardiac contractile and diastolic function, but also with the indices insulin resistance.

5.6 Limitations

This study is limited by a relatively small sample size, in line with its proof-of-principle nature.

Of the 42 patients with T2DM, 9 patients (21%) did not consent to have CCTA performed and as such it is possible that occult coronary artery disease could be present in this minority of patients.

Whilst the release of various adipokines including Adiponectin and Leptin has been considered among the important actions of adipocytes, in this study the circulating levels of Adiponectin or Leptin were not assessed

5.7 Conclusion

When compared to lean T2DM patients, obese patients with T2DM exhibit ectopic/visceral fat deposition and impaired cardiac systolic strain. This ectopic/visceral fat deposition is associated with liver fibrosis and inflammation, insulin resistance, and cardiac diastolic and systolic dysfunction. Myocardial steatosis is not associated with ectopic adiposity in other organs, and myocardial steatosis may thus represent a separate entity that is influenced by factors beyond ectopic/visceral adiposity. Importantly, as body fat distribution is modifiable, strategies aimed at reducing ectopic adiposity, may potentially improve contractile function and prognosis in patients with diabetes.

Chapter 6

7T versus 3T ^{31}Phosphorus Magnetic Resonance Spectroscopy in Patients with Type 2 Diabetes Mellitus

6.1 Abstract

Background and Aims

Phosphorus magnetic resonance spectroscopy (^{31}P-MRS) allows for unique insight into cardiac energetics but inherently has a low intrinsic signal-to-noise ratio (SNR). The theoretically predicted increased SNR at 7T compared to 3T, may allow detection of smaller changes in metabolite concentrations or measurement of changes in smaller patient groups.

Methods

Eleven normal weight / mildly overweight patients with T2DM were scanned at 3T and 7T scanners and SNR and PCr/ATP ratios compared. Matched data acquisition was performed at 3T and 7T, on 11 patients with T2DM who had no contraindications for being scanned at 7T, using coils of equal dimensions. Monte Carlo error propagation was used to calculate the Cramer-Ráo lower bounds (CRLB) in PCr concentration assessment as a measure of error. The CRLB quantify the minimum precision of the fitted parameters, therefore it is a measure of accuracy.

Results

In the paired 3T-vs-7T study (N = 11), at 3T the mean PCr/ATP value was 1.68 ± 0.24 compared to 1.72 ± 0.39 at 7T (P = 0.775). The PCr/ATP ratio was consistent between the two field strengths; with no statistically significant difference. PCr SNR increased 1.54x at 7T relative to 3T (19.4 ± 7.2 vs 12.6 ± 3.9, P = 0.024), the CRLB in PCr concentration decreased

1.7x (7.6 ± 2.3 vs 13.0 ± 3.6 respectively, P = 0.009), the PCr/ATP standard deviation (SD) remained unchanged (20.4 ± 8.2 vs 20.3 ± 3.8, P = 0.955). The decrease in CRLB at higher strength field represents the fact that the metabolites are indeed quantified more precisely at 7T compared to 3T.

Conclusions

This study has demonstrated for cardiac ^{31}P-MRS at 7T is feasible for assessment of patients with T2DM and well tolerated. Cardiac ^{31}P-MRS at 7T has higher SNR and the spectra can be quantified more precisely than at 3T. 7T may be recommended as the field strength of choice for future clinical applications of ^{31}P-MRS.

6.2 Introduction

^{31}P-MRS revolutionised our understanding of cardiac and skeletal muscle metabolism[160-163]. Myocardial ^{31}P-MRS reveals the biochemistry of ATP, ADP and phosphocreatine (PCr), which are critical to the supply of energy for contractile work in the myocardium[164]. Derangement of the ratio of concentrations of PCr to ATP measured by ^{31}P-MRS (the 'PCr/ATP ratio') is predictive of mortality[161]; reduction of the creatine-kinase flux is seen in patients with myocardial infarction[165]; and changes in the PCr/ATP ratio during pharmacological stress are associated with cardiac pathologies, as also demonstrated by the work in this thesis, possibly as result of metabolic as well as microvascular dysfunction[109]. However, clinical applications of ^{31}P-MRS have not yet seen widespread acceptance, mainly as a consequence of the method's low intrinsic signal-to-noise ratio (SNR) (^{31}P-MRS has ~10^{-5}x lower $\mathrm{SNR}/\sqrt{t}$ than ^{1}H MRI) [166].

MR physics predicts that the quality of the raw ^{31}P-MRS signal ($\mathrm{SNR}\cdot t^{-1/2}$) would increase approximately in proportion to the scanner's magnetic field strength B_0 [167, 168]. Increasing B_0 would thus offer the potential for significant increases in ^{31}P-MRS performance, provided that the anticipated gains in ^{31}P Boltzmann equilibrium magnetization and RF receive sensitivity outweigh any exacerbation of the effects of B_0-inhomogeneity, RF-induced heating and increased RF thermal noise at the higher field strength. At 3T, ^{31}P-MRS typically takes at shortest ~9min and at longest ~30min to acquire metabolite concentrations in three 5.6mL voxels covering the interventricular septum[118]. The spectral SNR at 3T is 2.1x greater than was the case using equivalent methods at 1.5T[169], making 3T the more popular

choice for cardiac ^{31}P-MRS for investigators. However, even at 3T, wider application of ^{31}P-MRS has remained constrained by its limited SNR.

^{31}P capability of the whole-body 7T MRI scanners has recently been demonstrated in healthy volunteers[121]. The theoretical predictions are as such that cardiac ^{31}P-MRS may show a further significant (approximately 2.3x) increase in $\mathrm{SNR}/\sqrt{t}$ compared to the performance available at 3T. This gain in $\mathrm{SNR}/\sqrt{t}$ would be important as it may potentially 1) Lower variability to allow reliable individual subject comparisons; 2) Give sufficient spatial resolution to study focal disease; 3) Detect metabolites that cannot be detected at lower fields, such as inorganic phosphate.

The inherently long acquisition times associated with cardiac ^{31}P MRS is another major limitation of the method, making cardiac ^{31}P-MRS unfeasible for studies of highly symptomatic patients, children, or for the application of cardiac exercise stress testing. A common approach to reducing ^{31}P-MRS acquisition times is to reduce the spatial resolution (increase voxel size). The downside of this approach is the consequent reduction of specificity of cardiac signal acquisition, resulting in contamination from neighbouring tissues. However, these issues were addressed at 3T in a previous study in our centre and signal contamination arising from adjacent voxels was solved by the use of saturation pulses issued over neighbouring tissues[170, 171]. This essentially saturates any signal from the tissue covered by the saturation bands. This study used a protocol at 3T that has adopted a reduced resolution approach achieving an acquisition time of 9 minutes (nominal voxel volume 11.2 ml, true voxel volume is 93 ml) but it still maintained myocardial specificity by

using acquisition weighting, and by careful placement of muscle and liver saturation bands to reduce the potential contamination still further as described before[171].

Dramatic increase in SNR has been demonstrated in a previous proof-of-principle study for 7T human cardiac ^{31}P-MRS in normal volunteers[121]. The study had compared similar length protocols (30 min acquisition in both fields), however the current study is the first to compare the 30 min protocol at 7T to the currently most frequently practiced shorter (9 min) protocol at 3T in patients with T2DM.

Thus, the aims of this project were to 1) Demonstrate a proof-of-principle of 7T cardiac ^{31}P-MRS in patients with T2DM, a metabolic disease of epidemic proportions, and 2) To compare the performance at the 7T longer protocol against an established protocol at 3T. It was hypothesised that cardiac ^{31}P-MRS at 7T would have higher SNR and the spectra could be quantified more precisely than at 3T, with a decreased error in PCr concentration, and decreased PCr/ATP standard deviation, potentially allowing for smaller numbers of study populations recruited to show differences.

6.3 Methods

Subjects

11 patients with T2DM were enrolled. Inclusion and exclusion criteria were as in Chapter 2, however scanning at 7T had extra considerations. The 7T safety information is provided in Appendix 1.

All subjects underwent ^{31}P-MRS at 3T and 7T field strengths.

Protocol

3T ^{31}P-MRS acquisition protocol

Scans at 3T used a Trio MRI scanner (Siemens, Germany) equipped with a 10cm ^{31}P Tx/Rx loop coil (PulseTeq, UK). Subjects were scanned in a prone position. Pilot images of the vertical long axis, the horizontal long axis and a 3D stack of short axis images were initially acquired. Localization at 3T was performed with bSSFP and CINE images acquired using the body coil.

Eight non-localised inversion recovery spectra, consisting of a 1000 μs hard inversion pulse with inversion delay varied from 0.1 to 3 seconds, were acquired to measure the flip angle in a phenyl phosphoric acid (PPA) reference fixed inside the radio frequency (RF) coil housing. Using home-written software in Matlab 6.5 (Mathworks, Natick, USA), the measured flip angle achieved at the PPA reference was combined with a calculated RF field

profile of the RF coil and short-axis stack of images to determine the subject specific flip angle at the selected voxel of interest.

All ^{31}P MRS data was acquired with a three dimensional acquisition weighted chemical shift imaging technique (AW-CSI)[172] with 10 averages at the centre of K-space and ultrashort TE[173] to minimise T2 effects and first order phase artefacts. An optimised RF pulse[118] centred between γ and α ATP resonance frequencies was used to ensure uniform excitation of all spectral peaks. Five Nuclear overhauser effect (NOE) pulses (2.5 ms, 222.2 V separated by 80.5 ms) were used to increase signal to noise (correction factors detailed below). Acquisition matrix was 16 x 8 x 8 mm^3 for the 3T protocol. Field of view was 240 x 240 x 200 mm^3. The high resolution acquisition was run with TR of 720 ms. The 3T protocol employed two 25 mm saturation bands placed over chest wall muscle and an additional 25 mm saturation band placed over liver.

The CSI grid was placed with a central voxel in the mid-ventricular septum on the first short axis image in which the papillary muscle was visible. The CSI grid was positioned such that the voxel was orientated down the long axis of the intra-ventricular septum, and rotated to maximise coverage of the septal myocardium by one low resolution voxel.

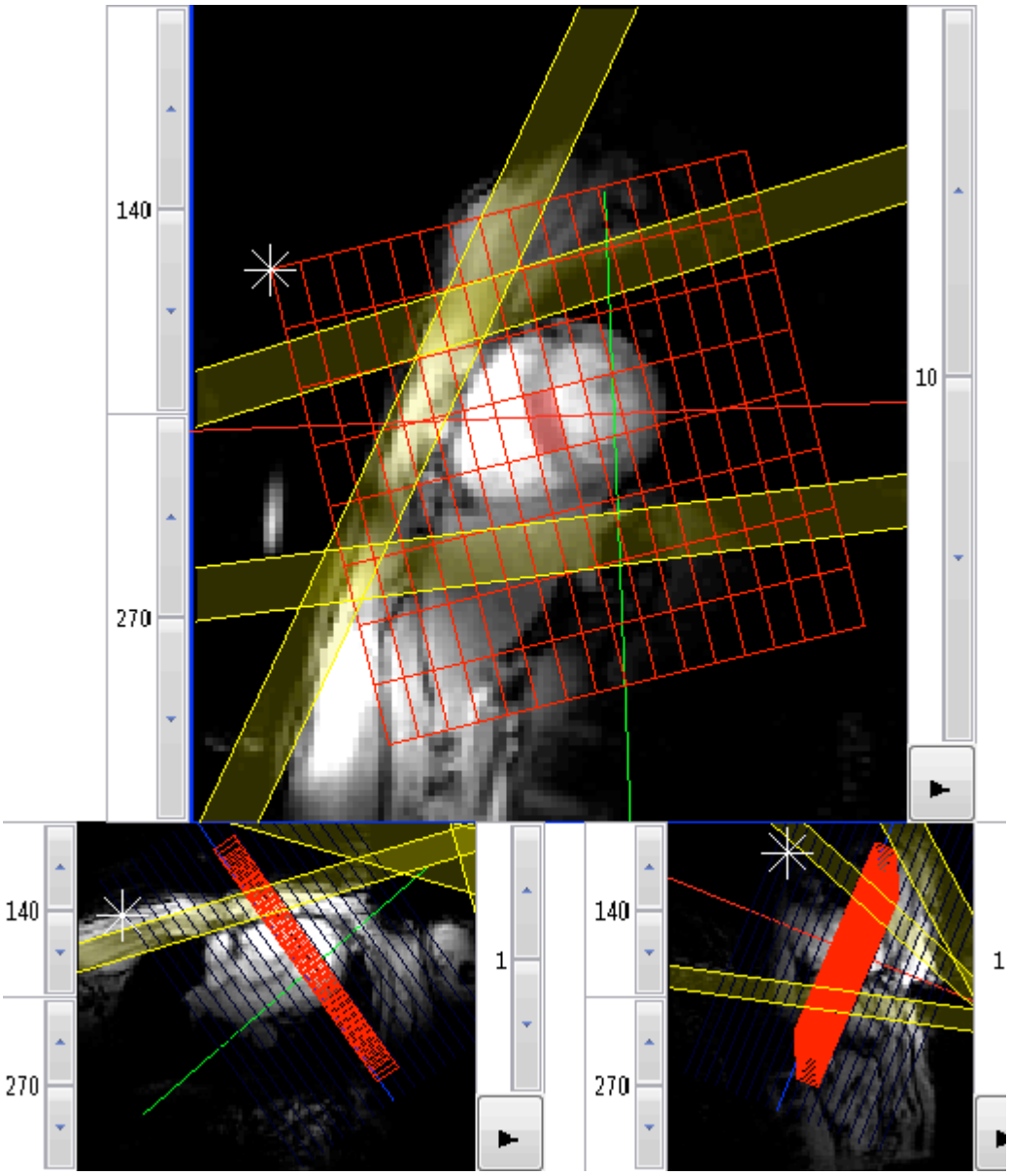

Figure 6.1: *Voxel selection at 3T.*

7T ^{31}P-MRS acquisition protocol

Scans at 7T used a Magnetom 7T scanner (Siemens, Germany), with a T/R switch and preamplifier module (Virtumed, MN, USA), and a purpose-built 10cm ^{31}P Tx/Rx loop coil whose housing has the same subject–coil distance as the 3T coil. As 7T scanners do not

have built-in body coils, localization at 7T was performed using a separate 10cm ^{1}H loop surface coil to record CINE FLASH images with pulse oximeter gating (Siemens, Germany). The ^{1}H coil was then removed and replaced with the 10cm ^{31}P loop coil in the same position above the interventricular septum. Subjects were scanned supine to facilitate the exchange of ^{1}H and ^{31}P coils at 7T, but since the body coil was not an issue at 3T, acquisitions were carried out prone at 3T field strength. Prone and supine ^{31}P-MRS spectra acquisitions were compared by a previous study and no discernible difference was detected[174]. Spectroscopy sequences used no gating to avoid the possibility of bias due to increased mis-triggering at 7T[175].

Spectroscopy acquisitions used the ultra-short-TE chemical shift imaging (UTE-CSI) pulse sequence[169]. The protocol and sequence parameters were adapted to accommodate the more restrictive limits on peak B_1^+ and SAR at 7T, starting from what has been used for several years at 3T[169].

Then, a set of non-localized inversion recovery free induction decays (FIDs) and a set of images (^{31}P FLASH projection images covering 3 orthogonal planes at 7T) were recorded. From these, the coil location, transmit efficiency and B_1 profile were computed with custom Matlab (MathWorks, Natick, MA) code.

For each subject, the mid-septal voxel in the most basal short-axes plane showing the papillary muscles was chosen for further analysis. Spectra were recorded using the UTE-CSI pulse sequence with a 16x16x8 matrix, 15x15x25 mm^3 (i.e. 5.6 mL) nominal voxel size, acquisition weighting with 10 averages at k = 0 and T_R = 1 s. At 7T, excitation was always at

the full power supported by the coil (270 V) giving a flip angle of ~20° in the inter-ventricular septum. A 25 mm-thick saturation band was placed to suppress signal from skeletal muscle in the anterior chest wall. The exact voltage was set to the maximum permissible given the SAR limits for each subject. The HS8 excitation pulse bandwidth of R/Tp = 11/8 = 1.4 kHz was selected to minimise the chemical shift displacement artefact while still giving effective saturation.

The final uncertainty in metabolite concentrations was expressed using Monte Carlo error propagation to calculate the Cramer-Ráo lower bounds (CRLB)[176]. The CRLB quantify the minimum precision of the fitted parameters, therefore it is a measure of accuracy. Statistical comparisons were made in Matlab using paired comparisons wherever possible[177].

Image Analysis

After each scan, the following analysis was performed using a purpose-made Matlab program. First, the voxel lying at the centre of the inter-ventricular septum was extracted for analysis. The spectrum there was fitted using AMARES[178] together with prior knowledge specifying 11 Lorentzian peaks (α,β,γ-ATP, PCr, PDE and 2x 2,3-DPG) and fixed amplitude ratios and scalar couplings for the multiplets. The fitted amplitudes were then corrected for blood contamination by subtracting 30% of the average of the two 2,3-DPG signals from each of the ATP amplitudes[179]. The remaining PCr and ATP signals were corrected for the effects of partial saturation[180] using the flip angle at the centre of the voxel, assuming no motion effects and with the T_1s. The final PCr/ATP ratio was taken as the ratio of the blood

and saturation-corrected values of PCr / γ-ATP, discounting the α-ATP peak since it has contributions from $NADPH^+$ and the β-ATP peak had a phase artefact in some subjects at 7T. Finally, the spectral SNR was determined by applying a matched filter and then measuring the SNR as the peak height / baseline SD[181].

6.4 Results

Study Population

Eleven, normal/mildly overweight T2DM patients (9 male, mean age 55 ± 9 years, BMI 24.6 ± 2.5 kg/m^2), mean HBA1c of 7.6 ± 1.6%, were studied. For each subject, both scans were performed in mornings, to minimise physiological variation.

3T vs 7T

In the paired 3T-vs-7T study (N = 11), the PCr/ATP ratio was consistent between the two field strengths; with no statistically significant difference **(Figure 6.2).** PCr SNR increased 1.54x at 7T relative to 3T (19.4 ± 7.2 vs 12.6 ± 3.9, P = 0.024), the Cramer-Ráo uncertainty (CRLB) in PCr concentration decreased 1.7x (7.6 ± 2.3 vs 13.0 ± 3.6 respectively, P = 0.009, **Figure 6.3**) , the PCr/ATP SD remained unchanged (20.4 ± 8.2 vs 20.3 ± 3.8, P = 0.955). At 3T the mean PCr/ATP value was 1.68 ± 0.24 compared to 1.72 ± 0.39 at 7T (P = 0.775). The CRLB gives a lower bound to the accuracy of the fitted parameters. The decrease in CRLB at higher strength field represents an improved precision in metabolite quantitation at 7T

compared to 3T. The SNR improvement with field strength varied noticeably between subjects (e.g., PCr SNR increased 1.38, 1.40, 1.32, 1.55, 0.92, 0.85, 4.37, 1.09, 1.37, 2.9).

Linewidths previously reported at 3T for PCr are in the order of 21 ± 8 Hz [169], the mean PCr linewidth favourably increased at 7T to 36 ± 12, by 1.7x (P = 0.004)(**Figure 6.4**). In this study only "tune up" B_0 shims were used because of difficulties with 1H image-based shimming at 7T due to the inhomogeneous B1 from the 1H loop. Therefore, the 7T ^{31}P linewidths here represent an (although encouragingly good) worst case for future studies.

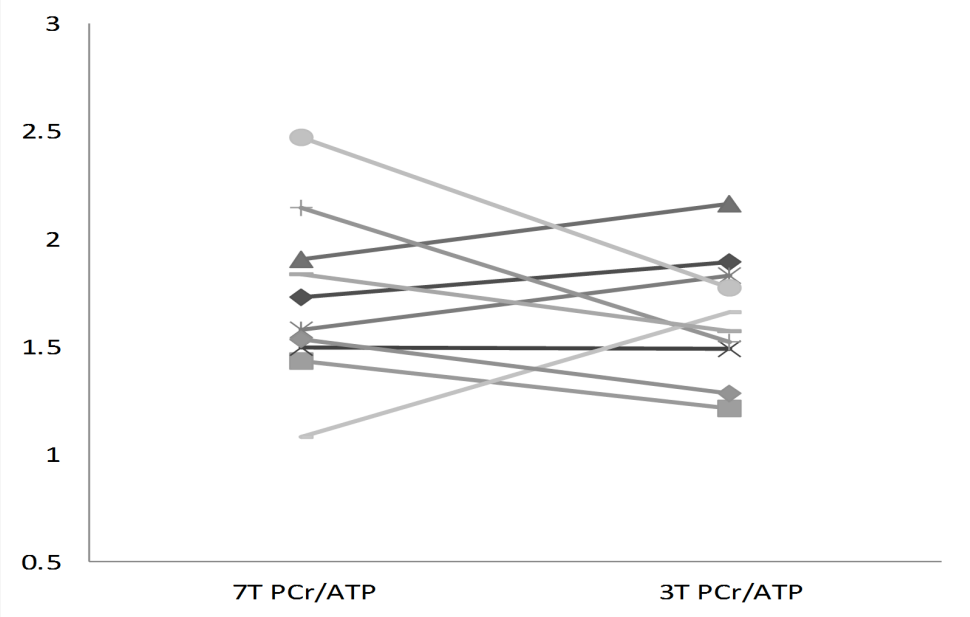

Figure 6.2: *The mean PCr/ATP paired comparison between two strength fields.*

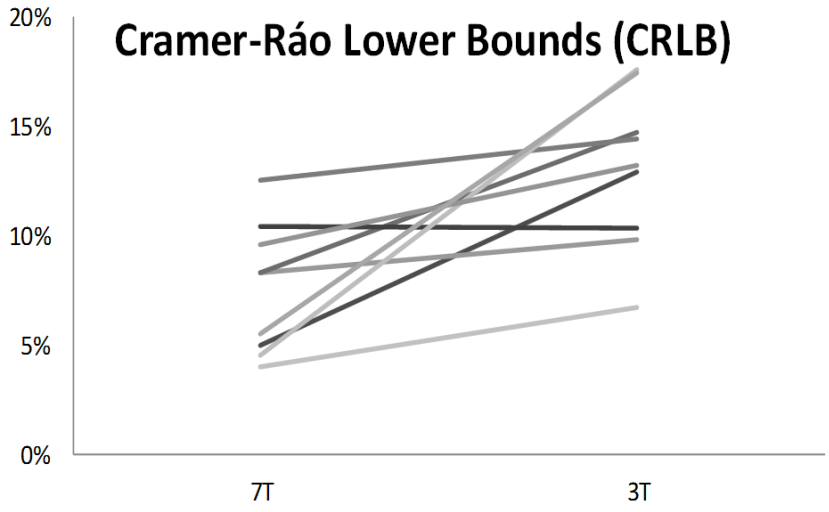

Figure 6.3: *The Cramer-Ráo Lower Bounds (CRLB) comparison between 7T vs 3T.*

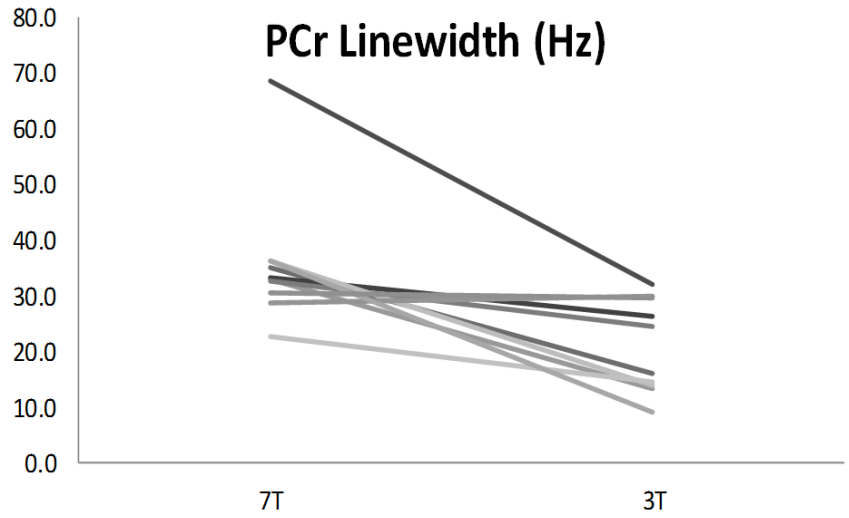

Figure 6.4: *The comparison in PCr linewidth between 7T vs 3T.*

6.5 Discussion

3T vs 7T comparison

This study reports the first 7T cardiac ^{31}P spectra in patients with T2DM, showing marked superiority of cardiac ^{31}P spectra at 7T relative to 3T, with increased SNR and increased precision in metabolite quantification. The CRLB gives a lower bound to the accuracy of the fitted parameters. Hence, this decrease in CRLB of PCr represents a desirable increased precision in metabolite quantitation at 7T compared to 3T.

The SNR improvement with field strength varies noticeably between subjects and this is most likely the result of the challenge of accurate coil positioning with a small loop coil. Even if optimally placed, a 10 cm Tx/Rx loop will show significant variation in receive sensitivity and B_1^+ homogeneity at the interventricular septum due to variations in body shape and in the coil – septum distance. The fraction of the voxel filled with myocardium will also vary between subjects. These effects are consistent with previous reports regarding the positioning of ^{31}P-MRS surface coils[169, 182].

In this study, PCr SNR increased by 1.54x. This value demonstrates that, with this protocol, the increase in SNR was lower than predicted by theory (2.4x improvement arising from the increase in B_0 alone as predicted by theory[167, 183]). The reasons for this may be:

1) The challenge of accurate coil positioning with a small loop coil. Even if optimally placed, a 10cm Tx/Rx loop will show significant variation in receiver sensitivity and B_1^+ homogeneity

at the interventricular septum due to variations in body shape and in the coil – septum distance.

2)The acquisition time was longer at 7T (fixed at 30 min at 7T compared to 9 min at 3T) which might have led to movement artefacts due to poorer compliance of the participants to the instruction to stay motionless.

3) Difficulties with ^{1}H image-based shimming at 7T due to the inhomogeneous B1 from the ^{1}H loop.

6.6 Limitations

This study does not answer the main question whether cardiac ^{31}P spectroscopy will be established for use in clinical Cardiology practice or remain a research tool for specialized academic centers. The main obstacle for implementation of cardiac MRS in routine Cardiology practice has been, and remains, that it is a tool with significant technical complexity, with limited signal and resolution. Major technical advances are needed to improve the spatial resolution from the current ~25 ml to ~1 ml sizes. Simultaneously, the temporal resolution must improve to acceptable acquisition times, such as < 5 min. Reduction in variability (< 5%) and high reproducibility are other important goals. 7T with increased SNR may achieve these goals for academic settings in the future, but issue of financial constraints is likely to remain an important consideration impeding wider application of this high field strength scanner for clinical purposes.

6.6 Conclusions

This study has demonstrated proof-of-principle that cardiac ^{31}P-MRS at 7T is feasible for assessment of patients with T2DM. Significant improvements in spectral SNR relative to the previous gold-standard field strength of 3T has been demonstrated. Finally, cardiac ^{31}P-MRS shows good potential at 7T. 7T could be recommended as the field strength of choice for clinical ^{31}P-MRS applications.

Chapter 7
General Conclusions

This work was carried out to explore cardiac energy metabolism at rest and during exercise in patients with T2DM. This thesis is the first to report on the further worsening of cardiac energetics as measured by PCr/ATP during exercise in T2DM. As the determinants of cardiac energetics are multifactorial, it is possible that a decrease in energy supply may coexist with the intrinsic metabolic dysfunction, such as the mitochondrial dysfunction and metabolic inefficiency, in the diabetic heart. This thesis explored the relationship between microvascular dysfunction and tissue oxygenation (measured using the BOLD technique) in T2DM. To my knowledge, this is the first report of myocardial perfusion and oxygenation in the diabetic heart. A modest correlation between these parameters suggested that some degree of dissociation exists between flow and oxygenation. However, the most striking finding was the blunted increase in myocardial tissue oxygenation in response to adenosine stress in T2DM. Both MPRI and oxygenation response to vasodilator stress correlated with PCr/ATP during exercise.

The impact of cardiac and hepatic steatosis, as well as epicardial fat accumulation on left ventricular function and geometry created by differences in lean and obese diabetes patients were also explored. This work has shown concentric LV remodelling in diabetes may potentially be explained by cardiac steatosis, and since cardiac steatosis is modifiable, strategies aimed at reducing myocardial triglycerides may be beneficial in reversing concentric remodelling.

This work has demonstrated that obesity, in the presence of diabetes, is associated with higher epicardial fat volumes, significant NAFLD and liver fibrosis, higher insulin resistance,

cardiac diastolic and systolic dysfunction, but not with an exacerbated deficit in myocardial energetic status or more pronounced cardiac steatosis compared to diabetes of the lean. Myocardial steatosis was shown to be dissociated from the ectopic adiposity in other organs, which could represent a separate entity that is influenced by factors beyond ectopic/visceral adiposity, such as a scarring process. The differences in cardiac and hepatic disease phenotype between the obese and the lean diabetes groups suggest that therapeutic trials should consider lean and obese T2DM as distinct groups.

This work has also demonstrated that despite the presence of concentric remodelling, and differences in myocardial energetics, cardiac steatosis, impaired myocardial perfusion reserve, blunted oxygenation response and subtle contractile dysfunction in patients with diabetes, diastolic function was not significantly different between the patients and the weight matching non-diabetic controls, although diastolic dysfunction is a common finding in other diabetes studies. Diastolic dysfunction has been demonstrated in obesity and the controls in this study were overweight and this finding might in fact be the result of the subtle diastolic impairment in the control group. In the future, it will be important to assess diastolic function in a similarly overweight non-diabetic cohort in comparison to healthy, normal weight individuals to prove this.

Overall, however, as these studies are observational, it is not possible to determine whether the observed associations between high-energy phosphate metabolism, steatosis and cardiac structural and functional changes are causal.

By far the greatest part of the work described in this thesis used Cardiac ^{31}P-MRS, which is the only non-invasive in vivo technique for the determination of cardiac high energy phosphate metabolism. Broader applications of ^{31}P-MRS have not yet seen widespread acceptance as a consequence of the method's low intrinsic signal-to-noise ratio. Higher field strength application of the technique may overcome this limitation. This work has also compared clinical applications of cardiac 31P-MRS at 7 Tesla field strength to 3 Tesla in patients with diabetes, and demonstrated that 7T offers significant improvements in spectral signal to noise relative to the 3T, with improved precision in metabolite quantitation.

Future work should address the limitations of the work in this thesis. One major limitation is the absence of invasive coronary angiography for assessment of endothelium-dependent coronary vasodilatation and vascular smooth muscle cell responsiveness, as endothelium has been recognised to be a major regulator of vascular tone and growth and clinical studies have demonstrated the association between diabetes and endothelium-dependent relaxation impairment[130, 131]. Although the impaired myocardial perfusion reserve demonstrated is commonly attributed to microvascular disease, this does not allow mechanistically differentiation between endothelial dysfunction and impaired smooth vessel relaxation as potential causes for the observed changes in diabetes. Therefore, future work should also focus on the endothelial function, especially since it is unknown whether there is a relationship between myocardial high-energy phosphate metabolism, myocardial oxygenation and endothelial dysfunction in diabetic heart disease. This can be

done invasively by coronary angiography, through assessment of the percent increase in coronary blood flow in response to endothelium-dependent vasodilator (commonly acetylcholine) infusion.

Finally, another exciting potential point of focus for future studies is comparison of the effects of acute ingestion of ketone metabolism, carbohydrate metabolism and fat metabolism on stress myocardial energetics. There is currently little information available about the myocardial metabolism in diabetic patients under stress and such studies may offer mechanistic insights into substrate metabolism in diabetic humans.

Science has progressed significantly in its understanding of disease mechanisms in T2DM. This thesis provides further insight into the role of energetics, perfusion, oxygenation and steatosis in the diabetic heart. Nonetheless, in search of improved treatments and a possible cure for these conditions, the road ahead still promises to be long.

The answers provided by this body of work stimulate further questions. Larger studies as well as longitudinal follow up is needed to further clarify rest and exercise PCr/ATP and oxygenation signal change during stress as means of predicting risk of developing significant cardiomyopathy in the diabetic heart.

Bibliography

1. Kannel WB and McGee DL. Diabetes and cardiovascular disease: The Framingham study. *Journal of the American Medical Association*. 1979;241:2035-2038.
2. Woodfield SL, Lundergan CF, Reiner JS, Thompson MA, Rohrbeck SC, Deychak Y, Smith JO, Burton JR, McCarthy WF, Califf RM, White HD, Weaver WD, Topol EJ and Ross AM. Gender and Acute Myocardial Infarction: Is There a Different Response to Thrombolysis? *Journal of the American College of Cardiology*. 1997;29:35-42.
3. Takahashi N, Iwasaka T, Sugiura T, Hasegawa T, Tarumi N, Kimura Y, Kurihara S, Onoyama H and Inada M. Left Ventricular Regional Function After Acute Anterior Myocardial Infarction in Diabetic Patients. *Diabetes Care*. 1989;12:630-635.
4. Hansson L, Zanchetti A, Carruthers SG, Dahlöf B, Elmfeldt D, Julius S, Ménard J, Rahn KH, Wedel H and Westerling S. Effects of intensive blood-pressure lowering and low-dose aspirin in patients with hypertension: principal results of the Hypertension Optimal Treatment (HOT) randomised trial. *The Lancet*. 1998;351:1755-1762.
5. Rubler S, Dlugash J, Yuceoglu YZ, Kumral T, Branwood AW and Grishman A. New type of cardiomyopathy associated with diabetic glomerulosclerosis. *The American journal of cardiology*. 1972;30:595-602.
6. Garcia MJ , McNamara PM, Gordon T and Kannel W. Morbidity and mortality in diabetics in the Framingham population. Sixteen year follow-up study. *Diabetes*. 1974;23(2): 105-11.
7. Levy D, Garrison RJ, Savage DD, Kannel WB and Castelli WP. Prognostic Implications of Echocardiographically Determined Left Ventricular Mass in the Framingham Heart Study. *New England Journal of Medicine*. 1990;322:1561-1566.
8. Bluemke DA, Kronmal RA, Lima JAC, Liu K, Olson J, Burke GL and Folsom AR. The Relationship of Left Ventricular Mass and Geometry to Incident Cardiovascular Events: The MESA Study. *Journal of the American College of Cardiology*. 2008;52:2148-2155.
9. Devereux RB, Roman MJ, Paranicas M, O'Grady MJ, Lee ET, Welty TK, Fabsitz RR, Robbins D, Rhoades ER and Howard BV. Impact of diabetes on cardiac structure and function: the strong heart study. *Circulation*. 2000;101:2271-6.
10. Taegtmeyer H, McNulty P and Young ME. Adaptation and Maladaptation of the Heart in Diabetes: Part I: General Concepts. *Circulation*. 2002;105:1727-1733.
11. Dhalla NS, Liu X, Panagia V and Takeda N. *Subcellular remodeling and heart dysfunction in chronic diabetes*; 1998.
12. Hardin NJ. The myocardial and vascular pathology of diabetic cardiomyopathy. *Coronary Artery Disease*. 1996;7:99-108.
13. Scheuermann-Freestone M, Madsen PL, Manners D, Blamire AM, Buckingham RE, Styles P, Radda GK, Neubauer S and Clarke K. Abnormal Cardiac and Skeletal Muscle Energy Metabolism in Patients With Type 2 Diabetes. *Circulation*. 2003;107:3040-3046.

14. Shivu GN, Phan TT, Abozguia K, Ahmed I, Wagenmakers A, Henning A, Narendran P, Stevens M and Frenneaux M. Relationship Between Coronary Microvascular Dysfunction and Cardiac Energetics Impairment in Type 1 Diabetes Mellitus. *Circulation*. 2010;121:1209-1215.
15. McGavock JM, Lingvay I, Zib I, Tillery T, Salas N, Unger R, Levine BD, Raskin P, Victor RG and Szczepaniak LS. Cardiac steatosis in diabetes mellitus: a 1H-magnetic resonance spectroscopy study. *Circulation*. 2007;116:1170-5.
16. Rijzewijk LJ, van der Meer RW, Smit JWA, Diamant M, Bax JJ, Hammer S, Romijn JA, de Roos A and Lamb HJ. Myocardial Steatosis Is an Independent Predictor of Diastolic Dysfunction in Type 2 Diabetes Mellitus. *Journal of the American College of Cardiology*. 2008;52:1793-1799.
17. Galderisi M, Anderson KM, Wilson PWF and Levy D. Echocardiographic evidence for the existence of a distinct diabetic cardiomyopathy (The Framingham Heart Study). *The American journal of cardiology*. 1991;68:85-89.
18. Lieb W, Xanthakis V, Sullivan LM, Aragam J, Pencina MJ, Larson MG, Benjamin EJ and Vasan RS. Longitudinal Tracking of Left Ventricular Mass Over the Adult Life Course: Clinical Correlates of Short- and Long-Term Change in the Framingham Offspring Study. *Circulation*. 2009;119:3085-3092.
19. Devereux RB, Roman MJ, Paranicas M, O'Grady MJ, Lee ET, Welty TK, Fabsitz RR, Robbins D, Rhoades ER and Howard BV. Impact of Diabetes on Cardiac Structure and Function: The Strong Heart Study. *Circulation*. 2000;101:2271-2276.
20. Carugo S, Giannattasio C, Calchera I, Paleari F, Gorgoglione MG, Grappiolo A, Gamba P, Rovaris G, Failla M and Mancia G. Progression of functional and structural cardiac alterations in young normotensive uncomplicated patients with type 1 diabetes mellitus. *Journal of Hypertension*. 2001;19:1675-1680.
21. Beljic T and Miric M. Improved metabolic control does not reverse left ventricular filling abnormalities in newly diagnosed non-insulin-dependent diabetes patients. *Acta Diabetologica*. 1994;31:147-150.
22. Bonito PD, Cuomo S, Moio N, Sibilio G, Sabatini D, Quattrin S and Capaldo B. Diastolic Dysfunction in Patients with Non-insulin-dependent Diabetes Mellitus of Short Duration. *Diabetic Medicine*. 1996;13:321-324.
23. Khan JN, Wilmot EG, Leggate M, Singh A, Yates T, Nimmo M, Khunti K, Horsfield MA, Biglands J, Clarysse P, Croisille P, Davies M and McCann GP. Subclinical diastolic dysfunction in young adults with Type 2 diabetes mellitus: a multiparametric contrast-enhanced cardiovascular magnetic resonance pilot study assessing potential mechanisms. *European Heart Journal - Cardiovascular Imaging*. 2014;15:1263-1269.
24. Boyer JK, Thanigaraj S, Schechtman KB and JE. P. Prevalence of ventricular diastolic dysfunction in asymptomatic, normotensive patients with diabetes mellitus. *American Heart Journal*. 2004;93(7):870-875.
25. Goldin A, Beckman JA, Schmidt AM and Creager MA. Advanced Glycation End Products: Sparking the Development of Diabetic Vascular Injury. *Circulation*. 2006;114:597-605.
26. Borisov AB, Ushakov AV, Zagorulko AK, Novikov NY, Selivanova KF, Edwards CA and Russell MW. Intracardiac lipid accumulation, lipoatrophy of muscle cells and expansion of myocardial infarction in type 2 diabetic patients. *Micron*. 2008;39:944-951.
27. Cheung N, Wang JJ, Rogers SL, Brancati F, Klein R, Sharrett AR and Wong TY. Diabetic Retinopathy and Risk of Heart Failure. *Journal of the American College of Cardiology*. 2008;51:1573-1578.
28. Neubauer S, Horn M, Cramer M, Harre K, Newell JB, Peters W, Pabst T, Ertl G, Hahn D, Ingwall JS and Kochsiek K. Myocardial Phosphocreatine-to-ATP Ratio Is a Predictor of Mortality in Patients With Dilated Cardiomyopathy. *Circulation*. 1997;96:2190-2196.

29. Neubauer S. The Failing Heart — An Engine Out of Fuel. *New England Journal of Medicine*. 2007;356:1140-1151.
30. Crilley JG, Boehm EA, Blair E, Rajagopalan B, Blamire AM, Styles P, McKenna WJ, Ostman-Smith I, Clarke K and Watkins H. Hypertrophic cardiomyopathy due to sarcomeric gene mutations is characterized by impaired energy metabolism irrespective of the degree of hypertrophy. *Journal of the American College of Cardiology*. 2003;41:1776-82.
31. Jung WI, Sieverding L, Breuer J, Schmidt O, Widmaier S, Bunse M, van Erckelens F, Apitz J, Dietze GJ and Lutz O. Detection of phosphomonoester signals in proton-decoupled 31P NMR spectra of the myocardium of patients with myocardial hypertrophy. *Journal of Magnetic Resonance*. 1998;133:232-5.
32. Jung WI, Hoess T, Bunse M, Widmaier S, Sieverding L, Breuer J, Apitz J, Schmidt O, van Erckelens F, Dietze GJ and Lutz O. Differences in cardiac energetics between patients with familial and nonfamilial hypertrophic cardiomyopathy. *Circulation*. 2000;101:E121.
33. Shivu GN, Abozguia K, Phan TT, Ahmed I, Henning A and Frenneaux M. (31)P magnetic resonance spectroscopy to measure in vivo cardiac energetics in normal myocardium and hypertrophic cardiomyopathy: Experiences at 3T. *Eur J Radiol*. 2008.
34. Neubauer S, Krahe T, Schindler R, Horn M, Hillenbrand H, Entzeroth C, Mader H, Kromer EP, Riegger GA, Lackner K et al. 31P magnetic resonance spectroscopy in dilated cardiomyopathy and coronary artery disease. Altered cardiac high-energy phosphate metabolism in heart failure. *Circulation*. 1992;86:1820-1818.
35. Neubauer S, Horn M, Pabst T, Godde M, Lubke D, Jilling B, Hahn D and Ertl G. Contributions of 31P-magnetic resonance spectroscopy to the understanding of dilated heart muscle disease. *Eur Heart J*. 1995;16 Suppl O:115-8.
36. Neubauer S, Horn M, Pabst T, Harre K, Stromer H, Bertsch G, Sandstede J, Ertl G, Hahn D and Kochsiek K. Cardiac high-energy phosphate metabolism in patients with aortic valve disease assessed by 31P-magnetic resonance spectroscopy. *J Investig Med*. 1997;45:453-62.
37. Sardanelli F, Zandrino F, Molinari G, Cordone S, Delfino L and Levrero F. Magnetic resonance spectroscopy of ischemic heart disease. *Rays*. 1999;24:149-64.
38. Okada M, K. M, Inubushi T and Kinoshita M. Influence of aging or left ventricular hypertrophy on the human heart: Contents of phosphorus metabolites measured by 31P MRS. *MRM*. 1998;39:772-782.
39. Beer M, Sandstede J, Landschütz W, Seyfarth T, Lipke C, Köstler H, Pabst T, Kenn W, Meininger M, von Kienlin M, Horn M, Harre K, Hahn D and Neubauer S. Absolute concentrations of myocardial high-energy phosphate metabolites in normal, hypertrophied and failing human myocardium, measured non-invasively with 31P-SLOOP-magnetic resonance spectroscopy. *Journal of the American College of Cardiology*. 2002;40:1267-74.
40. Conway MA, Allis J, Ouwerkerk R, Niioka T, Rajagopalan B and Radda GK. Detection of low phosphocreatine to ATP ratio in failing hypertrophied human myocardium by 31P magnetic resonance spectroscopy. *Lancet*. 1991;338:973-6.
41. Carley AN, Taegtmeyer H and Lewandowski ED. Matrix revisited: mechanisms linking energy substrate metabolism to the function of the heart. *Circulation research*. 2014;114:717-29.
42. Taegtmeyer H, Wilson CR, Razeghi P and Sharma S. Metabolic energetics and genetics in the heart. *Annals of the New York Academy of Sciences*. 2005;1047:208-18.
43. Zhang J, Duncker DJ, Ya X, Zhang Y, Pavek T, Wei H, Merkle H, Ugurbil K, From AHL and Bache RJ. Effect of Left Ventricular Hypertrophy Secondary to Chronic Pressure Overload on Transmural Myocardial 2-Deoxyglucose Uptake: A 31P NMR Spectroscopic Study. *Circulation*. 1995;92:1274-1283.

44. Bittl JA and Ingwall JS. Reaction rates of creatine kinase and ATP synthesis in the isolated rat heart. A 31P NMR magnetization transfer study. *Journal of Biological Chemistry*. 1985;260:3512-3517.
45. Boudina S and Abel ED. Diabetic cardiomyopathy revisited. *Circulation*. 2007;115:3213-23.
46. Kuo TH, Moore KH, Giacomelli F and Wiener J. Defective Oxidative Metabolism of Heart Mitochondria from Genetically Diabetic Mice. *Diabetes*. 1983;32:781-787.
47. Matsumoto Y, Kaneko M, Kobayashi A, Fujise Y and Yamazaki N. Creatine kinase kinetics in diabetic cardiomyopathy. *The American journal of physiology*. 1995;268:E1070-6.
48. Stanley WC, Lopaschuk GD and McCormack JG. Regulation of energy substrate metabolism in the diabetic heart. *Cardiovascular research*. 1997;34:25-33.
49. Taegtmeyer H. Adaptation and Maladaptation of the Heart in Diabetes: Part I: General Concepts. *Circulation*. 2002;105:1727-1733.
50. Rodrigues B, Cam M and McNeill J. Metabolic disturbances in diabetic cardiomyopathy. *Molecular and cellular biochemistry*. 1998;180:53-57.
51. Himms-Hagen J and Harper M-E. Physiological Role of UCP3 May Be Export of Fatty Acids from Mitochondria When Fatty Acid Oxidation Predominates: An Hypothesis. *Experimental Biology and Medicine*. 2001;226:78-84.
52. Bratis K, Child N, Terrovitis J, Nanas J, Felekos I, Aggeli C, Stefanadis C, Mastorakos G, Chiribiri A, Nagel E and Mavrogeni S. Coronary microvascular dysfunction in overt diabetic cardiomyopathy. *IJC Metabolic & Endocrine*. 2014;5:19-23.
53. Larghat AM, Swoboda PP, Biglands JD, Kearney MT, Greenwood JP and Plein S. The microvascular effects of insulin resistance and diabetes on cardiac structure, function, and perfusion: a cardiovascular magnetic resonance study. *European heart journal cardiovascular Imaging*. 2014;15:1368-76.
54. Bagi Z, Koller A and Kaley G. Superoxide-NO interaction decreases flow- and agonist-induced dilations of coronary arterioles in Type 2 diabetes mellitus. *American journal of physiology. Heart and circulatory physiology*. 2003;285:H1404-10.
55. De Lorenzo A, Lima RSL, Siqueira-Filho AG and Pantoja MR. Prevalence and prognostic value of perfusion defects detected by stress technetium-99m sestamibi myocardial perfusion single-photon emission computed tomography in asymptomatic patients with diabetes mellitus and no known coronary artery disease. *The American journal of cardiology*. 2002;90:827-832.
56. Spoladore R, Fisicaro A, Faccini A and Camici PG. Myocardial disease: Coronary microvascular dysfunction in primary cardiomyopathies. *Heart*. 2014;100:10 806-813.
57. Asbun J and Villarreal FJ. The Pathogenesis of Myocardial Fibrosis in the Setting of Diabetic Cardiomyopathy. *Journal of the American College of Cardiology*. 2006;47:693-700.
58. Eguchi K, Boden-Albala B, Jin Z, Rundek T, Sacco RL, Homma S and Di Tullio MR. Association Between Diabetes Mellitus and Left Ventricular Hypertrophy in a Multiethnic Population. *The American journal of cardiology*. 2008;101:1787-1791.
59. Taskiran M, Fritz-Hansen T, Rasmussen V, Larsson HBW and Hilsted J. Decreased Myocardial Perfusion Reserve in Diabetic Autonomic Neuropathy. *Diabetes*. 2002;51:3306-3310.
60. Murthy VL, Naya M, Foster CR, Gaber M, Hainer J, Klein J, Dorbala S, Blankstein R and Di Carli MF. Association Between Coronary Vascular Dysfunction and Cardiac Mortality in Patients With and Without Diabetes Mellitus. *Circulation*. 2012;126:1858-1868.
61. Grove TH, Ackerman JJ, Radda GK and Bore PJ. Analysis of rat heart in vivo by phosphorus nuclear magnetic resonance. *Proc Natl Acad Sci U S A*. 1980;77:299-302.
62. Bottomley PA. Noninvasive study of high-energy phosphate metabolism in human heart by depth-resolved 31P NMR spectroscopy. *Science*. 1985;229:769-72.

63. Rider OJ, Francis JM, Tyler D, Byrne J, Clarke K and Neubauer S. Effects of weight loss on myocardial energetics and diastolic function in obesity. *International Journal of Cardiovascular Imaging*. 2013;29:1043-1050.
64. Fox CS, Massaro JM, Hoffmann U, Pou KM, Maurovich-Horvat P, Liu C-Y, Vasan RS, Murabito JM, Meigs JB, Cupples LA, D'Agostino RB and O'Donnell CJ. Abdominal Visceral and Subcutaneous Adipose Tissue Compartments: Association With Metabolic Risk Factors in the Framingham Heart Study. *Circulation*. 2007;116:39-48.
65. Okura T, Nakata Y, Yamabuki K and Tanaka K. Regional Body Composition Changes Exhibit Opposing Effects on Coronary Heart Disease Risk Factors. *Arteriosclerosis, Thrombosis, and Vascular Biology*. 2004;24:923-929.
66. Fantuzzi G and Mazzone T. Adipose Tissue and Atherosclerosis: Exploring the Connection. *Arteriosclerosis, Thrombosis, and Vascular Biology*. 2007;27:996-1003.
67. Montani JP, Carroll JF, Dwyer TM, Antic V, Yang Z and Dulloo AG. Ectopic fat storage in heart, blood vessels and kidneys in the pathogenesis of cardiovascular diseases. *International journal of obesity and related metabolic disorders* . 2004;28:S58-S65.
68. Rabinowitz D and Zierler KL. Forearm metabolism in obesity and its response to intra-arterial insulin. Characterization of insulin resistance and evidence for adaptive hyperinsulinism. *Journal of Clinical Investigation*. 1962;41:2173-2181.
69. Felig P, Wahren J, Hendler R and Brundin T. Splanchnic glucose and amino acid metabolism in obesity. *Journal of Clinical Investigation*. 1974;53:582-590.
70. Caro JF, Dohm LG, Pories WJ and Sinha MK. Cellular alterations in liver, skeletal muscle, and adipose tissue responsible for insulin resistance in obesity and type II diabetes. *Diabetes/Metabolism Reviews*. 1989;5:665-689.
71. Fox CS, Gona P, Hoffmann U, Porter SA, Salton CJ, Massaro JM, Levy D, Larson MG, D'Agostino RB, O'Donnell CJ and Manning WJ. Pericardial Fat, Intrathoracic Fat, and Measures of Left Ventricular Structure and Function: The Framingham Heart Study. *Circulation*. 2009;119:1586-1591.
72. Fox CS, Massaro JM, Schlett CL, Lehman SJ, Meigs JB, O'Donnell CJ, Hoffmann U and Murabito JM. Periaortic Fat Deposition Is Associated With Peripheral Arterial Disease: The Framingham Heart Study. *Circulation: Cardiovascular Imaging*. 2010;3:515-519.
73. Rijzewijk LJ, Jonker JT, van der Meer RW, Lubberink M, de Jong HW, Romijn JA, Bax JJ, de Roos A, Heine RJ, Twisk JW, Windhorst AD, Lammertsma AA, Smit JWA, Diamant M and Lamb HJ. Effects of Hepatic Triglyceride Content on Myocardial Metabolism in Type 2 Diabetes. *Journal of the American College of Cardiology*. 2010;56:225-233.
74. Greenstein AS, Khavandi K, Withers SB, Sonoyama K, Clancy O, Jeziorska M, Laing I, Yates AP, Pemberton PW, Malik RA and Heagerty AM. Local Inflammation and Hypoxia Abolish the Protective Anticontractile Properties of Perivascular Fat in Obese Patients. *Circulation*. 2009;119:1661-1670.
75. Lee Y-C, Chang H-H, Chiang C-L, Liu C-H, Yeh J-I, Chen M-F, Chen P-Y, Kuo J-S and Lee TJF. Role of Perivascular Adipose Tissue–Derived Methyl Palmitate in Vascular Tone Regulation and Pathogenesis of Hypertension. *Circulation*. 2011;124:1160-1171.
76. Rider OJ, Tayal U, Francis JM, Ali MK, Robinson MR, Byrne JP, Clarke K and Neubauer S. The effect of obesity and weight loss on aortic pulse wave velocity as assessed by magnetic resonance imaging. *Obesity (Silver Spring)*. 2010;18:2311-6.
77. Association AD. Standards of Medical Care in Diabetes—2007. *Diabetes Care*. 2007;30:S4-S41.

78. Pennell DJ, Sechtem UP, Higgins CB, Manning WJ, Pohost GM, Rademakers FE, van Rossum AC, Shaw LJ and Yucel EK. Clinical indications for cardiovascular magnetic resonance (CMR): Consensus Panel report. *Journal of Cardiovascular Magnetic Resonance*. 2004;6:727-65.
79. Axel L and Dougherty L. MR imaging of motion with spatial modulation of magnetization. *Radiology*. 1989;171:841-845.
80. Sharma P, Socolow J, Patel S, Pettigrew RI and Oshinski JN. Effect of Gd-DTPA-BMA on blood and myocardial T1 at 1.5T and 3T in humans. *Journal of Magnetic Resonance Imaging*. 2006;23:323-30.
81. Jerosch-Herold M, Seethamraju RT, Swingen CM, Wilke NM and Stillman AE. Analysis of myocardial perfusion MRI. *Journal of Magnetic Resonance Imaging*. 2004;19:758-70.
82. Nagel E, Klein C, Paetsch I, Hettwer S, Schnackenburg B, Wegscheider K and Fleck E. Magnetic resonance perfusion measurements for the noninvasive detection of coronary artery disease. *Circulation*. 2003;108:432-7.
83. Al-Saadi N, Nagel E, Gross M, Bornstedt A, Schnackenburg B, Klein C, Klimek W, Oswald H and Fleck E. Noninvasive detection of myocardial ischemia from perfusion reserve based on cardiovascular magnetic resonance. *Circulation*. 2000;101:1379-83.
84. Petersen SE, Jerosch-Herold M, Hudsmith LE, Robson MD, Francis JM, Doll HA, Selvanayagam JB, Neubauer S and Watkins H. Evidence for microvascular dysfunction in hypertrophic cardiomyopathy: new insights from multiparametric magnetic resonance imaging. *Circulation*. 2007;115:2418-25.
85. Piechnik S, Ferreira V, Dall'Armellina E, Cochlin L and Robson M. Shortened Modified Look Locker Inversion recovery (Sh-MOLLI) cardiac gated mapping of T1 - Theory and phantom verification. *26th Annual Scientific Meeting, ESMRMB Oct 1-3, 2009 2009; Antalya, Turkey*. 2009:485.
86. White SK, Sado DM, Fontana M, Banypersad SM, Maestrini V, Flett AS, Piechnik SK, Robson MD, Hausenloy DJ, Sheikh AM, Hawkins PN and Moon JC. T1 Mapping for Myocardial Extracellular Volume Measurement by CMR: Bolus Only Versus Primed Infusion Technique. *Journal of the American College of Cardiology: Cardiovascular Imaging*. 2013;6:955-962.
87. Jerosch-Herold M, Sheridan DC, Kushner JD, Nauman D, Burgess D, Dutton D, Alharethi R, Li D and RE. H. Cardiac magnetic resonance imaging of myocardial contrast uptake and blood flow in patients affected with idiopathic or familial dilated cardiomyopathy. *American journal of physiology Heart and circulatory physiology*. 2008;295(3):H1234-H1242.
88. Rial B, Robson MD, Neubauer S and Schneider JE. Rapid quantification of myocardial lipid content in humans using single breath-hold 1H MRS at 3 Tesla. *Magnetic resonance in medicine : official journal of the Society of Magnetic Resonance in Medicine / Society of Magnetic Resonance in Medicine*. 2011;66:619-24.
89. Bella JN, Devereux RB, Roman MJ, Palmieri V, Liu JE, Paranicas M, Welty TK, Lee ET, Fabsitz RR and Howard BV. Separate and joint effects of systemic hypertension and diabetes mellitus on left ventricular structure and function in American Indians (the Strong Heart Study). *The American journal of cardiology*. 2001;87:1260-1265.
90. Gjesdal O, Bluemke DA and Lima JA. Cardiac remodeling at the population level[mdash]risk factors, screening, and outcomes. *Nature Reviews Cardiology*. 2011;8:673-685.
91. Gao H, Feng X-j, Li Z-m, Li M, Gao S, He Y-h, Wang J-j, Zeng S-y, Liu X-p, Huang X-y, Chen S-r and Liu P-q. Downregulation of adipose triglyceride lipase promotes cardiomyocyte hypertrophy by triggering the accumulation of ceramides. *Archives of Biochemistry and Biophysics*. 2015;565:76-88.

92. Glenn DJ, Cardema MC, Ni W, Zhang Y, Yeghiazarians Y, Grapov D, Fiehn O and Gardner DG. Cardiac steatosis potentiates angiotensin II effects in the heart. *American Journal of Physiology - Heart and Circulatory Physiology*. 2015;308:H339-H350.
93. Glenn DJ, Wang F, Nishimoto M, Cruz MC, Uchida Y, Holleran WM, Zhang Y, Yeghiazarians Y and Gardner DG. A Murine Model of Isolated Cardiac Steatosis Leads to Cardiomyopathy. *Hypertension*. 2011;57:216-222.
94. Nelson MD, Victor RG, Szczepaniak EW, Simha V, Garg A and Szczepaniak LS. Cardiac Steatosis and Left Ventricular Hypertrophy in Patients With Generalized Lipodystrophy as Determined by Magnetic Resonance Spectroscopy and Imaging. *The American journal of cardiology*. 2013;112:1019-1024.
95. Banerjee R, Rial B, Holloway CJ, Lewandowski AJ, Robson MD, Osuchukwu C, Schneider JE, Leeson P, Rider OJ and Neubauer S. Evidence of a Direct Effect of Myocardial Steatosis on LV Hypertrophy and Diastolic Dysfunction in Adult and Adolescent Obesity. *Journal of the American College of Cardiology: Cardiovasc Imaging*. 2015 Mar 12. doi: 10.1016/j.jcmg.2014.12.019.
96. Weber KT and Brilla CG. Pathological hypertrophy and cardiac interstitium. Fibrosis and renin-angiotensin-aldosterone system. *Circulation*. 1991;83:1849-65.
97. van Heerebeek L, Hamdani N, Handoko ML, Falcao-Pires I, Musters RJ, Kupreishvili K, Ijsselmuiden AJJ, Schalkwijk CG, Bronzwaer JGF, Diamant M, Borbély A, van der Velden J, Stienen GJM, Laarman GJ, Niessen HWM and Paulus WJ. Diastolic Stiffness of the Failing Diabetic Heart: Importance of Fibrosis, Advanced Glycation End Products, and Myocyte Resting Tension. *Circulation*. 2008;117:43-51.
98. Liu S, Han J, Nacif M, Jones J, Kawel N, Kellman P, Sibley C and Bluemke D. Diffuse myocardial fibrosis evaluation using cardiac magnetic resonance T1 mapping: sample size considerations for clinical trials. *Journal of Cardiovascular Magnetic Resonance*. 2012;14:90.
99. Verdecchia P, Schillaci G, Borgioni C, Ciucci A, Gattobigio R, Zampi I, Santucci A, Santucci C, Reboldi G and Porcellati C. Prognostic value of left ventricular mass and geometry in systemic hypertension with left ventricular hypertrophy. *American Journal of Cardiology*. 78:197-202.
100. Rosen BD, Edvardsen T, Lai S, Castillo E, Pan L, Jerosch-Herold M, Sinha S, Kronmal R, Arnett D, Crouse JR, Heckbert SR, Bluemke DA and Lima JAC. Left Ventricular Concentric Remodeling Is Associated With Decreased Global and Regional Systolic Function: The Multi-Ethnic Study of Atherosclerosis. *Circulation*. 2005;112:984-991.
101. Monji A, Mitsui T, Bando YK, Aoyama M, Shigeta T and Murohara T. Glucagon-like peptide-1 receptor activation reverses cardiac remodeling via normalizing cardiac steatosis and oxidative stress in type 2 diabetes. *American Journal of Physiology - Heart and Circulatory Physiology*. 2013;305:H295-H304.
102. Ramírez E, Klett-Mingo M, Ares-Carrasco S, Picatoste B, Ferrarini A, Rupérez FJ, Caro-Vadillo A, Barbas C, Egido J, Tuñón J and Lorenzo Ó. Eplerenone attenuated cardiac steatosis, apoptosis and diastolic dysfunction in experimental type-II diabetes. *Cardiovascular diabetology*. 2013;12:172-172.
103. Palmieri V, Bella JN, Arnett DK, Liu JE, Oberman A, Schuck MY, Kitzman DW, Hopkins PN, Morgan D, Rao DC and Devereux RB. Effect of type 2 diabetes mellitus on left ventricular geometry and systolic function in hypertensive subjects: Hypertension Genetic Epidemiology Network (HyperGEN) study. *Circulation*. 2001;103:102-7.
104. Finck BN, Lehman JJ, Leone TC, Welch MJ, Bennett MJ, Kovacs A, Han X, Gross RW, Kozak R, Lopaschuk GD and Kelly DP. The cardiac phenotype induced by PPARα overexpression mimics that caused by diabetes mellitus. *The Journal of Clinical Investigation*. 2002;109:121-130.
105. Schmieder RE, Hilgers KF, Schlaich MP and Schmidt BMW. Renin-angiotensin system and cardiovascular risk. *The Lancet*. 369:1208-1219.

106. Randle PJ, Garland PB, Hales CN and Newsholme EA. The glucose fatty-acid cycle, its role in insulin sensitivity and the metabolic disturbances of diabetes mellitus. *The Lancet*. 281:785-789.
107. Damsgaard EM, Frøland A, Jørgensen OD and Mogensen CE. Prognostic value of urinary albumin excretion rate and other risk factors in elderly diabetic patients and non-diabetic control subjects surviving the first 5 years after assessment. *Diabetologia*. 1993;36:1030-1036.
108. Ingwall JS. Energy metabolism in heart failure and remodelling. *Cardiovascular research*. 2009;81:412-419.
109. Rider OJ, Francis JM, Ali MK, Holloway C, Pegg T, Robson MD, Tyler D, Byrne J, Clarke K and Neubauer S. Effects of Catecholamine Stress on Diastolic Function and Myocardial Energetics in Obesity. *Circulation*. 2012;125:1511-1519.
110. Karamitsos TD, Leccisotti L, Arnold JR, Recio-Mayoral A, Bhamra-Ariza P, Howells RK, Searle N, Robson MD, Rimoldi OE, Camici PG, Neubauer S and Selvanayagam JB. Relationship between regional myocardial oxygenation and perfusion in patients with coronary artery disease: insights from cardiovascular magnetic resonance and positron emission tomography. *Circulation Cardiovascular imaging*. 2010;3:32-40.
111. Jahnke C, Gebker R, Manka R, Schnackenburg B, Fleck E and Paetsch I. Navigator-Gated 3D Blood Oxygen Level–Dependent CMR at 3.0-T for Detection of Stress-Induced Myocardial Ischemic Reactions. *Journal of the American College of Cardiology: Cardiovascular Imaging*. 2010;3:375-384.
112. Vohringer M, Flewitt JA, Green JD, Dharmakumar R, Wang J, Jr., Tyberg JV and Friedrich MG. Oxygenation-sensitive CMR for assessing vasodilator-induced changes of myocardial oxygenation. *Journal of Cardiovascular Magnetic Resonance*. 2010;12:20.
113. Alberti KG and Zimmet P. Definition, diagnosis and classification of diabetes mellitus and its complications. Part 1: diagnosis and classification of diabetes mellitus provisional report of a WHO consultation. *Diabetic Medicine*. 1998;15(7):539-53.
114. Vanhamme L, van den Boogaart A and S. VH. Improved method for accurate and efficient quantification of MRS data with use of prior knowledge. *Journal of Magnetic Resonance*. 1997;129:35-43.
115. Hudsmith LE, Neubauer S. Magnetic Resonance Spectroscopy in Myocardial Disease. *Journal of the American College of Cardiology: Imaging.* 2009;2(1):87-96.
116. Zhang X, Heberlein K, Sarkar S and X. H. A multiscale approach for analyzing in vivo spectroscopic imaging data. *Magnetic resonance in medicine.* 2000;43:331-334.
117. Purvis LAB, Clarke WT, Biasiolli L, Robson MD and Rodgers CT. Linewidth constraints in Matlab AMARES using per-metabolite T2 and per-voxel ΔB0. *ISMRM*. 2014 abstract 2885.
118. Tyler DJ, Emmanuel Y, Cochlin LE, Hudsmith LE, Holloway CJ, Neubauer S, Clarke K and Robson MD. Reproducibility of 31P cardiac magnetic resonance spectroscopy at 3 T. *NMR in biomedicine*. 2009;22:405-13.
119. Bottomley PA and Ouwerkerk R. Optimum flip-angles for exciting NMR with uncertain T1 values. *Magnetic Resonance in Medicine*. 1994;32:137-141.
120. Dass S, Cochlin L, Holloway C, Suttie J, Johnson A, Tyler D, Watkins H, Robson M, Clarke K and Neubauer S. Development and validation of a short 31P cardiac magnetic resonance spectroscopy protocol. *Journal of Cardiovascular Magnetic Resonance*. 2010;12:P123.
121. Rodgers CT, Clarke WT, Snyder C, Vaughan JT, Neubauer S and Robson MD. Human cardiac (31)P magnetic resonance spectroscopy at 7 tesla. *Magnetic Resonance in Medicine*. 2014;72:304-315.
122. Korosoglou G, Humpert PM, Ahrens J, Oikonomou D, Osman NF, Gitsioudis G, Buss SJ, Steen H, Schnackenburg B, Bierhaus A, Nawroth PP and Katus HA. Left ventricular diastolic function in

type 2 diabetes mellitus is associated with myocardial triglyceride content but not with impaired myocardial perfusion reserve. *Journal of Magnetic Resonance Imaging*. 2012;35:804-811.
123. Turko IV and Murad F. Quantitative Protein Profiling in Heart Mitochondria from Diabetic Rats. *Journal of Biological Chemistry*. 2003;278:35844-35849.
124. Friedrich MG and Karamitsos TD. Oxygenation-sensitive cardiovascular magnetic resonance. *Journal of Cardiovascular Magnetic Resonance*. 2013;15:43-43.
125. Kaul S and Jayaweera AR. Myocardial Capillaries and Coronary Flow Reserve. *Journal of the American College of Cardiology*. 2008;52:1399-1401.
126. Beache GM, Herzka DA, Boxerman JL, Post WS, Gupta SN, Faranesh AZ, Solaiyappan M, Bottomley PA, Weiss JL, Shapiro EP and Hill MN. Attenuated Myocardial Vasodilator Response in Patients With Hypertensive Hypertrophy Revealed by Oxygenation-Dependent Magnetic Resonance Imaging. *Circulation*. 2001;104:1214-1217.
127. Karamitsos TD, Dass S, Suttie J, Sever E, Birks J, Holloway CJ, Robson MD, Jerosch-Herold M, Watkins H and Neubauer S. Blunted Myocardial Oxygenation Response During Vasodilator Stress in Patients With Hypertrophic Cardiomyopathy. *Journal of the American College of Cardiology*. 2013;61:1169-1176.
128. Herrero P, Peterson LR, McGill JB, Matthew S, Lesniak D, Dence C and Gropler RJ. Increased Myocardial Fatty Acid Metabolism in Patients With Type 1 Diabetes Mellitus. *Journal of the American College of Cardiology*. 2006;47:598-604.
129. Tune JD, Yeh C, Setty S, Zong P and Downey HF. Coronary blood flow control is impaired at rest and during exercise in conscious diabetic dogs. *Basic Res Cardiol*. 2002;97:248-257.
130. Cosson E, Pham I, Valensi P, Pariès J, Attali J-R and Nitenberg A. Impaired Coronary Endothelium–Dependent Vasodilation Is Associated With Microalbuminuria in Patients With Type 2 Diabetes and Angiographically Normal Coronary Arteries. *Diabetes Care*. 2006;29:107-112.
131. Nitenberg A, Valensi P, Sachs R, Cosson E, Attali J-R and Antony I. Prognostic Value of Epicardial Coronary Artery Constriction to the Cold Pressor Test in Type 2 Diabetic Patients With Angiographically Normal Coronary Arteries and No Other Major Coronary Risk Factors. *Diabetes Care*. 2004;27:208-215.
132. Jellis CL, Jenkins C, Leano R, Martin JH and Marwick TH. Reduced end-systolic pressure-volume ratio response to exercise: a marker of subclinical myocardial disease in type 2 diabetes. *Circulation Cardiovascular imaging*. 2010;3:443-9.
133. Juha N Mustonen, Matti IJ Uusitupa, Kari Tahvanainen, Sunil Talwar, Markku Laakso, Esko Länsimies, Jyrki T. Kuikka and Kalevi Pyörälä. Impaired left ventricular systolic function during exercise in middle-aged insulin-dependent and noninsulin-dependent diabetic subjects without clinically evident cardiovascular disease. *The American journal of cardiology*. 1988;62:1273-9.
134. Neglia D, De Caterina A, Marraccini P, Natali A, Ciardetti M, Vecoli C, Gastaldelli A, Ciociaro D, Pellegrini P, Testa R, Menichetti L, L'Abbate A, Stanley WC and Recchia FA. Impaired myocardial metabolic reserve and substrate selection flexibility during stress in patients with idiopathic dilated cardiomyopathy. *American journal of physiology Heart and circulatory physiology*. 2007;293:H3270-8.
135. Marfella R, Esposito K, Nappo F, Siniscalchi M, Sasso FC, Portoghese M, Pia Di Marino M, Baldi A, Cuzzocrea S, Di Filippo C, Barboso G, Baldi F, Rossi F, D'Amico M and Giugliano D. Expression of Angiogenic Factors During Acute Coronary Syndromes in Human Type 2 Diabetes. *Diabetes*. 2004;53:2383-2391.
136. Petta S, Argano C, Colomba D, Cammà C, Di Marco V, Cabibi D, Tuttolomondo A, Marchesini G, Pinto A, Licata G and Craxì A. Epicardial fat, cardiac geometry and cardiac function in patients

with non-alcoholic fatty liver disease: Association with the severity of liver disease. *Journal of Hepatology*. 2015;62:928-933.
137. Goland S, Shimoni S, Zornitzki T, Knobler H, Azoulai O, Lutaty G, Melzer E, Orr A, Caspi A and Malnick S. Cardiac Abnormalities as a New Manifestation of Nonalcoholic Fatty Liver Disease: Echocardiographic and Tissue Doppler Imaging Assessment. *Journal of Clinical Gastroenterology*. 2006;40:949-955.
138. Banerjee R, Pavlides M, Tunnicliffe EM, Piechnik SK, Sarania N, Philips R, Collier JD, Booth JC, Schneider JE, Wang LM, Delaney DW, Fleming KA, Robson MD, Barnes E and Neubauer S. Multiparametric magnetic resonance for the non-invasive diagnosis of liver disease. *Journal of Hepatology*. 2014;60:69-77.
139. Matthews DR, Hosker JP, Rudenski AS, Naylor BA, Treacher DF and Turner RC. Homeostasis model assessment: insulin resistance and β-cell function from fasting plasma glucose and insulin concentrations in man. *Diabetologia*. 1985;28:412-419.
140. Targher G, Bertolini L, Padovani R, Rodella S, Tessari R, Zenari L, Day C and Arcaro G. Prevalence of Nonalcoholic Fatty Liver Disease and Its Association With Cardiovascular Disease Among Type 2 Diabetic Patients. *Diabetes Care*. 2007;30:1212-1218.
141. Birkenfeld AL and Shulman GI. Non Alcoholic Fatty Liver Disease, Hepatic Insulin Resistance and Type 2 Diabetes. *Hepatology (Baltimore, Md)*. 2014;59:713-723.
142. Iacobellis G and Leonetti F. Epicardial Adipose Tissue and Insulin Resistance in Obese Subjects. *The Journal of Clinical Endocrinology & Metabolism*. 2005;90:6300-6302.
143. Youm Y-H, Yang H, Amin R, Smith SR, Leff T and Dixit VD. Thiazolidinedione treatment and constitutive-PPARγ activation induces ectopic adipogenesis and promotes age-related thymic involution. *Aging cell*. 2010;9:478-489.
144. Klöting N, Fasshauer M, Dietrich A, Kovacs P, Schön MR, Kern M, Stumvoll M and Blüher M. Insulin-sensitive obesity. *American Journal of Physiology - Endocrinology and Metabolism*. 2010;299:E506-E515.
145. Murdolo G, Bartolini D, Tortoioli C, Piroddi M, Iuliano L and Galli F. Lipokines and oxysterols: Novel adipose-derived lipid hormones linking adipose dysfunction and insulin resistance. *Free Radical Biology and Medicine*. 2013;65:811-820.
146. Johannsen DL, Tchoukalova Y, Tam CS, Covington JD, Xie W, Schwarz J-M, Bajpeyi S and Ravussin E. Effect of 8 Weeks of Overfeeding on Ectopic Fat Deposition and Insulin Sensitivity: Testing the "Adipose Tissue Expandability" Hypothesis. *Diabetes Care*. 2014;37:2789-2797.
147. Dresner A, Laurent D, Marcucci M, Griffin ME, Dufour S, Cline GW, Slezak LA, Andersen DK, Hundal RS, Rothman DL, Petersen KF and Shulman GI. Effects of free fatty acids on glucose transport and IRS-1–associated phosphatidylinositol 3-kinase activity. *Journal of Clinical Investigation*. 1999;103:253-259.
148. Roden M, Price TB, Perseghin G, Petersen KF, Rothman DL, Cline GW and Shulman GI. Mechanism of free fatty acid-induced insulin resistance in humans. *Journal of Clinical Investigation*. 1996;97:2859-2865.
149. Thakur ML, Sharma S, Kumar A, Bhatt SP, Luthra K, Guleria R, Pandey RM and Vikram NK. Nonalcoholic fatty liver disease is associated with subclinical atherosclerosis independent of obesity and metabolic syndrome in Asian Indians. *Atherosclerosis*. 2012;223:507-511.
150. Mazurek T, Zhang L, Zalewski A, Mannion JD, Diehl JT, Arafat H, Sarov-Blat L, O'Brien S, Keiper EA, Johnson AG, Martin J, Goldstein BJ and Shi Y. Human Epicardial Adipose Tissue Is a Source of Inflammatory Mediators. *Circulation*. 2003;108:2460-2466.

151. Dubois SG, Heilbronn LK, Smith SR, Albu JB, Kelley DE, Ravussin E and Look AARG. Decreased Expression of Adipogenic Genes in Obese Subjects with Type 2 Diabetes. *Obesity (Silver Spring, Md)*. 2006;14:1543-1552.
152. Iacobellis G and Bianco AC. Epicardial adipose tissue: emerging physiological, pathophysiological and clinical features. *Trends in Endocrinology & Metabolism*. 2011;22:450-457.
153. Granér M, Nyman K, Siren R, Pentikäinen MO, Lundbom J, Hakkarainen A, Lauerma K, Lundbom N, Nieminen MS and Taskinen M-R. Ectopic Fat Depots and Left Ventricular Function in Nondiabetic Men With Nonalcoholic Fatty Liver Disease. *Circulation: Cardiovascular Imaging*. 2015;8 doi: 10.1161/CIRCIMAGING.114.001979..
154. Granér M, Siren R, Nyman K, Lundbom J, Hakkarainen A, Pentikäinen MO, Lauerma K, Lundbom N, Adiels M, Nieminen MS and Taskinen M-R. Cardiac Steatosis Associates With Visceral Obesity in Nondiabetic Obese Men. *The Journal of Clinical Endocrinology & Metabolism*. 2013;98:1189-1197.
155. de Marco R, Locatelli F, Zoppini G, Verlato G, Bonora E and Muggeo M. Cause-specific mortality in type 2 diabetes. The Verona Diabetes Study. *Diabetes Care*. 1999;22:756-761.
156. Perry RJ, Samuel VT, Petersen KF and Shulman GI. The role of hepatic lipids in hepatic insulin resistance and type 2 diabetes. *Nature*. 2014;510:84-91.
157. Yilmaz Y, Kurt R, Yonal O, Polat N, Celikel CA, Gurdal A, Oflaz H, Ozdogan O, Imeryuz N, Kalayci C and Avsar E. Coronary flow reserve is impaired in patients with nonalcoholic fatty liver disease: Association with liver fibrosis. *Atherosclerosis*. 2010;211:182-186.
158. Kim D, Choi S-Y, Park EH, Lee W, Kang JH, Kim W, Kim YJ, Yoon J-H, Jeong SH, Lee DH, Lee H-s, Larson J, Therneau TM and Kim WR. Nonalcoholic fatty liver disease is associated with coronary artery calcification. *Hepatology*. 2012;56:605-613.
159. Hallsworth K, Hollingsworth KG, Thoma C, Jakovljevic D, MacGowan GA, Anstee QM, Taylor R, Day CP and Trenell MI. Cardiac structure and function are altered in adults with non-alcoholic fatty liver disease. *Journal of Hepatology*. 2013;58:757-762.
160. Bottomley PA. NMR Spectroscopy of the Human Heart. In: R. K. Harris and R. E. Wasylishen, eds. *Encylcopedia of Magnetic Resonance* Chichester: John Wiley; 2009.
161. Neubauer S. Mechanisms of disease - The failing heart - An engine out of fuel. *N Engl J Med*. 2007;356:1140-1151.
162. Lee JH, Komoroski RA, Chu WJ and Dudley JA. Methods and Applications of Phosphorus NMR Spectroscopy In Vivo. *Annu Rep Nmr Spectro*. 2012;75:115-160.
163. Hudsmith LE and Neubauer S. Detection of myocardial disorders by magnetic resonance spectroscopy. *Nature Clinical Practice Cardiovascular Medicine*. 2008;5:S49-S56.
164. Bottomley PA. Noninvasive Study of High-Energy Phosphate-Metabolism in Human-Heart by Depth-Resolved P-31 Nmr-Spectroscopy. *Science*. 1985;229:769-772.
165. Bottomley PA, Wu KC, Gerstenblith G, Schulman SP, Steinberg A and Weiss RG. Reduced Myocardial Creatine Kinase Flux in Human Myocardial Infarction An In Vivo Phosphorus Magnetic Resonance Spectroscopy Study. *Circulation*. 2009;119:1918-1924.
166. Holloway CJ, Suttie J, Dass S and Neubauer S. Clinical Cardiac Magnetic Resonance Spectroscopy. *Prog Cardiovasc Dis*. 2011;54:320-327.
167. Redpath TW. Signal-to-noise ratio in MRI. *Br J Radiol*. 1998;71:704-707.
168. De Graaf RA. *In vivo NMR spectroscopy: principles and techniques.* 2nd ed. Chichester: John Wiley & Sons; 2007.
169. Tyler DJ, Hudsmith LE, Clarke K, Neubauer S and Robson MD. A comparison of cardiac P-31 MRS at 1.5 and 3 T. *NMR Biomed*. 2008;21:793-798.

170. Blamire AM, Rajagopalan B and Radda GK. Measurement of myocardial pH by saturation transfer in man. *Magnetic Resonance in Medicine*. 1999;41:198-203.
171. Dass S, Cochlin LE, Holloway CJ, Suttie JJ, Johnson AW, Tyler DJ, Watkins H, Robson MD, Clarke K and Neubauer S. Development and validation of a short 31P cardiac magnetic resonance spectroscopy protocol. *Journal of Cardiovascular Magnetic Resonance* 2010;12:123.
172. Pohmann R and von Kienlin M. Accurate phosphorus metabolite images of the human heart by 3D acquisition-weighted CSI. *Magnetic Resonance in Medicine*. 2001;45:817-26.
173. Robson MD, Tyler DJ and Neubauer S. Ultrashort TE chemical shift imaging (UTE-CSI). *Magnetic resonance in medicine : official journal of the Society of Magnetic Resonance in Medicine / Society of Magnetic Resonance in Medicine*. 2005;53:267-74.
174. Schroeder JL, Tyler DJ, Emmanuel Y, Robson MD, Scheuermann-Freestone M, Neubauer S and Clarke K. Effect of Patient Orientation on Cardiac ^{31}P-MRS. Paper presented at: Proceedings of the ISMRM; 2006.
175. Frauenrath T, Hezel F, Renz W, d'Orth TdG, Dieringer M, von Knobelsdorff-Brenkenhoff F, Prothmann M, Schulz-Menger J and Niendorf T. Acoustic cardiac triggering: a practical solution for synchronization and gating of cardiovascular magnetic resonance at 7 Tesla. *Journal of Cardiovascular Magnetic Resonance*. 2010;12:1-14 (DOI: 10.1186/1532-429X-12-67).
176. Cavassila S, Deval S, Huegen C, van Ormondt D and Graveron-Demilly D. Cramer-Rao bounds: an evaluation tool for quantitation. *NMR in biomedicine*. 2001;14:278-283.
177. Ross SM. *Introduction to probability and statistics for engineers and scientists.* 3rd ed. ed. Amsterdam ; London: Elsevier Academic Press; 2004.
178. Vanhamme L, van den Boogaart A and Van Huffel S. Improved method for accurate and efficient quantification of MRS data with use of prior knowledge. *Journal of Magnetic Resonance*. 1997;129:35-43.
179. Horn M, Kadgien M, Schnackerz K and Neubauer S. P-31-nuclear magnetic resonance spectroscopy of blood: A species comparison. *Journal of Cardiovascular Magnetic Resonance*. 2000;2:143-149.
180. Ernst RR and Anderson WA. Application of Fourier Transform Spectroscopy to Magnetic Resonance. *Review of Scientific Instruments*. 1966;37:93-102.
181. Ernst RR, Bodenhausen G and Wokaun A. *Principles of nuclear magnetic resonance in one and two dimensions*. Oxford: Clarendon Press; 1987.
182. Hardy CJ, Bottomley PA, Rohling KW and Roemer PB. An NMR Phased Array for Human Cardiac ^{31}P Spectroscopy. *Magnetic Resonance in Medicine*. 1992;28:54-64.
183. Redpath TW and Wiggins CJ. Estimating achievable signal-to-noise ratios of MRI transmit-receive coils from radiofrequency power measurements: applications in quality control. *Physics in medicine and biology*. 2000;45:217-227.

Appendix 1: 7T Safety Regulations

Important Information

- Under no circumstances should this list be given to volunteers.
- This safety information in this list is only applicable for the FMRIB Magnetom 7T.
- Without the risk versus benefit analysis that exists for clinical MRI, we must be much more cautious in a research environment.
- Therefore a volunteer is excluded from having an MRI at FMRIB will, in many cases, be able to undergo a clinical MRI examination at a lesser field strength.

Screening

- It is a requirement that you go through the 7T Volunteer Screening Form at the initial recruitment stage.
- Any 'yes' responses that are not covered by the scanner specific Surgery and Implant Safe List must be checked with the radiographers via MRIsafety@fmrib.ox.ac.uk
- Implants & surgeries that fall under FIR are likely to be excluded for 7T. The overriding concern, even with apparently trivial surgery, is the use of surgical clips, which while safe at 3T, pose a safety hazard at 7T.

Using The List

- Anything NOT on this list must be treated as Further Information Required.
- With very few exceptions, 6 weeks must have passed between surgery and scanning.

Using MRIsafety@fmrib.ox.ac.uk

- If you have an MRI safety query that is not covered in the list, classified as Further Information Required or as Likely Exclusion, you should email MRIsafety@fmrib.ox.ac.uk
  - The subject line of your email should contain FMRIB study number, the volunteer's date of birth (DD/MM/YYYY) and their gender eg "2013_50 – 01/01/1980 – M".
  - The body of the email should contain your query along with
    - A description of the procedure
    - The manufacturer, model name or number of any implants used

- The date of the procedure, hospital and country of surgery if not the UK

- Please send a separate email for each volunteer.
- This is a ticked system and on submission you will receive a reply with a reference number for your query. Please reply to this acknowledgment email if you wish to add further information to your query.
- The radiographers will then investigate the MRI compatibility of the surgery or implant.
- Please note that manufacturers can take several weeks to provide compatibility information.
- If scanning is approved you should bring a copy of this email to the scanning session.

High Value Subjects

- In exceptional cases it may still be possible to scan a high value subject that has an implant.
- Examples include where manufacturer safety information either doesn't exist or contraindicates scanning, or implant information cannot be obtained.
- Applications to scan such subjects need to demonstrate that their exclusion will have a significant detrimental effect on the study.
- If an application is accepted an implant risk assessment will be carried out along with an examination of any ethical and legal considerations.

Head and Brain Surgery/Implants

Safe

- Cysts removed from scalp (as long as no bone was cut), stitches/staples for lacerations (as long as removed and no bone was cut), removal of nasal polyps, tonsillectomies and adenoidectomies

Further information required

- In general any participant with a history of brain surgery, including burr holes or biopsies, will be excluded from scanning (the risk comes from clips that may have been used during the surgery and not recorded)

- Other aspects that need to be considered include the presence of any implants including, but not limited to, cranial fixation devices, shunts (fixed or programmable), clips on sensitive structures, stents, coils.

Likely Exclusion

- Participants with aneurysm clips, neurostimulators

Eye Surgery/Implants

Safe

- Squint surgery, minor cosmetic surgery, laser eye surgery for vision correction, cataract surgery done post 2000

Further information required

- All other eye operations including, but not limited to, surgery for a detached retina, lens implants not associated with cataract surgery, cataract surgery done prior to 2000
- All eye implants eg eye prostheses, metal weights in eyelids, eye lid springs

Likely Exclusion

- Any subjects with a history of a metallic penetrating eye injury where there is no radiological evidence of it being removed (even if removed medically)

Ear Surgery/Implants

Safe

- Grommets are safe to scan regardless of when they were implanted or whether they are still present, cosmetic ear procedures (eg pinoplasy)

Further information required

- All other ear surgeries eg stapedectomies, stapedotomies, surgery for a ruptured ear drum Likely Exclusion
- Participants with cochlear implants

Spine Surgery/Implants

Safe

- Any surgeries that have not introduced any metallic implants or clips eg discectomies, micro-discectomies, decompressions, laminectomies

Further information required

- Spinal fusions, Anterior Cervical Discectomies and Fusions (ACDFs)

Likely Exclusion

- Harrington rods, spinal cord stimulators

Thoracic Surgery/Implants

Safe

- Nil

Further information required

- Lumpectomies, mastectomies, lobectomies, breast implants, tissue expanders

Heart Surgery/Implants

Safe

- Diagnostic angiography of coronary vessels

Further information required

- Coronary bypasses (including sternal wiring), coronary stents, PFO closure devices, artificial heart valves, if there is any history of a pacemaker or defibrillator that has now been removed (pacing wires aren't always removed)

Likely Exclusion

- Pacemakers, defibrillators

Abdominal Surgery/Implants

Safe

- Haemorrhoidectomies, endoscopies (after 6 weeks)

Further information required

- All other IUDs, contraceptive coils and diaphragms
- Appendectomies, cholecystectomies, sterilisations, vasectomies, C-sections, gynaecological procedures, hysterectomies
- Hernia repairs involving mesh, filters, stents, implanted drug delivery devices, colostomies, cystoscopies, diaphragms, pessaries, insulin or infusion pumps, implanted drug infusion devices, urinary catheters, penile implants

Likely Exclusion

- Capsule endoscopy devices eg pill cam (until they have passed)

Contraceptive Implants

Safe

- The Mirena IUS is safe provided it is outside of the transmit volume of the coil eg studies that are only using the 32 channel TxRx coil
- Nexplanon and Implanon contraceptive implants

Further Information Required

- All other IUDs, contraceptive coils and diaphragms

Orthopaedic Surgery/Implants

Safe

- Arthroscopies, any surgery not involving implanted devices or clips

Further information required

- Open Reduction Internal Fixations (ORIFs) followed by removal of metallic implants (often removal can be incomplete)
- All joint replacements, ORIFS, bone/joint pins, screws, nails, wires, plates, etc

Vessel Surgery/Implants

Safe

- Nil

Further information required

- Varicose veins (clips can be used), vessel grafts, stents, filters, vascular access ports and/or catheters

Dental Surgery/Implants

Safe

- Fillings, crowns, dental posts (entirely within the tooth) associated with root canal treatment

Further information required

- Retainers, bridges, braces
- Dental implants (are screwed into the jaw)
- Jaw surgery – need to identify precisely what they've had done before a decision can be made re safety and artefact

Metallic Foreign Bodies - Orbits

- Any participants with a history of an orbital metallic FB should firstly have the risks associated with scanning, including blindness, explained to them
- In cases of penetrative injuries, scanning must not proceed unless there is a written radiological opinion confirming the absence of any metallic fragments
- In cases of non-penetrative intraocular metallic foreign body scanning cannot proceed unless the participant can state categorically that all metal fragments have been removed medically

- It is not ethical for a research participant to be subjected to x-rays in order to clear them for a research MRI scan. However if a written radiological opinion can be obtained on existing imaging that rules out a metallic foreign body the participant can be scanned.

Metallic Foreign Bodies - Non-Orbits

- Unless the participant can state categorically that all of the metal fragments have been removed by a doctor, they should be excluded from scanning.
- It is not appropriate for a research participant to be subjected to x-rays in order to clear them for a research MRI scan. However if a written radiological opinion can be obtained on existing imaging that rules out a metallic foreign body being present, then the participant can be scanned.

Miscellaneous

- Artificial limbs, prosthetics eg false eyes, callipers, braces or corsets
  - Must be removed prior to entering the MR CONTROLLED AREA (scanner side of 7T console room)
  - We have MR SAFE walking sticks or an MR SAFE wheelchair if required

- Medicated patches
  - All medicated patches must be removed prior to scanning eg nicotine, contraceptive, pain relief, nitro
  - If the patch is for a prescription medicine the participant must check with their GP that it can be removed safely for the duration of the scan
  - It is recommended that the participant brings a replacement patch as it is not always possible to reapply a patch after it has been removed

- Mascara and Eyeliner
  - Mascara and eyeliner needs to be removed prior to the scan
  - While fMRIB has makeup removing solution it is recommended that participants are warned so they can bring their own remover and makeup to reapply afterwards

- Tattoos and Permanent Makeup
  - Participants with tattoos that will be **within** the area of the transmit coil will be excluded from scanning, eg lip or eyebrow tattoos for head imaging
  - Participants with tattoos outside of the transmit coil should be warned of the rare complication of heating and to inform the radiographer or scanop immediately if they feel any uncomfortable heating
  - Furthermore participants with new tattoos will not be scanned until 48 hours after to avoid the risk of smearing or blurring

- Body piercing jewellery
  - All metallic body piercing jewellery must be removed for scanning
  - Jewellery that is entirely plastic can remain in place
  - It is recommended that participants change metal piercings to plastic piercings prior to attending for their scan (some piercings may have to be swapped by the original piercer)

- Transdermal anchors
  - Participants with transdermal anchors should be excluded from imaging unless there is manufacturer information regarding MR compatibility

- Rings
  - All rings should be removed if possible
  - If not then the participant should be warned re heating and to alert the scanop if this happens.

Appendix 2: Conference Abstracts

1) Oral Abstract Presentation, 17th Annual Society for Cardiovascular Magnetic Resonance Scientific Sessions, 16-19/1/2014

E Levelt, M Mahmod, C Wainwright, SK Piechnik, JM Francis, JE Schneider, P Leeson, TD Karamitsos, C Holloway, K Clarke, S Neubauer. **"Myocardial steatosis, impaired energetics and reduced circumferential strain are early manifestations of diabetic cardiomyopathy and precede structural changes"** Journal of Cardiovascular Magnetic Resonance 2014, 16(Suppl 1):O114 doi:10.1186/1532-429X-16-S1-O114

2) Oral Abstract Presentation at 2015 SCMR/EuroCMR Joint Scientific Session

E Levelt, CT Rodgers, W Clarke, M Mahmod, R Ariga, JM Francis, Liu A, C Holloway, K Clarke, TD Karamitsos, S Neubauer: **"Effect of exercise on myocardial energy metabolism and relationship between coronary microvascular dysfunction and abnormal myocardial energetics in diabetic cardiomyopathy "***Journal of Cardiovascular Magnetic Resonance* 2015, **17**(Suppl 1):O98 doi:10.1186/1532-429X-17-S1-O98

3) Oral Abstract Presentation at 2015 BSCMR 10th Annual Meeting

E Levelt, CT Rodgers, W Clarke, M Mahmod, R Ariga, JM Francis, Liu A, C Holloway, K Clarke, TD Karamitsos, S Neubauer. Title: **"The effect of exercise on myocardial energy metabolism in patients with type 2 diabetes mellitus and relationship between coronary microvascular function, myocardial energetics and myocardial oxygenation"**

Moderated Poster Presentations

1) British Cardiovascular Society Annual Conference, Manchester, 2015

E Levelt, C Holloway, CT Rodgers, W Clarke, M Mahmod, R Ariga, JM Francis, Liu A, K Clarke, TD Karamitsos, S Neubauer . Abstract Title: "*Relationship between coronary microvascular dysfunction, myocardial oxygenation and abnormal myocardial energetics at rest and stress in patients with type 2 Diabetes Mellitus"*

2) 10th British Society of Cardiovascular Magnetic Resonance Annual Meeting, London, 2015

Levelt E; Pavlides M; Kelly C; Mahmod M; Francis JM[1]; Schneider J; Clarke K; Neubauer S

Title: **"***Non-alcoholic fatty liver disease is associated with impaired cardiac function in patients with type 2 diabetes mellitus* **"**

3) 10th British Society of Cardiovascular Magnetic Resonance Annual Meeting, London, 2015

Levelt E; Rider OJ; Mahmod M; Ariga R; Piechnick SK; Francis JM; Schneider J; Holloway CJ; Karamitsos TD; Clarke K; Neubauer S

Title: *Left ventricular concentric remodelling is a prominent feature of diabetic cardiomyopathy and it is associated with functional and metabolic changes.*

4) EASL - The International Liver Congress™, Vienna, 2015

Levelt E; Pavlides M; Kelly C; Mahmod M; Francis JM; Schneider J; Clarke K; Neubauer S. Abstract Title: *"Non-alcoholic fatty liver disease is a common finding in asymptomatic, uncomplicated type 2 diabetes mellitus patients assessed by multiparametric magnetic resonance liver imaging"*

5) 2015 SCMR/EuroCMR Joint Scientific Sessions (walking poster presentation session)

Levelt E, Piechnick S, Mahmod M, Ferreira V, Ariga R, Francis JM, Liu A, Robson M , Clarke K, Neubauer S, Karamitsos TD "*Adenosine stress native T1 mapping detects microvascular disease in diabetic cardiomyopathy, without the need for gadolinium-based contrast*"

6) American Heart Association Scientific Sessions 2014, Chicago

R Upton, **E Levelt**, J Gamble, K Clarke, T Betts, S Neubauer, P Leeson. Abstract Title: *Strain Dispersion is an Early Subclinical Manifestation of Diabetic Cardiomyopathy Assessed by 3D Echocardiography*. Circulation 2014;130:A12183

7) RDM Symposium, University of Oxford, 2015.

R Upton, **E Levelt**, J Gamble, K Clarke, T Betts, S Neubauer, P Leeson. *Myocardial and Fluid Mechanics by Echocardiography Detect Subclinical Changes in Type 2 Diabetes Mellitus*.

8) BHF Symposium, University of Oxford, 2014.

R Upton, **E Levelt**, J Gamble, K Clarke, T Betts, S Neubauer, P Leeson. Abstract Title: *Changes in Ventricular Deformation and Fluid Dynamics Assessed by Echocardiography are Subclinical Manifestations of Diabetic Cardiomyopathy*.

9) British Cardiovascular Society Annual Conference, Manchester, 2014

E Levelt, N Ntusi, M Mahmod, C Wainwright, SK Piechnik, JM Francis, A Davis, JE Schneider, P Leeson, TD Karamitsos, C Holloway, K Clarke, S Neubauer, "*Early Manifestations of*

Diabetic Cardiomyopathy Assessed by Cardiac Magnetic Resonance Imaging and Spectroscopy", *Heart 2014;100:Suppl 3 A73-A74 doi:10.1136/heartjnl-2014-306118.127*

10) 9th British Society of Cardiovascular Magnetic Resonance Annual Meeting, Southampton, 12/3/2014 (walking poster presentation session)

E Levelt, M Mahmod, N Ntusi, R Ariga, R Upton, SK Piechnick, JM Francis, J Schneider, TD Karamitsos, P Leeson, CJ Holloway, K Clarke, S Neubauer, *"Assessment of early phenotypes in diabetic heart disease by cardiac magnetic resonance imaging and magnetic resonance spectroscopy"*

11) EuroCMR 12th International Congress on Cardiovascular Magnetic Resonance, Vienna, 15-17/5/2014

E Levelt, M Mahmod, NAB Ntusi, R Ariga, R Upton, SK Piechnick, JM Francis, JE Schneider, V Stoll, A Davis, TD Karamitsos, P Leeson, CJ Holloway, K Clarke, S Neubauer, *"Early phenotypes of diabetic cardiomyopathy assessed by multiparametric magnetic resonance imaging and magnetic resonance spectroscopy"*